# Green's Function for Poisson Equation in Layered Nano-Structures including Graphene

by

Naijing Kang

A thesis
presented to the University of Waterloo
in fulfillment of the
thesis requirement for the degree of
Master of Mathematics
in
Applied Math

Waterloo, Ontario, Canada, 2015

I hereby declare that I am the sole author of this thesis. This is a true copy of the thesis, including any required final revisions, as accepted by my examiners.

I understand that my thesis may be made electronically available to the public.

**Abstract**

The purpose of this thesis is to focus on the electrostatic properties of graphene-based nanostructures consisting of different materials, as well as their interactions with external electric charges, by solving the boundary value problem (BVP) corresponding to the electrostatic potential with the method of Green's function (GF). In the first part, we derive the Poisson equation and the corresponding GF for electrostatic potential in a layered structure without graphene from Maxwell's equations in the non-retarded approximation, together with the electrostatic boundary and matching conditions at the sharp boundaries between adjacent regions with different dielectric properties from the integral form of Maxwell's equations. Owing to the translational invariance in the layered structure, and taking the advantage of the infinitesimally thin layer of the graphene sheet, we continue to show that the GF for the layered structure with graphene integrated at an arbitrary position can be expressed in terms of the GF of the same structure without graphene by means of Dyson-Schwinger equation.

The main goal of this work is to analyze the electrostatic interaction of graphene with external charges and electric fields, mediated by the varying dielectric properties of the surrounding layered structure. As a starting point, we present full expressions for the GF after performing a two-dimensional (2D) Fourier Transform (FT) and applying the method of undetermined coefficients in structures consisting of two and three dielectric layers, where each region contains material with constant dielectric properties. Based on those basic results, a further application of the simple two-dielectric layer structure is then presented, where we consider the case with a randomly rough interface between two infinite dielectric layers. Describing the surface by a random profile function with zero mean, we calculate the average values of the perturbative solution for the undetermined coefficients in the GF to the second order in the surface roughness.

Another aspect of our study in the application of the three-layer structure is the dynamic response of a metallic slab due to the polarization by the passage of external charged particles. In this thesis, both the local and non-local descriptions of the electron gas (EG) in the metallic slab are presented in a sequence. In order to introduce nonlocal effects in the local hydrodynamic (LHD) model of the EG, we first introduce the quantum pressure term in the equation of motion for EG, which yields the standard hydrodynamic (SHD) model. By using the GF from a three-layered structure, we solve the resulting second-order wave equation for the perturbed charge density and the Poisson equation for the electric potential. In addition, by further introducing a Bohm quantum potential term into the equation of motion for EG, we arrive at the quantum hydrodynamic model (QHD). As a consequence of the new quantum term being in the form of a gradient correction to the perturbed charge density, a fourth-order wave equation for the density is acquired, which requires additional boundary condition (ABC) in order to form a well-posed

BVP. In addition, the dispersion relations arising from the excitation of the collective oscillation of electrons in the thin metal film are studied for all three cases of the hydrodynamic model.

Finally, we consider a special configuration of the field effect transistor (FET), where the graphene is implemented between a Stern layer and an oxide layer of finite thickness, with a semi-infinite region above the Stern layer occupied by an aqueous electrolyte containing mobile ions. In this model a nonlinear Poisson-Boltzmann (PB) equation is generated for the electrostatic potential in the electrolyte. After reviewing the construction of a GF for the fully linearized PB equation in the Debye-Hückel approximation, we show that it is possible to solve the so-called partially linearized PB equation by first obtaining an averaged part of the solution for the surface average of all quantities, and then developing a GF for the resulting linear equation with non-constant coefficients describing the fluctuating part of the potential.

## Acknowledgements

First and foremost, I would like to express my sincere gratitude to my supervisor, Dr. Zoran Miskovic, for the precious time he devoted to me, providing guidance and support in my research journey. My work would not have been produced as elegantly without the hard work of my supervisor. I am so deeply grateful for his patience and the courage he gave me throughout the duration of my masters.

In addition, I would also like to express appreciation to Yingying Zhang, Keenan Lyon, Puneet Sharma, and Vivek Thampi, for their valuable advice in my research and for all the joy they brought. I would like to also thank Tawsif Khan, Amenda Chow, Kexue Zhang, and Cesar Ramirez Ibanez, who have helped in many ways. A special thanks to Hanzhe (Tom) Chen for all the support and company during my graduate career in Waterloo.

Last but not least, I would like to thank my mother for her unconditional love and support throughout my journey.

# Table of Contents

# List of Figures

# List of Acronyms

| | |
|---|---|
| 0D | Zero-dimensional |
| 1D | One-dimensional |
| 2D | Two-dimensional |
| 3D | Three-dimensional |
| ABC | Additional boundary condition |
| BC | Boundary condition |
| BVP | Boundary value problem |
| PDE | Partial differential equation |
| DFT | Density Functional Theory |
| DH | Debye-Hückel |
| DS | Dyson-Schwinger |
| EDL | Electric double layer |
| EG | Electron gas |
| FET | Field effect transistor |
| FT | Fourier Transform |
| FTGF | Fourier Transform of the Green's Function |
| GF | Green's Function |

| | |
|---|---|
| LDA | Local density approximation |
| LHD | Local hydrodynamic |
| MC | Matching condition |
| ODE | Ordinary differential equation |
| PB | Poisson-Boltzmann |
| QHD | Quantum hydrodynamic |
| SHD | Standard hydrodynamic |
| SRM | Specular reflection model |
| TF | Thomas-Fermi |

# Chapter 1

# Introduction

## 1.1 Layered Nanostructures

Mathematical modeling of layered materials has a very long history in the development of semi-conductor heterostructures for applications in traditional silicon-based microelectronic devices. The need for miniaturization of such devices at the sub-micron scale and an expansion of the range of their applications for sensing devices gave rise to a whole new area of nano-electronics where novel devices are engineered by integrating layers of various materials with different electrical and optical properties [1]. In addition, the new area of nano-plasmonics has been developed over the past decade or so, which explores optical properties of the so-called meta-materials that often include stacked layers of thin metal sheets separated by some transparent insulating material [2]. An example of a nano-plasmonic waveguide is given in Fig. 1.1, which is designed so that a thin metallic conductor layer is sandwiched between two layers of dielectric insulators (cladding) that are separated from the conductor with thin gaps of other insulators [3]. Such structure can be designed to achieve long-ranged guiding of electromagnetic waves at dimensions smaller than their wavelengths.

While the typical thickness of layers in the novel nano-electronic and nano-plasmonic devices is on the order of some 10 nm, there has been increased interest in the past few years to integrate layers of a material that is only one atom thick, such as graphene, into those devices [4, 5].

Graphene is a two-dimensional (2D) arrangement of carbon atoms forming a densely packed honeycomb lattice. It is the thinnest known material in the universe so far, which was discovered in 2004 by Novoselov, Geim, *et al*. [6], who received a Nobel Prize for Physics in 2010 for their discovery of graphene. Graphene can be viewed as mother of other allotrope forms

| High-index cladding | $n_{\mathrm{d}}$ | |
|---|---|---|
| Low-index gap | $n_{\mathrm{g}}$ | $t$ |
| Conductor | $\varepsilon_{\mathrm{m}}$ | $d$ |
| Low-index gap | $n_{\mathrm{g}}$ | $t$ |
| High-index cladding | $n_{\mathrm{d}}$ | |
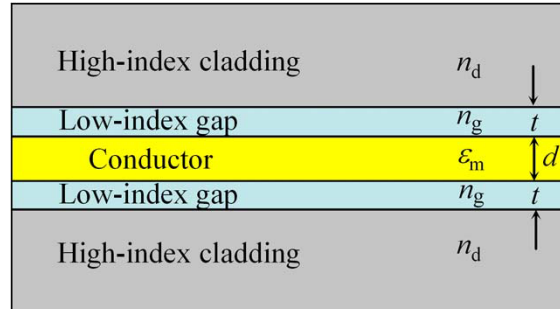
Figure 1.1: Schematic diagram of a nano-plasmonic waveguide. Adapted from Ref. [3].

of carbon: it can be wrapped into a zero-dimensional (0D) fullerene molecule, rolled up into a one-dimensional (1D) carbon nanotube and stacked into three-dimensional (3D) multilayered graphite. Owing to its exceptional mechanical, electrical and optical properties, graphene is extensively studied in devices for applications in nano-electronics and nano-plasmonics [4, 5]. Such devices are typically operated in the regime of a field effect transistor (FET) where graphene provides an active channel that accumulates charge on its surface and/or conducts electrical current. The charge and the current are efficiently modified by applying electrostatic potential to an external electrode called gate, which is typically placed parallel to graphene, providing a means of controlling graphene's electrical capacitance and/or conductivity [7, 8]. The materials used for such gates have characteristics of a metal, which contains large density of free electrons, and hence it must be electrically insulated from the graphene's channel to prevent the flow of electrical current between the gate and graphene. Such insulation is typically provided by inserting a layer of some oxide such as $SiO_2$ or $Al_2O_3$.

Figure 1.2 shows schematic diagrams of graphene based FETs with one gate (the so-called back gate, BG, a heavily doped silicon layer) and two gates (having both the back gate, BG, and a top gate, TG), which are used to control the density of charge carriers in graphene by applying external voltage to them. Those gates are separated from the graphene sheet by insulating layers of the $SiO_2$ and $Al_2O_3$ oxides. The surface density of charge carriers determines the magnitude of electrical current that flows between the source (S) and the drain (D) electrodes when a small voltage difference between those electrodes.

Graphene is also extensively studied in the FET devices for applications in biological and chemical sensors [9, 10, 11]. Such devices typically operate exposed to an electrolyte solu-
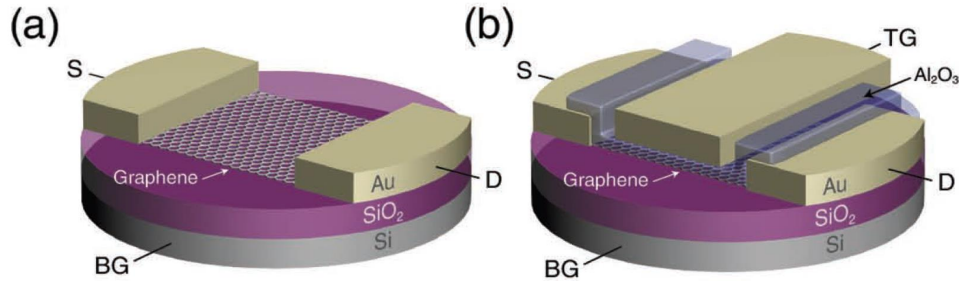
Figure 1.2: Graphene-based field effect transistor with one (a) and two (b) metallic gates, separated from graphene by insulating oxide layers. Adapted from Ref. [5].

tion containing mobile charges, such as dissolved salt ions, as well as some biological macromolecules [1]. The surface of graphene is known to be chemically inert, which diminishes its chemical sensitivity in such devices, but enables increasing its electrical sensitivity to the composition of an electrolytic solution because graphene may be safely exposed to the electrolyte without significant "leaking" of its charge carriers into it [12, 13]. Moreover, by applying the potential to an external top gate through the electrolyte, one can achieve an improved control of graphene's conductivity and capacitance compared to both the back-gated devices in Fig. 1.2(a) [14] and the more traditional electrolyte-insulator-semiconductor FETs [1]. Figure 1.3 shows a schematic diagram of a graphene-based FET exposed to an electrolytic solution that may be used to analyze the concentration of, e.g., dissolved salt ions, or charged bio-molecules, by controlling its electrical conductivity via the reference gate Ag/AgCl immersed in the electrolyte.

Because graphene is essentially a zero-thickness material, which only possesses a two-sided surface, its conductivity is strongly affected by: the dielectric properties of the surrounding material, the presence of external electrodes, the electric charges in its surrounding, as well as external electric fields [7, 8]. Whereas interaction of graphene with the external electromagnetic radiation is of interest in nano-plasmonic applications of graphene based meta-materials [16], there are several types of interaction of graphene with external charges that are of interest in various applications. The interactions with fast-moving charged particles are of interest for electron- or ion–beam spectroscopies of graphene. On the other hand, static charges near graphene are of interest for controlling its electrical conductivity by deposition of dopant particles near graphene sheet in a FET device that may act as charge donors or acceptors. At the same time, there always exist unwanted residual impurity atoms or molecules near graphene that are left as a consequence

3
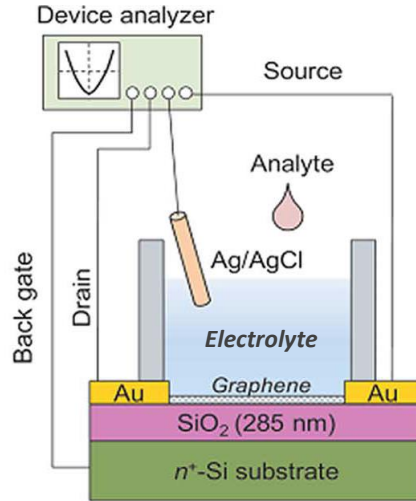
Figure 1.3: Electrolytically top-gated graphene-based field effect transistor for sensor applications. Adapted from Ref. [15].

of using various laboratory procedures for creating a graphene based FET device. In addition, graphene is often insulated by some oxide material, which may contain large amount of charged impurities that act as trapping centers for charge carriers in graphene. Finally, graphene applications for biochemical sensing involve interactions of charge carriers in graphene with some biological macromolecules in a solution adjacent to the surface of graphene.

For mathematical modeling of layered nano-structures it is often sufficient to assume that the area of the active channel, that is, graphene sheet, is large compared to the thickness of individual layers in the structure, as well as compared to the typical lateral dimension of the external charge distribution. In other words, one may often neglect the so-called end effects in such structures and invoke their translational invariance in 2D, which enables taking advantage of the 2D FT. On the other hand, the propagation of electromagnetic fields across nano-structures can often be described by Maxwell's equations in the so-called non-retarded approximation, i.e., by assuming that the speed of light is infinite [17]. In that case, all the relevant interactions with electrical fields and external charges are well described by the Poisson equation for the electrostatic potential, which is the main ingredient of the mathematical model developed in this work. Poisson equation is an elliptic partial differential equation (PDE), whose solution has to satisfy certain conditions at the boundaries between spatial regions occupied by the materials with different electric properties, which follow from the structure of Maxwell's equations. We are

specifically considering the so-called macroscopic form of Maxwell's equation, where atomic-scale fluctuations of the electric and magnetic fields are "smoothed-out", so that changes in the material properties may be considered as abrupt when crossing a boundary between two different materials [17]. Maxwell's equations then imply that Poisson equation must be supplemented by the boundary conditions (BCs) for the electrostatic potential of the Dirichlet and Neumann type [17].

When it comes to modeling the properties of various materials in a layered nano-structure, one may conveniently use the concept of a (relative) dielectric constant [17]. So, typically insulating layers of oxide, as well as the solvent in electrolyte are described by assigning numerical values to those constants, e.g., 3.9 for $SiO_2$ and 80 for water. On the other hand, the response of metallic layers to external fields or to the moving charges involves a time-dependent response of quasi-free electrons in the metal. Considering those electrons as a charged fluid, it is noteworthy that their dynamics is coupled with the electrostatic potential via Poisson equation, giving rise to a restoring force effect in the charged fluid that causes oscillations in the electron density in metals, known as plasma oscillations, or plasmons. Owing to the time-invariance of Maxwell's equations, the study of those oscillations may be translated into the frequency domain by performing a FT with respect to time, in which case the dielectric constants of metallic regions become functions of frequency. It was shown that plasmons in noble metals, such as gold or silver, which are of interest in the traditional plasmonic applications [2], may be adequately described by simple dielectric functions that only depend on frequency. However, when the typical size in plasmonic structures is reduced to a nanometer or so, it became obvious that one has to introduce the so-called spatial non-locality in the plasma oscillation of electrons in a metallic nano-particle, which may be then described by a wave equation for the charge density of electron fluid in the metal that involves spatial dispersion [18, 19, 20, 21].

When a single sheet of graphene is included in a layered structure, its 2D character gives rise to a rather complicated behavior of its charge carriers (electrons and/or holes) in response to external fields and charged particles. This response may be adequately described in the Fourier space-time transformed domain by means of the so-called polarization function, or polarizability, that includes both the 2D spatial dispersion and frequency dependence [22]. While the derivation of polarizability of graphene requires quantum-mechanical considerations, we can take advantage of its linear character, where the induced charge density on graphene is proportional to the perturbation of the electrostatic potential on its surface. Then, incorporating graphene in a layered nano-structure may be treated as including a one-atom thick sheet of charge, which just gives rise to a BC of the Robin type for macroscopic Maxwell's equations.

Thus, solving the Poisson equation over various regions with different material properties, which may include graphene, must be supplemented by a set of suitable BCs, giving rise to a boundary value problem (BVP) . This problem can be made well-posed by careful consideration

5

of the existence, uniqueness and stability of its solution [23], which gives a prescription for the choice of proper BCs that are in accord with the physical phenomena. In this thesis we concentrate on the Green's function (GF) method of solving the Poisson equation because of its elegance and universality in expressing the electrostatic potential throughout a region as an integral over arbitrary distribution of external charges inside that region plus a term that includes preassigned values of the electrostatic potential (or its normal gradient) at the boundary of the region.

## 1.2   The method of Green's function

For the electrostatic phenomena, the Poisson equation is extensively used for the description of the electric field described by the Maxwell's equations. Considering the simplest case with an arbitrary charge density $\rho$ in an infinite free space, the electrostatic potential $\Phi$ can be directly deduced from the Coulomb law without solving the Poisson equation,

$$\Phi(\mathbf{R}) = \int_V \frac{\rho(\mathbf{R}')}{R} \, d^3\mathbf{R}', \tag{1.1}$$

where $R = \|\mathbf{R} - \mathbf{R}'\|$. Using the well-known result

$$\nabla^2(1/R) = -4\pi\delta(\mathbf{R} - \mathbf{R}'), \tag{1.2}$$

where $\delta(\mathbf{R} - \mathbf{R}')$ is a 3D Dirac's delta function, one may show that the potential satisfies the Poisson equation,

$$\nabla^2\Phi(\mathbf{R}) = -4\pi\rho(\mathbf{R}). \tag{1.3}$$

However, for the BVP of the Poisson equation (1.3) on a finite region involving prescribed conditions on its closed boundary, the method of GF is favored, not only because of the integral representation for the solution of the Poisson equation, but also because it can be used to prove the uniqueness of the solution with Dirichlet or Neumann BCs. Before we develop expressions for the GF for the Poisson equation, two identities due to George Green should be introduced as necessary tools. To begin with, by assuming that $V$ is a smooth domain in $\mathbb{R}^3$ bounded by the closed surface $S$, with two scalar fields $\phi, \psi \in C^2(V) \cap C(S)$, the Green's first identity follows as

$$\int_V \left(\phi\nabla^2\psi + \nabla\phi \cdot \nabla\psi\right) d^3\mathbf{R} = \oint_S \phi\frac{\partial\psi}{\partial n} \, dA, \tag{1.4}$$

whereas the Green's second identity can be deduced from Eq. (1.4) as

$$\int_V \left(\phi\nabla^2\psi - \psi\nabla^2\phi\right) d^3\mathbf{R} = \oint_S \left[\phi\frac{\partial\psi}{\partial n} - \psi\frac{\partial\phi}{\partial n}\right] dA. \tag{1.5}$$

Here, $\frac{\partial \psi}{\partial n} = \hat{\mathbf{n}} \cdot \nabla \psi$ is the normal derivative of the function $\psi$ with $\hat{\mathbf{n}}$ being the outer normal to the surface $S$.

In order to tackle the Poisson equation (1.3), we apply the Green's second identity by choosing $\phi = \Phi$ and $\psi = 1/R = 1/\|\mathbf{R} - \mathbf{R}'\|$. As a consequence of Eqs. (1.2) and (1.3), the potential in the domain $V$ may be expressed explicitly by an integral equation,

$$\Phi(\mathbf{R}) = \int_V \frac{\rho(\mathbf{R}')}{R} d^3\mathbf{R}' + \frac{1}{4\pi} \oint_S \left[ \frac{1}{R} \frac{\partial \Phi}{\partial n'} - \Phi \frac{\partial}{\partial n'} \left( \frac{1}{R} \right) \right] dA'. \tag{1.6}$$

Note that the potential of the electrostatic field for the free space in Eq. (1.1) can be regarded as a special case of Eq. (1.6), where the correction term in the form of surface integral in Eq. (1.6) diminishes if the surface $S$ goes to infinity. The integral statement in (1.6) shows that the potential in the closed region $V$ is expressed in terms of two prescribed conditions on its boundary: one is for the potential itself $\Phi$ known as the Dirichlet BC, and the other is for the normal derivative of the potential $\frac{\partial \Phi}{\partial n'}$ called the Neumann BC. This result indicates that the specification of both $\Phi$ and $\frac{\partial \Phi}{\partial n'}$ as the Cauchy data on the boundary would lead to an overdetermined BVP. One may conclude that the BVP for the Poisson equation would be well-posed only if it is subject to either Dirichlet or Neumann BCs on the surface $S$.

In order to analyze the uniqueness of the solution with either Dirichlet or Neumann BC by the method of Green Function, we assume that there exist two solutions, $\Phi_1$ and $\Phi_2$, satisfying the same BC. By denoting the difference of the two solutions as

$$U = \Phi_1 - \Phi_2, \tag{1.7}$$

we conclude that $U$ must also satisfy the Laplace equation $\nabla^2 U = 0$ inside the volume $V$, corresponding to either $U = 0$ for Dirichlet BVP or $\frac{\partial U}{\partial n} = 0$ for Neumann BVP on $S$. From the Green's first identity in Eq. (1.4), by taking $\phi = \psi = U$, we have

$$\int_V (U\nabla^2 U + \nabla U \cdot \nabla U) d^3\mathbf{R} = \oint_S U \frac{\partial U}{\partial n} dA. \tag{1.8}$$

This relation can be converted to the following equation for either BC,

$$\int_V \|\nabla U\|^2 d^3\mathbf{R} = 0, \tag{1.9}$$

which implies $\nabla U = 0$ due to the non-negative value inside the integral. Therefore, in $C^2(V) \cap C(S)$, the solution for the Poisson equation is unique for Dirichlet BC, while the solutions for the Neumann BC can only differ by a constant.

In order to develop a formal solution of the Poisson equation (1.3) in terms of the GF $G(\mathbf{R}, \mathbf{R}')$, we may follow the same idea as that used in deriving Eq. (1.6). Noticing that

$$\nabla'^2 \left( \frac{1}{\|\mathbf{R} - \mathbf{R}'\|} \right) = -4\pi\delta(\mathbf{R} - \mathbf{R}'), \tag{1.10}$$

one may require that the GF satisfies the same equation with the point source,

$$\nabla'^2 G(\mathbf{R}, \mathbf{R}') = -4\pi\delta(\mathbf{R} - \mathbf{R}'), \tag{1.11}$$

having a general solution given by

$$G(\mathbf{R}, \mathbf{R}') = \frac{1}{\|\mathbf{R} - \mathbf{R}'\|} + F(\mathbf{R}, \mathbf{R}'), \tag{1.12}$$

where the term $\frac{1}{\|\mathbf{R}-\mathbf{R}'\|}$ is a solution particularly assigned to the infinite domain, whereas $F(\mathbf{R}, \mathbf{R}')$ is a harmonic function satisfying the Laplace equation inside the volume $V$,

$$\nabla'^2 F(\mathbf{R}, \mathbf{R}') = 0. \tag{1.13}$$

According to the analysis of Eq. (1.6) above, one may realize that $\frac{1}{\|\mathbf{R}-\mathbf{R}'\|}$ is not a wise choice for GF due to the dependence on both $\Phi$ and $\partial\Phi/\partial n$ in the surface integral. In order to avoid the redundant Cauchy data in the surface integral, a modification for the GF is achieved by choosing the specific form for the free term $F(\mathbf{R}, \mathbf{R}')$ so that only one of the two surface integrals would remain in the expression for $\Phi$, Eq. (1.6), corresponding to either the Dirichlet or Neumann BCs for $\Phi$. By applying the Green's second identity (1.5) and using $\psi = G(\mathbf{R}, \mathbf{R}')$ and $\phi = \Phi(\mathbf{R})$, the general solution for $\Phi(\mathbf{R})$ by the method of GF becomes

$$\Phi(\mathbf{R}) = \int_V \rho(\mathbf{R}')G(\mathbf{R}, \mathbf{R}')\, d^3\mathbf{R}' + \frac{1}{4\pi} \oint_S \left[ G(\mathbf{R}, \mathbf{R}')\frac{\partial\Phi}{\partial n'} - \Phi\frac{\partial G(\mathbf{R}, \mathbf{R}')}{\partial n'} \right] dA'. \tag{1.14}$$

Thus, for the BVP subjected to the Dirichlet BC, one may choose the specific $F(\mathbf{R}, \mathbf{R}')$ which results in the corresponding Dirichlet BC for GF as

$$G_D(\mathbf{R}, \mathbf{R}') = 0 \qquad \text{for} \quad \mathbf{R}' \quad \text{on} \quad S. \tag{1.15}$$

Then, the unique solution for the Poisson equation (1.3) is given by

$$\Phi(\mathbf{R}) = \int_V \rho(\mathbf{R}')G_D(\mathbf{R}, \mathbf{R}')\, d^3\mathbf{R}' - \frac{1}{4\pi} \oint_S \Phi(\mathbf{R}')\frac{\partial G_D(\mathbf{R}, \mathbf{R}')}{\partial n'}dA'. \tag{1.16}$$

8

As for the Neumann BC, one might intuitively assume that $\partial G/\partial n' = 0$ following similar procedure as above. However, the zero outflux of the GF on $S$ contradicts Eq. (1.11) and the corresponding expression of the Gauss'law for $G(\mathbf{R}, \mathbf{R}')$. As a result, the simplest correction that can be used for the Neumann BC is

$$\frac{\partial G_N(\mathbf{R}, \mathbf{R}')}{\partial n'} = -\frac{4\pi}{A} \qquad \text{for} \quad \mathbf{R}' \quad \text{on} \quad S \tag{1.17}$$

where $A$ is the area of the boundary surface $S$. Then, the unique solution for the Poisson equation (1.3) is given by

$$\Phi(\mathbf{R}) = \langle \Phi \rangle_S + \int_V \rho(\mathbf{R}')G_N(\mathbf{R}, \mathbf{R}') \, d^3\mathbf{R}' + \frac{1}{4\pi} \oint_S \frac{\partial \Phi}{\partial n'} G_N(\mathbf{R}, \mathbf{R}')dA', \tag{1.18}$$

where $\langle \Phi \rangle_S$ is the average value of the potential over the entire surface $S$. This additional term in the solution indicates that the potential is defined up to an additive constant in the case of the Neumann BC on $S$. However, in most cases $A$ is extremely large or infinite, so that one may set $A \to \infty$ giving $\langle \Phi \rangle_S = 0$ in Eq. (1.18), whereas the corresponding Neumann BC for the GF in Eq. (1.17) becomes homogeneous.

## 1.3   Outline of the thesis

The thesis is organised in the following manner. In the Chapter 2, for the purpose of understanding the effects of all sorts of external charges or external electric fields on graphene, we first develop a mathematical model that describes the electrostatic potential in a layered structure of dielectric materials without graphene, which satisfies all the electrostatic boundary and MCs of the Dirichlet and Neumann type that follow from Maxwell's equations. We then show that the in-plane polarizability of a single layer of graphene gives rise to a new BC of the Robin type for the electrostatic potential at the plane occupied by graphene. Then, we show how the GF for the layered structure that includes graphene at an arbitrary position may be directly obtained from the GF for the same structure without graphene by solving the Dyson-Schwinger (DS) equation.

In Chapter 3 we show a detailed derivation of the results for the GF in the cases of two and three regions containing materials with constant dielectric properties, which are of interest for applications of graphene. In the first case, both regions are considered semi-infinite, representing a simple interface between two dielectrics that may contain graphene close to that interface, as in the case shown in Fig. 1.2(a) with graphene layer laying on a thick $SiO_2$ substrate and free space above it. In the second case, we consider a layer of finite thickness between two semi-infinite layers that may represent, e.g., the configuration shown in Fig. 1.2(b) of dual-gated graphene

with thick insulating layers around it. Notice that experiments show that graphene generally cannot lie directly on an interface between two materials, but rather that there are usually small gaps of free space around graphene, with the thickness about 3-4 Å.

For the Chapter 4, we derive a perturbative solution for the GF of the Poisson equation for electrostatic potential in the presence of two semi-infinite regions with different relative dielectric constants that are separated by a randomly rough boundary. In the case when one region is a metal described by a frequency dependent dielectric function, such configuration may be used to explore possible effects of the surface roughness on the the surface plasmon frequency of the metal. Describing the surface by a random profile function with zero mean, which is translationally invariant in 2D, we use a perturbative approach to implement the electrostatic BCs and obtain analytical expressions for the average value of the GF to the second order in the surface profile function.

In the case of Chapter 5, we consider a metallic layer of finite thickness sandwiched between two semi-infinite dielectric regions, similar to that in Fig. 1.1. The dynamic properties of the gas of quasi-free electrons in the metal are studied by means of different versions of the hydrodynamic equations for the electron gas (EG) coupled with the Poisson equation for the electrostatic potential. Firstly, we describe the dynamic polarization of the EG in a purely classical manner, which gives rise to the local hydrodynamic (LHD) model of the EG. Next, by keeping the quantum pressure term in the equation of motion for the EG we derive the standard hydrodynamic (SHD) model in order to characterize nonlocal effects in the EG. As a consequence, the perturbed charge density in the EG is described by a second-order wave equation (which becomes a second-order Helmholtz equation upon FT with resect to time), which is solved assuming that the normal component of the electron velocity vanishes at the impenetrable boundary of the metal. Finally, we add the quantum diffraction effects due to the Bohm potential in the equation of motion for the EG giving the quantum hydrodynamic model (QHD) , which results in a fourth-order wave (or Helmholtz) equation for the perturbed charge density in the EG. This equation then requires an additional boundary condition (ABC) for the perturbed electron density in the EG, and we show in Chapter that a consistent treatment of the fourth-order wave (Helmotlz) equation gives rise to two possibilities for an ABC. In addition, the plasmon dispersion relations in the metal layer are discussed in that chapter for all three versions of the hydrodynamic model.

In Chapter 6, we consider two dielectric layers of finite thickness and a semi-infinite region occupied by a liquid electrolyte that contains mobile charges. This situation corresponds to, e.g., a graphene based FET in Fig. 1.3 with the surface of graphene exposed to an aqueous solution of salt ions. When the surface of graphene is charged by the potential applied to the gate immersed deep in the bulk of electrolyte, then the ions of opposite charge are attracted to graphene and those with the same charge sign are repelled from graphene. Describing the charge density from those ions with the Boltzmann distribution gives rise to the Poisson-Boltzmann (PB) equation for

the electrostatic potential in electric double layer (EDL) formed in the electrolyte. While the PB equation is a nonlinear eqution, we show in that chapter that fluctuations of the potential about an equilibrium value given by a 2D average of the potential over a plane parallel to graphene may be described by a linearized equation with coefficients that depend on the perpendicular distance from graphene. This partially linearized treatment of the PB equation allows us to develop an analytical expression for the GF function describing fluctuations of the electrostatic potential in response to an arbitrary charge density perturbation in the electrolyte coming, e.g., from charged bio-molecules. Those fluctuations may be then directly used to estimate changes in the electrical conductivity of electrolytically gated graphene and hence asses its sensitivity to the presence of various concentrations of bio-molecules in the electrolyte.

In this thesis we use the so-called Gaussian electrostatic units, where the dielectric permittivity of vacuum $\epsilon_0$ satisfies the relation $4\pi\epsilon_0 = 1$.

# Chapter 2

# Green's function for the Poisson equation in a layered structure

In order to understand the effects of all sorts of external charges or external electric fields in a graphene based device, it is desirable to develop a mathematical model that describes the electrostatic interaction in a layered structure of dielectric materials containing a sheet of graphene. To analyze those structures macroscopically, it is justifiable to approach the problem from the electromagnetic aspect. This can be achieved by introducing Maxwell's equations, which are the laws governing the behavior of electric and magnetic fields or, specifically, how the electric and magnetic fields are generated and altered by each other and by the external electrical charges and currents. Since we are interested in the quasi-static regime, we discard magnetic field and show in this Chapter how the Poisson equation for the electrostatic potential is derived from Maxwell's equation in the electrostatic limit. In particular, we show how this equation can be solved in a piece-wise manner in a domain consisting of regions with different dielectric properties, which change in an abrupt manner when crossing the boundary surfaces between neighboring regions. This is achieved by identifying the so-called MCs for the potential and its normal derivative at those boundaries, which follow from the BCs implied by Maxwell's equations. Finally, a procedure is outlined on how to treat the presence of graphene in a layered structure as an ABC based on a linear-response relation between the induced charge density on graphene and the electrostatic potential on its surface.

## 2.1 Derivation of the Poisson's equation

In this thesis we start with the Maxwell's equations inside matter, which are all first considered in the spatial $\mathbf{R}$ and time $t$ domains, to show the dynamic interaction between magnetic field and electric field. First we look at two equations, known as the Gauss' law for the electric displacement, $\mathbf{D}$, and magnetic induction, $\mathbf{B}$, fields:

$$\nabla \cdot \mathbf{D}(\mathbf{R}, t) = 4\pi\rho(\mathbf{R}, t), \tag{2.1}$$

$$\nabla \cdot \mathbf{B}(\mathbf{R}, t) = 0, \tag{2.2}$$

where $\mathbf{R} = (x, y, z)$ is the position vector and $\nabla = (\partial/\partial x, \partial/\partial y, \partial/\partial z)$ is the gradient vector in a Cartesian coordinate system. Equation (2.1) describes how the divergence of the electric displacement vector field $\mathbf{D}$ is determined by external charges with the volume density $\rho$, which represents the number of unit (monopole) electric charges per unit volume. On the other hand, Eq. (2.2) tells us that the divergence of the magnetic induction field $\mathbf{B}$ is identically zero because there are no sources of the magnetic field in the form of a magnetic monopole. Another two equations that are coupled with Eq. (2.1) and Eq. (2.2) to form the full set of Maxwell's equation are the Faraday's law and the Ampere's law:

$$\nabla \times \mathbf{E}(\mathbf{R}, t) = -\frac{1}{c}\frac{\partial \mathbf{B}(\mathbf{R}, t)}{\partial t}, \tag{2.3}$$

$$\nabla \times \mathbf{H}(\mathbf{R}, t) = \frac{4\pi}{c}\mathbf{j}(\mathbf{R}, t) + \frac{1}{c}\frac{\partial \mathbf{D}(\mathbf{R}, t)}{\partial t}, \tag{2.4}$$

where $c$ is the speed of light in free space (i.e., vacuum or air). These equations reveal that a change in time of the magnetic induction results in a circulation of the electric field $\mathbf{E}$, whereas the circulation of the magnetic field $\mathbf{H}$ is governed by the external electric current density $\mathbf{j}$, which is related to $\rho$ by the continuity equation that expresses charge conservation:

$$\frac{\partial\rho(\mathbf{R}, t)}{\partial t} + \nabla \cdot \mathbf{j}(\mathbf{R}, t) = 0. \tag{2.5}$$

Note that the Maxwell's equations are written here in the so-called Gaussian electrostatic units, where the dielectric permittivity of vacuum $\epsilon_0$ satisfies the relation $4\pi\epsilon_0 = 1$.

For Maxwell's equations in matter, there also exist the so-called constitutive relations between the electric displacement and the electric field vectors, as well as between the magnetic induction and the magnetic field vectors, which may be written in a general form as

$$\mathbf{D}(\mathbf{R}, t) = \int d^3\mathbf{R}' \int_{-\infty}^{\infty} dt'\, \mathcal{E}(\mathbf{R}, \mathbf{R}', t - t')\, \mathbf{E}(\mathbf{R}', t'), \tag{2.6}$$

$$\mathbf{B}(\mathbf{R}, t) = \int d^3\mathbf{R}' \int_{-\infty}^{\infty} dt'\, \mathcal{M}(\mathbf{R}, \mathbf{R}', t - t')\, \mathbf{H}(\mathbf{R}', t'), \tag{2.7}$$

where $\mathcal{E}$ and $\mathcal{M}$ are called the dielectric response function and the magnetic response function, respectively. Notice that the above constitutive relations are nonlocal, both in the space and time variables, because the values of the fields $\mathbf{D}(\mathbf{R}, t)$ and $\mathbf{B}(\mathbf{R}, t)$ are determined by integrating over a range of positions $\mathbf{R}'$ (notice that $d^3\mathbf{R}' \equiv dx'\, dy'\, dz'$) and time $t'$ where the electric and magnetic fields have values $\mathbf{E}(\mathbf{R}', t')$ and $\mathbf{H}(\mathbf{R}', t')$, respectively.

In this work, we are interested in the so-called quasi-static limit of the Maxwell's equations, where one may neglect the retardation effects due to finite time it takes perturbations in the electric and magnetic fields to propagate across a nanometer-sized object at the speed of light $c$. This limit is mathematically achieved by simply taking the limit $c \to \infty$ in Eqs. (2.3) and (2.4). As a result, it can be shown that the magnetic fields may be discarded from the theory in the quasi-static limit, whereas the electric field becomes irrotational,

$$\nabla \times \mathbf{E}(\mathbf{R}, t) = 0. \tag{2.8}$$

Thus, $\mathbf{E}$ becomes a conservative vector field in the quasistatic limit and hence it may be expressed as a gradient of some scalar field, $\Phi(\mathbf{R}, t)$, called the electric (or electrostatic, in the present context) potential,

$$\mathbf{E}(\mathbf{R}, t) = -\nabla\Phi(\mathbf{R}, t). \tag{2.9}$$

If the system under study is stationary, e.g., if there is no temporal change in the macroscopic parameters of the structure, no moving boundaries between dielectrics, etc., we may apply a Fourier Transform (FT) with respect to time, which gives for the electric field a function $\hat{\mathbf{E}}(\mathbf{R}, \omega)$ in the FT space defined by

$$\hat{\mathbf{E}}(\mathbf{R}, \omega) = \int_{-\infty}^{\infty} e^{i\omega t}\mathbf{E}(\mathbf{R}, t)\, dt, \tag{2.10}$$

with similar definitions for $\hat{\mathcal{E}}$, $\hat{\rho}$ and $\hat{\Phi}$. Noting that the relation between $\mathbf{D}$ and $\mathbf{E}$ in Eq. (2.6) is a convolution with respect to time, we obtain a simpler relation between $\hat{\mathbf{D}}$ and $\hat{\mathbf{E}}$ in the FT space as

$$\hat{\mathbf{D}}(\mathbf{R}, \omega) = \int \hat{\mathcal{E}}(\mathbf{R}, \mathbf{R}', \omega)\hat{\mathbf{E}}(\mathbf{R}', \omega)\, d^3\mathbf{R}', \tag{2.11}$$

which implies that there may still exist a nonlocal relation between $\hat{\mathbf{D}}$ and $\hat{\mathbf{E}}$ involving their spatial dependencies. At the same time, note that $\hat{\mathbf{D}}$ and $\hat{\rho}$ satisfy the same local relation as in Eq. (2.1), and $\hat{\mathbf{E}}$ and $\hat{\Phi}$ satisfy the same local relation as in Eq. (2.9) in the time domain.

We shall now consider two special cases of the constitutive relation in Eq. (2.18) of interest in this thesis.

- **Spatially local structure**.
  If we assume that the dielectric response of a material is spatially local by writing

$$\hat{\mathcal{E}}(\mathbf{R}, \mathbf{R}', \omega) = \epsilon(\mathbf{R}, \omega)\,\delta(\mathbf{R} - \mathbf{R}'), \tag{2.12}$$

  where $\delta(\mathbf{R} - \mathbf{R}')$ is the Dirac's delta function in the spatial coordinates, then we obtain from Eq. (2.18)

$$
\begin{aligned}
\hat{\mathbf{D}}(\mathbf{R}, \omega) &= \int_{-\infty}^{\infty} \epsilon(\mathbf{R}, \omega)\,\delta(\mathbf{R} - \mathbf{R}')\hat{\mathbf{E}}(\mathbf{R}', \omega)\,d^3\mathbf{R}' \\
&= \epsilon(\mathbf{R}, \omega)\hat{\mathbf{E}}(\mathbf{R}, \omega).
\end{aligned}
\tag{2.13}
$$

  Therefore, by combining Eqs. (2.13), (2.9) and (2.1) we derive the Poisson equation for the electric potential in the FT space as

$$\nabla \cdot \left[\epsilon(\mathbf{R}, \omega)\nabla\hat{\Phi}(\mathbf{R}, \omega)\right] = -4\pi\hat{\rho}(\mathbf{R}, \omega). \tag{2.14}$$

  Note that the function $\epsilon(\mathbf{R}, \omega)$ introduced in Eq. (2.12) generally depends on the position $\mathbf{R}$ in a nonhomogeneous structure, containing layers of different materials with different relative dielectric constants, each of which may depend on frequency $\omega$.

- **Spatially and temporally local structure**.
  If the structure is also strictly static, in addition to being spatially local, i.e., if there is no frequency dependence of dielectric constants so that $\epsilon(\mathbf{R}, \omega) = \epsilon(\mathbf{R})$, then we may write the inverse of the dielectric response function in Eq. (2.12) as

$$
\begin{aligned}
\mathcal{E}(\mathbf{R}, \mathbf{R}', t - t') &= \delta(\mathbf{R} - \mathbf{R}')\frac{1}{2\pi}\int_{-\infty}^{\infty} \mathrm{e}^{-i\omega(t-t')}\epsilon(\mathbf{R})\,d\omega, \\
&= \epsilon(\mathbf{R})\delta(\mathbf{R} - \mathbf{R}')\delta(t - t'),
\end{aligned}
\tag{2.15}
$$

  showing that the dielectric response is both local in time and space. Therefore, we obtain from the general relation in Eq. (2.6)

$$\mathbf{D}(\mathbf{R}, t) = \epsilon(\mathbf{R})\mathbf{E}(\mathbf{R}, t), \tag{2.16}$$

  which when combined with Eqs. (2.1) and (2.9) gives the Poisson equation in the time domain as

$$\nabla \cdot [\epsilon(\mathbf{R})\nabla\Phi(\mathbf{R}, t)] = -4\pi\rho(\mathbf{R}, t). \tag{2.17}$$

In the interest of obtaining a general mathematical framework relevant to both the frequency dependent and static forms of the Poisson equation given in Eqs. (2.14) and (2.17), respectively, we notice that those equations, as well as the corresponding constitutive relations Eq. (2.13) and Eq. (2.16) and the accompanying BCs are all isomorphic in the spatial domain. Hence, we may simply drop $\omega$ and $\hat{}$ from the notation in the first case and drop the time dependence in the second case and consider only the spatial dependence, giving a constitutive relation,

$$\mathbf{D}(\mathbf{R}) = \epsilon(\mathbf{R})\mathbf{E}(\mathbf{R}), \tag{2.18}$$

and the Poisson equation,

$$\nabla \cdot [\epsilon(\mathbf{R})\nabla\Phi(\mathbf{R})] = -4\pi\rho(\mathbf{R}). \tag{2.19}$$

Specifically, in layered structures of dielectrics, which are of interest for graphene applications, we often find that different materials occupy different regions of space with a sharp boundary between them. Therefore, when crossing from one region to another region, the relative dielectric constant $\epsilon(\mathbf{R})$ exhibits finite jump at the boundary between the regions. Since we want to solve the Poisson equation Eq. (2.19) for all points $\mathbf{R}$ in a 3D space, we must specify the behavior of the electrostatic potential at the boundaries where the relative dielectric constant exhibits jumps. This can be accomplished by considering the electrostatic BCs that follow from Maxwell's equations.

## 2.2 Electrostatic boundary conditions

By focusing on the electrostatic behavior of dieletric material when it is placed in an electric field, the required conditions on the electrostatic potential at the boundary between two dielectric media may be deduced from the so-called electrostatic BCs for the electric and displacement fields, $\mathbf{E}$ and $\mathbf{D}$, which we can deduce from the Gauss's Law for $\mathbf{D}$ as in Eq. (2.1) and Eq. (2.8). By choosing the Gauss's law for electric displacement $\mathbf{D}$, the effect of polarization of a dielectric material is considered since $\mathbf{D}$ includes both the field attributable to bound charges due to polarization and the field attributable to free charges.

More generally, suppose we have a curved surface $S$ that acts as a boundary between two different dielectric media in a 3D space, $\mathbb{R}^3$. We now notice that $\mathbb{R}^3$ has been divided into two regions by $S$. For convenience, we denote the region below $S$ (the part including $z = -\infty$ in a Cartesian coordinate system) as $V_1$ and assume that the vector fields in that region are given by $\mathbf{D}_1$ and $\mathbf{E}_1$. Similarly, let the region above $S$ (the part including $z = \infty$) be $V_2$ with the corresponding vector fields $\mathbf{D}_2$ and $\mathbf{E}_2$. Also note that $V_1 \bigcup V_2 = \mathbb{R}^3$. Accordingly, assume that

the functions $\epsilon(\mathbf{R})$ and $\Phi(\mathbf{R})$ are defined as

$$\epsilon(\mathbf{R}) = \begin{cases} \epsilon_1 & \text{for} \quad \mathbf{R} \in V_1 \\ \epsilon_2 & \text{for} \quad \mathbf{R} \in V_2 \end{cases} \tag{2.20}$$

$$\Phi(\mathbf{R}) = \begin{cases} \Phi_1(\mathbf{R}) & \text{for} \quad \mathbf{R} \in V_1 \\ \Phi_2(\mathbf{R}) & \text{for} \quad \mathbf{R} \in V_2 \end{cases} \tag{2.21}$$

The expression for BCs can be explicitly deduced from the integral form of Maxwell's equations.

## 2.2.1 Normal component of displacement field

First considering $\mathbf{D}$, let us integrate both sides of Eq. (2.1) over a small closed domain $V$, which contains part of the boundary $S$, as shown in Fig. 2.1, giving

$$\int_V \nabla \cdot \mathbf{D}(\mathbf{R}) \, dV = \int_V 4\pi\rho(\mathbf{R}) \, dV \tag{2.22}$$
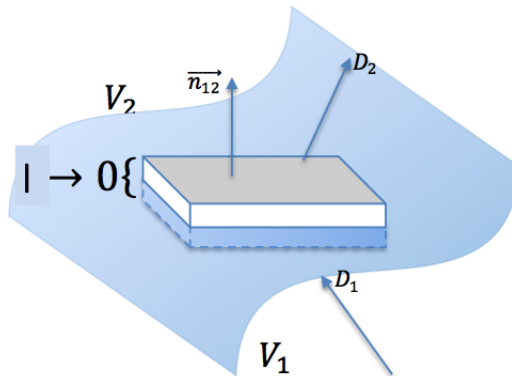


Figure 2.1: Wafer-thin Gaussian pillbox

In general case, we suppose the domain $V$ is a wafer-thin Gaussian pillbox, extending just barely over the edge along $S$, the surface between two media, in each direction. Let us denote

17

by $\ell$ the thickness of the pillbox and assume that $\ell$ goes to zero. Also we denote $\mathbf{n}_{21}$ as the unit normal vector on $\mathbf{S}$ that goes from region $V_2$ to $V_1$, and $\mathbf{n}_{12}$ as the unit normal vector that goes from $V_1$ to $V_2$. By the Gauss' divergence theorem we have that the LHS of Eq. (2.22) becomes

$$
\begin{aligned}
LHS &= \oint_{\partial V} \mathbf{D} \cdot d\mathbf{S} \\
&= \oint_{\partial V} \mathbf{D} \cdot \hat{\mathbf{n}} \, dS \\
&= \int_A (\mathbf{D}_2 \cdot \mathbf{n}_{12} - \mathbf{D}_1 \cdot \mathbf{n}_{12}) \, dA
\end{aligned}
\tag{2.23}
$$

where $\partial V$ is the closed boundary of the pillbox $V$ with the outer unit normal vector $\hat{\mathbf{n}}$, and $A$ is the area of its upper and lower lids. Note that the sides of the pillbox contribute nothing to the integral over the closed surface $\partial V$, nor does any volume charge density in the regions $V_1$ or $V_2$, as $\ell$ goes to zero.

Next, we assume that there may exist charges that are localized on the boundary $S$, which are characterized by the surface charge density $\sigma$, that is, the number of unit charges per unit area. Then, the RHS of Eq. (2.22) gives the total charge contained in the pillbox $V$ as

$$
RHS = \int_A 4\pi\sigma \, dA.
\tag{2.24}
$$

Combining Eq. (2.24) and Eq. (2.23), the BC becomes,

$$
\int_A (\mathbf{D}_2 \cdot \mathbf{n}_{12} - \mathbf{D}_1 \cdot \mathbf{n}_{12} - 4\pi\sigma) \, dA = 0
\tag{2.25}
$$

Note that all terms in the above integrand may depend on the position $\mathbf{R}$ but, since the area $A$ is arbitrary, we can deduce local relation from Eq. (2.25) as

$$
(\mathbf{D}_2 - \mathbf{D}_1) \cdot \mathbf{n}_{12} = 4\pi\sigma \quad \text{for all} \quad \mathbf{R} \in S,
\tag{2.26}
$$

which expresses the well-known jump condition for the normal component of the displacement field at the boundary $S$ containing the surface charge of density $\sigma$.

Then, by Eq. (2.9) and the constitutive relation Eq. (2.18) used in each of the regions $V_1$ and $V_2$, we get the required jump BCs for electric potential $\Phi$:

$$
-\epsilon_2 \mathbf{n}_{12} \cdot \nabla\Phi_2 + \epsilon_1 \mathbf{n}_{12} \cdot \nabla\Phi_1 = 4\pi\sigma \quad \text{for all} \quad \mathbf{R} \in S.
\tag{2.27}
$$

It is instructive to give specific details of the above derivation for a layered structure, where the surface $S$ may be assumed to be the plane $z = 0$ in a 3D Cartesian coordinate system with the coordinates $\mathbf{R} = (x, y, z)$. Then, the surface density of charge $\sigma(x, y)$ on $S$ may be described by defining the volume density of charge as

$$\rho(x, y, z) = \sigma(x, y)\delta(z) \tag{2.28}$$

where $\delta(z)$ is the Dirac's delta function peaked at $z = 0$, expressing the physical nature of a sharp boundary between the regions $V_1$ and $V_2$. It can easily be verified that Eq. (2.28) satisfies the relation

$$
\begin{aligned}
\int \rho(x, y, z)\, dz &= \int \sigma(x, y)\delta(z)\, dz \\
&= \sigma(x, y) \int \delta(z)\, dz \\
&= \sigma(x, y), \tag{2.29}
\end{aligned}
$$

which is used in deriving Eq. (2.24).

Now, the unit normal vector at $S$ is given by $\mathbf{n}_{12} = \hat{\mathbf{k}}$, where $\hat{\mathbf{k}}$ is the unit vector in the positive direction of the $z$ axis. So, the LHS of Eq. (2.27) becomes

$$LHS = \epsilon_1 \left.\frac{\partial \Phi_1}{\partial z}\right|_{z=0} - \epsilon_2 \left.\frac{\partial \Phi_2}{\partial z}\right|_{z=0} \tag{2.30}$$

So finally, the BC for the special case when boundary $S$ is at $z = 0$ becomes:

$$\epsilon_1 \left.\frac{\partial \Phi_1}{\partial z}\right|_{z=0} - \epsilon_2 \left.\frac{\partial \Phi_2}{\partial z}\right|_{z=0} = 4\pi\sigma. \tag{2.31}$$

We note that $\sigma(x, y)$ in this expression is considered to be some sort of external charge sheet with atomic thickness. Hence, $\sigma(x, y)$ may as well be the surface charge density on a single layer of graphene placed in the plane $z = 0$.

### 2.2.2 Tangential components of electric field

We now consider $\mathbf{E}$ and integrate both sides of Eq. (2.8) over a thin, closed rectangular loop $C$ that crosses the boundary $S$ between the regions $V_1$ and $V_2$, as shown in Fig. 2.2, giving

$$\oint_C \mathbf{E} \cdot d\mathbf{l} = 0. \tag{2.32}$$

19
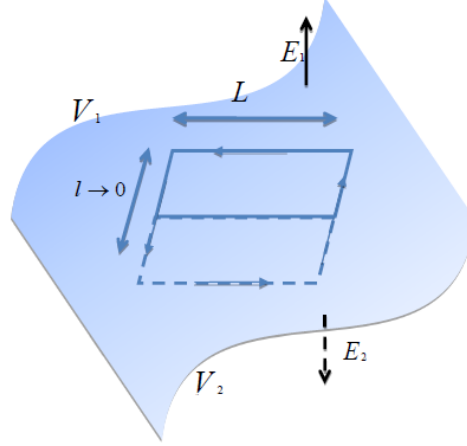
Figure 2.2: Thin Amperian loop straddling the surface

We suppose that $C$ is a thin "Amperian" loop straddling the surface $S$, which is traversed counterclockwise as the positive direction. In the integral (2.32) we assume that the width $\ell$ of the loop goes to zero, which means that the segments passing through $S$ give nothing to the integral.

So, now only the components of electric field $\mathbf{E}$ that are parallel to the surface $S$ remain to be integrated in Eq. (2.32) along the two oppositely directed line segments, $\mathbf{L}$ and $-\mathbf{L}$, giving

$$\int_{\mathbf{L}} \mathbf{E}_2 \cdot d\mathbf{l} + \int_{-\mathbf{L}} \mathbf{E}_1 \cdot d\mathbf{l} = 0, \tag{2.33}$$

where $\mathbf{E}_1$ and $\mathbf{E}_2$ are the values of the electric field in the regions $V_1$ and $V_2$, respectively. Since $\mathbf{L}$ is a segment of the curve $C$ that is parallel to the surface $S$, but is otherwise arbitrary, we can deduce a local relation

$$(\mathbf{E}_2 - \mathbf{E}_1) \cdot \mathbf{L} = 0 \Rightarrow \mathbf{E}_{2t} = \mathbf{E}_{1t} \quad \text{for all} \quad \mathbf{R} \in S, \tag{2.34}$$

where $\mathbf{E}_{2t}$ and $\mathbf{E}_{1t}$ are the tangential components of $\mathbf{E}_2$ and $\mathbf{E}_1$, respectively. This relation expresses the well-known continuity of the tangential component of the electric field along a dielectric boundary.

Then by Eq. (2.9) we may get the above condition in terms of the electric potential $\phi$. Specifically, if the surface $S$ is the plane $z = 0$ in 3D Cartesian coordinate system, we have

$$\frac{\partial \Phi_1}{\partial x} = \frac{\partial \Phi_2}{\partial x}, \quad \frac{\partial \Phi_1}{\partial y} = \frac{\partial \Phi_2}{\partial y}, \quad \text{for} \quad z = 0. \tag{2.35}$$

Finally, as regards the electric potential, $\Phi(\mathbf{R})$, Eq. (2.31) implies that the normal derivative of that potential has finite jump at a dielectric boundary, whereas Eq. (2.35) implies that the derivatives of the potential in the tangential directions are continuous. In addition to those conditions, it is a common assumption in the electrostatics that the electric potential is itself a continuous scalar function of the position $\mathbf{R}$. It is also common to assume that the value of the potential at a gate, which is represented as an ideal metallic electrode, is constant across the entire surface of the gate and takes a prescribed value. At infinitely remote points in a 3D space, the potential is assumed to also take a constant value, which is often set to be zero. All the above considerations now allow us to write the Poisson equation for the electric potential as a BVP in 3D.

## 2.3    Construction of the Poisson boundary value problem

So, we wish to solve the Poisson equation for the electric potential $\Phi(\mathbf{R})$ in a region $V$, which satisfies the Dirichlet BCs on its closed boundary $S$

$$\begin{cases} \nabla \cdot (\epsilon(\mathbf{R})\nabla\Phi(\mathbf{R})) & = -4\pi\rho(\mathbf{R}), \quad \text{for} \quad \mathbf{R} \in V, \\ \Phi(\mathbf{R}) & = \text{prescribed}, \quad \text{when} \quad \mathbf{R} \in S, \end{cases} \tag{2.36}$$

where $\mathbf{R} = (x, y, z)$ is the position vector and $\nabla = (\partial/\partial x, \partial/\partial y, \partial/\partial z)$ is the gradient vector in a 3D Cartesian coordinate system. In our applications to layered structures, the prescribed value of the potential on $S$ will be typically given by a constant value at the surface of a gate, or zero at points $\|\mathbf{R}\| \to \infty$. In the above, one notices that the source function of the Poisson equation is $-4\pi\rho(\mathbf{R})$, where $\rho(\mathbf{R})$ is the volume density of the external charges and $\epsilon$ is the relative dielectric constant, whose dependence on the position $\mathbf{R}$ reflects the variation in dielectric properties of various materials surrounding graphene. Note that our use of the so-called electrostatic Gaussian units gives rise to the factor $4\pi$ in the source function in Eq. (2.36). Now we get that Eq. (2.36) is a BVP, which is a second-order, nonhomogeneous PDE of the elliptic type. Instead of using separation of variables or other methods, the method of a GF is used in this thesis. This method has many advantages, e.g, it is particularly suitable to solve BVPs, especially when the BCs are fixed but the nonhomogeneous part varies.

We now follow the method described in section 1.2, which leads to the equation satisfied by GF on the same region $V$, Eq. (1.11), which satisfies a homogeneous Dirichlet BC, Eq. (1.15). While those two equations were written with $\mathbf{R}' = (x', y', z')$ being a variable and the source point in Eq. (1.11) being at $\rho(\mathbf{R})$, we reverse here the notation and invoke the Maxwell's symmetry of the GF, $G(\mathbf{R}, \mathbf{R}') = G(\mathbf{R}', \mathbf{R})$. Hence, we shall determine the GF $G(\mathbf{R}, \mathbf{R}')$ as a function

of $\mathbf{R} = (x, y, z)$ by solving an equation analogous to (2.36) where the charge density $\rho(\mathbf{R})$ is replaced by the density of a unit point charge centered at some fixed but arbitrarily positioned source point $\mathbf{R}' = (x', y', z')$, and imposing a homogeneous version of the BC in Eq. (2.36),

$$\begin{cases} \nabla \cdot (\epsilon(\mathbf{R})\nabla G(\mathbf{R}, \mathbf{R}')) = & -4\pi\delta(\mathbf{R} - \mathbf{R}'), \quad \text{for} \quad \mathbf{R} \in V, \\ \qquad\qquad G(\mathbf{R}, \mathbf{R}') = & 0, \qquad\qquad\quad \text{when} \quad \mathbf{R} \in S, \end{cases} \tag{2.37}$$

where $\delta(\mathbf{R} - \mathbf{R}')$ is a shorthand for $\delta(x - x')\delta(y - y')\delta(z - z')$, which is the Dirac's delta function in 3D.

Recall that the use of Green's second identity in section 1.2 gave Eq. (1.16), which expresses the solution of the Dirichlet BVP in Eq. (2.36) for the potential $\Phi(\mathbf{R})$ as a 3D integral involving arbitrary density of external charge $\rho(\mathbf{R})$ in the region $V$ plus a surface integral over the boundary $S$ of $V$ involving the prescribed value of the potential on the boundary,

$$\Phi(\mathbf{R}) = \int_V \rho(\mathbf{R}')G(\mathbf{R}, \mathbf{R}') \, d^3\mathbf{R}' - \frac{1}{4\pi} \oint_S \Phi(\mathbf{R}')\frac{\partial G(\mathbf{R}, \mathbf{R}')}{\partial n'} dA'. \tag{2.38}$$

The most difficult part for solving Eq. (2.37) is the $\mathbf{R}$–dependence of $\epsilon$. In the special case of an infinitely large homogeneous region $V$ with $\epsilon = \text{const.}$, the GF is easily obtained from Eq. (2.37) as

$$G(\mathbf{R}, \mathbf{R}') = \frac{1}{\epsilon} \frac{1}{\|\mathbf{R} - \mathbf{R}'\|} = \frac{1}{\epsilon\sqrt{(x - x')^2 + (y - y')^2 + (z - z')^2}}, \tag{2.39}$$

by using a 3D FT with respect to $\mathbf{R}$. An important finding here is that the GF of a translationally invariant system in 3D only depends on the difference of its variables, $G(\mathbf{R}, \mathbf{R}') = G(\mathbf{R} - \mathbf{R}')$. This means that the solution of the Poisson equation Eq. (2.36) given in Eq. (2.38) with $\Phi(\mathbf{R}) \to 0$ when $\|\mathbf{R}\| \to \infty$ is simply a 3D convolution of the arbitrary charge density with the GF,

$$\begin{aligned} \Phi(\mathbf{R}) &= \int G(\mathbf{R} - \mathbf{R}') \, \rho(\mathbf{R}') \, d^3\mathbf{R}' \\ &= \frac{1}{\epsilon} \int \frac{\rho(\mathbf{R}')}{\|\mathbf{R} - \mathbf{R}'\|} \, d^3\mathbf{R}'. \end{aligned} \tag{2.40}$$

Eq. (2.40) is also known as Coulomb law for the electrostatic potential due to an arbitrary distribution of charges, which may be directly obtained by solving the Poisson equation Eq. (2.36) by means of a 3D FT.

In a more general case when the function $\epsilon(\mathbf{R})$ is defined in piece-wise manner throughout a finite region $V$, there are various methods to solve for the GF in Eq. (2.37) – the image point

method, conformal mapping method, eigenfunction method, *etc*. [24, 25]. However, since we are interested exclusively in layered structures, the GF is obtained by exploiting a special property of the translational invariance of such structures in directions parallel to the, say, $(x, y)$ plane of a Cartesian coordinate system and taking advantage of a 2D FT with respect to $x$ and $y$. This will be described more in the next section.

## 2.4 Translational invariance and two-dimensional Fourier Transform

Considering a layered structure, we first assume that several dielectric layers are stacked into slabs with sharp boundaries between them, which are parallel to the $(x, y)$ plane in a 3D Cartesian coordinate system. Secondly assume that the dielectric properties of the material are constant throughout each layer, so that we can define a piece-wise constant dielectric function $\epsilon(z)$ on the $z$ axis. This means that translations of the entire structure in directions parallel to the $(x, y)$ plane do not change its dielectric properties. These assumptions have two advantages; one is that we can reduce a 3D PDE to an ODE by using 2DFT with respect to the $(x, y)$ plane, another is that we can solve that equation in a piece-wise manner along the $z$ axis.

In addition, the layered structure may generally extend over a finite interval along the $z$-axis with the endpoints at, say, $z_1$ and $z_2 > z_1$, where the electrostatic potential is considered to take prescribed values $\Phi(\mathbf{r}, z_1) = \phi_1(\mathbf{r})$ and $\Phi(\mathbf{r}, z_2) = \phi_2(\mathbf{r})$, which may be determined, e.g., placing structures with planar electrodes at the planes $z = z_1$ and $z = z_2$. Therefore we have a Dirichlet BVP for the Poisson equation with a formal solution for the electrostatic potential in the interval $z \in [z_1, z_2]$ given in Eq. (2.38) in terms of a Dirichlet-type GF, which vanish at $z = z_1$ and $z = z_2$ by construction. Now let's see how we can simplify the problem of determining such GF.

When the dielectric properties of the structure only vary along the $z$ axis, we can rewrite Eq. (2.37) as

$$\nabla \cdot (\epsilon(z)\nabla G(\mathbf{R}, \mathbf{R}')) = -4\pi\delta(\mathbf{R} - \mathbf{R}'). \tag{2.41}$$

It is convenient to write $\mathbf{R} = (\mathbf{r}, z)$ where $\mathbf{r} = (x, y)$ is a 2D position vector parallel to the $(x, y)$ plane. Looking on the right hand side of Eq. (2.41) the only dependence on the variable $\mathbf{r} = (x, y)$ comes from $\delta(x - x')\delta(y - y') = \delta(\mathbf{r} - \mathbf{r}')$. This suggests that the GF, which is the only function containing the variable $\mathbf{r} = (x, y)$ on the left side must also depend on the difference $\mathbf{r} - \mathbf{r}'$. Thus, the translational invariance in 2D requires that the GF must be of the form $G(\mathbf{R}, \mathbf{R}') = G(\mathbf{r} - \mathbf{r}'; z, z')$. This means that the expression for the potential in Eq. (2.38)

contains terms having the form of a 2D convolution in the $\mathbf{r}$ space,

$$
\begin{aligned}
\Phi(\mathbf{r}, z) \;=\; & \int_{z_1}^{z_2} dz' \int d^2\mathbf{r}'\, G(\mathbf{r} - \mathbf{r}'; z, z')\, \rho(\mathbf{r}', z') \\
& - \frac{1}{4\pi} \int d^2\mathbf{r}'\, \phi_2(\mathbf{r}')\, \frac{\partial}{\partial z'} G(\mathbf{r} - \mathbf{r}'; z, z') \bigg|_{z'=z_2} \\
& + \frac{1}{4\pi} \int d^2\mathbf{r}'\, \phi_1(\mathbf{r}')\, \frac{\partial}{\partial z'} G(\mathbf{r} - \mathbf{r}'; z, z') \bigg|_{z'=z_1}.
\end{aligned}
\tag{2.42}
$$

Now one can apply a 2DFT to $\Phi(\mathbf{r}, z)$, $G(\mathbf{r} - \mathbf{r}'; z, z')$ and $\rho(\mathbf{r}', z')$ with respect to $\mathbf{r} = (x, y)$ and introduce the corresponding vector $\mathbf{q} = (q_x, q_y)$. First express GF via its 2DFT, $\widetilde{G}(\mathbf{q}; z, z')$, as

$$
\begin{aligned}
G(\mathbf{r} - \mathbf{r}'; z, z') \;=\; & \int \frac{dq_x}{2\pi} \int \frac{dq_y}{2\pi}\, e^{iq_x(x-x')}\, e^{iq_y(y-y')}\, \widetilde{G}(q_x, q_y; z, z') \\
\;=\; & \int \frac{d^2\mathbf{q}}{(2\pi)^2}\, e^{i\mathbf{q}\cdot(\mathbf{r}-\mathbf{r}')}\, \widetilde{G}(\mathbf{q}; z, z').
\end{aligned}
\tag{2.43}
$$

By the same process as above, the potential may be expressed in terms of its 2DFT, $\widetilde{\Phi}(\mathbf{q}, z)$, as

$$
\Phi(\mathbf{r}, z) = \int \frac{d^2\mathbf{q}}{(2\pi)^2}\, e^{i\mathbf{q}\cdot\mathbf{r}}\, \widetilde{\Phi}(\mathbf{q}, z),
\tag{2.44}
$$

and the external charge density in terms of its 2DFT, $\widetilde{\rho}(\mathbf{q}, z)$, as

$$
\rho(\mathbf{r}, z) = \int \frac{d^2\mathbf{q}}{(2\pi)^2}\, e^{i\mathbf{q}\cdot\mathbf{r}}\, \widetilde{\rho}(\mathbf{q}, z).
\tag{2.45}
$$

One can apply the convolution theorem for the 2DFT with respect to $\mathbf{r}$ in Eq. (2.42) to obtain the 2DFT of the potential as

$$
\widetilde{\Phi}(\mathbf{q}, z) = \int_{z_1}^{z_2} dz'\, \widetilde{G}(\mathbf{q}; z, z')\, \widetilde{\rho}(\mathbf{q}, z') - \frac{1}{4\pi}\, \widetilde{\phi}_2(\mathbf{q})\, \frac{\partial}{\partial z'} \widetilde{G}(\mathbf{q}; z, z') \bigg|_{z'=z_2} + \frac{1}{4\pi}\, \widetilde{\phi}_1(\mathbf{q})\, \frac{\partial}{\partial z'} \widetilde{G}(\mathbf{q}; z, z') \bigg|_{z'=z_1}
\tag{2.46}
$$

where we denote the 2DFT of the external charge density by introducing the operator $\mathcal{F}$ as

$$
\widetilde{\rho}(\mathbf{q}, z) \equiv \mathcal{F}\{\rho(\mathbf{r}, z)\} = \int d^2\mathbf{r}\, e^{-i\mathbf{q}\cdot\mathbf{r}}\, \rho(\mathbf{r}, z),
\tag{2.47}
$$

24

and where $\widetilde{\phi}_{1,2}(\mathbf{q})$ are the 2DFT of the prescribed potential functions $\phi_{1,2}(\mathbf{r})$ at the boundary points $z_{1,2}$.

The form of the first term in Eq. (2.46) can be proved by substituting the GF from Eq. (2.43) and using the 2DFT of the external charge density $\widetilde{\rho}(\mathbf{q}, z)$ from (2.47) in the expression for the potential Eq. (2.42),

$$
\begin{aligned}
\Phi(\mathbf{r}, z) &= \int dz' \int d^2\mathbf{r}'\, G(\mathbf{r} - \mathbf{r}'; z, z')\, \rho(\mathbf{r}', z') &&(2.48) \\
&= \int d^2\mathbf{r}' \int dz' \int \frac{d^2\mathbf{q}}{(2\pi)^2}\, \mathrm{e}^{i\mathbf{q}\cdot(\mathbf{r}-\mathbf{r}')} \widetilde{G}(\mathbf{q}; z, z')\, \rho(\mathbf{r}', z') &&(2.49) \\
&= \int \frac{d^2\mathbf{q}}{(2\pi)^2} \mathrm{e}^{i\mathbf{q}\cdot\mathbf{r}} \int dz' \widetilde{G}(\mathbf{q}, z, z') \int d^2\mathbf{r}' \mathrm{e}^{-i\mathbf{q}\cdot\mathbf{r}'}\, \rho(\mathbf{r}', z') &&(2.50) \\
&= \int \frac{d^2\mathbf{q}}{(2\pi)^2} \mathrm{e}^{i\mathbf{q}\cdot\mathbf{r}} \int dz' \widetilde{G}(\mathbf{q}, z, z') \widetilde{\rho}(\mathbf{q}, z'). &&(2.51)
\end{aligned}
$$

Now, comparing the last step with Eq. (2.44) we obtain the first term in Eq. (2.46). The other two terms due to the Dirichlet BCs at the endpoints $z_{1,2}$ may be proved in the same manner.

It should be mentioned that, if either of the two endpoints of the layered structure is removed to infinity along the $z$-axis, $z_{1,2} \to \mp\infty$, the corresponding term(s) in Eqs. (2.42) and (2.46) should vanish on the account that Eq. (1.15) implies

$$
\frac{\partial}{\partial z'} G(\mathbf{r} - \mathbf{r}'; z, z')\Big|_{z'\to\pm\infty}
$$

for the Dirichlet type GF in a layered structure.

## 2.5   Differential equations for components of Green's function

Next, we label different dielectric layers by $j = 1, 2, 3\ldots$, and assume that the corresponding dielectric constants have values $\epsilon_j$. Thus, the electrical properties of the structure only vary in the direction of the $z$-axis. Accordingly, one can define a $z$-dependent dielectric function of the system of dielectric layers as $\epsilon(z) = \epsilon_j$ when $z \in I_j$, where $I_j$ is an interval on the $z$-axis occupied by the $j$th layer. Now we can also define the electric potential as a piece-wise function, $\Phi(\mathbf{R}) = \Phi_j(\mathbf{R})$ when $z \in I_j$, as well as the associated GF, $G(\mathbf{R}, \mathbf{R}') = G_j(\mathbf{R}, \mathbf{R}')$ when $z \in I_j$,

which then satisfy the following equations that follow from Eqs. (2.36) and (2.37),

$$\nabla^2 \Phi_j(\mathbf{R}) = \frac{-4\pi}{\epsilon_j} \rho(\mathbf{R}), \qquad \text{when} \quad z \in I_j \tag{2.52}$$

$$\nabla^2 G_j(\mathbf{R}, \mathbf{R}') = \frac{-4\pi}{\epsilon_j} \delta(\mathbf{R} - \mathbf{R}'), \qquad \text{when} \quad z \in I_j \tag{2.53}$$

for $j = 1, 2, 3 \ldots$. We see that the GF becomes easier to solve for in the piece-wise manner.

Now we want to find an ODE for the 2DFT of each GF, $G_j(\mathbf{R}, \mathbf{R}') = G_j(\mathbf{r} - \mathbf{r}'; z, z')$, as a function of $z$ by applying the 2DFT with respect to $\mathbf{r}$ in the equation for the GF (2.53). We can write and $\delta(\mathbf{R} - \mathbf{R}') = \delta(\mathbf{r} - \mathbf{r}') \delta(z - z')$ and set $\mathbf{r}' = \mathbf{0}$ because the system is translationally invariant in 2D. Then using Eq. (2.43) on the left hand side of (2.53) we have

$$\mathcal{F}\left\{ \nabla^2 G_j(\mathbf{r}; z, z') \right\} = \mathcal{F}\left\{ \left( \frac{\partial^2}{\partial x^2} + \frac{\partial^2}{\partial y^2} + \frac{\partial^2}{\partial z^2} \right) G_j(\mathbf{r}; z, z') \right\}, \tag{2.54}$$

$$\mathcal{F}\left\{ \frac{\partial^2}{\partial x^2} G_j(\mathbf{r}; z, z') \right\} = -q_x^2 \widetilde{G}_j(\mathbf{q}; z, z'), \tag{2.55}$$

$$\mathcal{F}\left\{ \frac{\partial^2}{\partial y^2} G_j(\mathbf{r}; z, z') \right\} = -q_y^2 \widetilde{G}_j(\mathbf{q}; z, z'), \tag{2.56}$$

$$\text{so} \quad \mathcal{F}\left\{ \nabla^2 G_j(\mathbf{r}; z, z') \right\} = \left( -q_x^2 - q_y^2 + \frac{\partial^2}{\partial z^2} \right) \widetilde{G}_j(\mathbf{q}; z, z'). \tag{2.57}$$

On the right hand side of (2.53) we use the result $\mathcal{F}\left\{ \delta(\mathbf{r} - \mathbf{r}') \right\} = 1$, which gives

$$\frac{\partial^2}{\partial z^2} \widetilde{G}_j(\mathbf{q}; z, z') - q^2 \widetilde{G}_j(\mathbf{q}; z, z') = -\frac{4\pi}{\epsilon_j} \delta(z - z'), \tag{2.58}$$

where $q = \|\mathbf{q}\| = \sqrt{q_x^2 + q_y^2}$. Thus, the former 3D PDE (2.37) becomes a system of second-order ODEs for the FT of the GF (FTGF) components $\widetilde{G}_j(\mathbf{q}; z, z')$ for $j = 1, 2, 3 \ldots$, where $q$ and $z'$ are parameters.

To be specific, we now consider a three-layer structure as in Refs. [7, 8, 26], with dielectric layers occupying the intervals along the $z$ axis defined by $I_1 = (-\infty, 0]$, $I_2 = [0, h]$ and $I_3 = [h, \infty)$, which are characterized by the relative dielectric constants $\epsilon_1$, $\epsilon_2$ and $\epsilon_3$, respectively. Thus, the total FTGF may be expressed in a piece-wise manner by solving just three differential equations in Eq. (2.58),

$$\widetilde{G}(\mathbf{q}; z, z') = \begin{cases} \widetilde{G}_1(\mathbf{q}; z, z'), & z \in I_1, \\ \widetilde{G}_2(\mathbf{q}; z, z'), & z \in I_2, \\ \widetilde{G}_3(\mathbf{q}; z, z'), & z \in I_3. \end{cases} \tag{2.59}$$
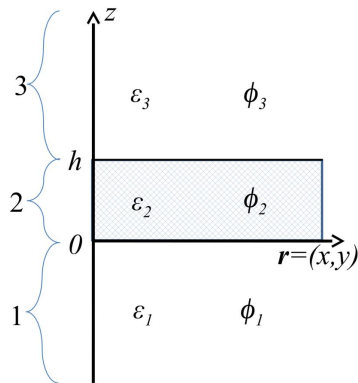
Figure 2.3: Schematic diagram showing three regions with a layer of dielectric (or metal) occupying the interval $0 \leq z \leq h$, and surrounded by two semi-infinite regions of dielectrics.

However, in the process of solving Eq. (2.58) the position of the source point $z'$ in the delta function on the right-hand sides of those equations is also important to be specified, because it will affect the inhomogeneous part of Eq. (2.58). So it is convenient to introduce a second index, $k$, in the above FTGF, which thus becomes a tensor function of the second rank, $\widetilde{G}_{jk}(z, z')$, where indices $j$ and $k$ correspond to the specific locations of the observation point, $z \in I_j$, and the source point, $z' \in I_k$, with $j, k = 1, 2, 3$. Now, the nine components of the FTGF are found as the solution of a set of ODEs written in the compact form as

$$\frac{\partial^2}{\partial z^2}\widetilde{G}_{jk}(\mathbf{q}; z, z') - q^2\widetilde{G}_{jk}(\mathbf{q}; z, z') = -\frac{4\pi}{\epsilon_j}\,\delta_{jk}\,\delta(z - z'), \quad \text{for} \quad z \in I_j \quad \text{and} \quad z' \in I_k, \quad (2.60)$$

where $\delta_{jk}$ is a Kronecker delta symbol with $j, k = 1, 2, 3$. Once we find all the components of the FTGF, we may write the solution of Eq. (2.52) by using the expression in Eq. (2.38), which is written in the in the 2DFT space in a piece-wise manner as

$$\widetilde{\Phi}_j(\mathbf{q}, z) = \sum_{k=1}^{3} \int_{I_k} \widetilde{G}_{jk}(\mathbf{q}; z, z')\widetilde{\rho}_k(\mathbf{q}, z')\,dz', \quad (2.61)$$

where $\widetilde{\rho}_k(\mathbf{q}, z)$ is the part of the external charge density that is defined over the interval $z \in I_k$, and where we have taken into account that the contributions from the endpoints in Eq. (2.46) vanish when the endpoints $z_{1,2} \to \mp\infty$.

We should also briefly discuss the Maxwell's symmetry property of a GF [24, 25], which can be expressed as $G(\mathbf{R}, \mathbf{R}') = G(\mathbf{R}', \mathbf{R})$. Notice that solutions of the equations for $\widetilde{G}_{jk}$ in Eq. (2.60) can only depend on the magnitude $q = \|\mathbf{q}\|$ of the vector $\mathbf{q}$, $\widetilde{G}_{jk}(\mathbf{q}; z, z') = \widetilde{G}_{jk}(q; z, z')$. Then Eq. (2.43) implies that $G(\mathbf{R}, \mathbf{R}') = G(\|\mathbf{r} - \mathbf{r}'\|; z, z')$, which means that the GF only depends on the magnitude of the vector $\mathbf{r} - \mathbf{r}'$ but not on its direction. This property means that the structure of dielectric layers is isotropic in the $(x, y)$ plane. Because we can write $G(\|\mathbf{r} - \mathbf{r}'\|; z, z') = G(\|\mathbf{r}' - \mathbf{r}\|; z, z')$, the Maxwell's symmetry property implies that we must also have $\widetilde{G}_{jk}(q; z, z') = \widetilde{G}_{kj}(q; z', z)$. This can easily be made intuitive by physical interpretation of GF: $G(q; z, z')$ is the response of the system at point $z$ to a unit source at point $z'$; if we interchange observation and source point we get the same value. This means that we only need to find six components of the tensor $\widetilde{G}_{jk}(q; z, z')$, particularly in this project we get $\widetilde{G}_{jk}(q; z, z')$ for $j \geq k$.

To simplify the notation, we shall drop the dependence on $q$ in the FTGF from now on.

## 2.6  Boundary and matching conditions

Now we discuss the BCs and the matching conditions (MCs) for the ordinary differential equations (ODEs) (2.60) for components of the FTGF. These conditions follow from the corresponding electrostatic conditions for the electric potential $\Phi(\mathbf{R})$ because the GF $G(\mathbf{R}, \mathbf{R}')$ is essentially an electric potential due to the point charge at $\mathbf{R}'$.

### 2.6.1  Boundary conditions at infinity

Referring to the BCs in Eq. (2.37), in which GF should vanish when $\|\mathbf{R}\| \to \infty$, the solutions of the equations (2.60) will satisfy the BCs for the full FTGF if we require

$$\begin{cases} \widetilde{G}_{1k}(-\infty, z') = 0 & \text{for} \quad k = 1, 2, 3 \\ \widetilde{G}_{3k}(\infty, z') = 0 & \text{for} \quad k = 1, 2, 3 \end{cases} \tag{2.62}$$

Note that these BCs only apply for the observation point which is placed at infinite region.

### 2.6.2  Continuity between intervals

The solutions of the equations (2.60) need to be matched at the boundary points $z = 0$ between the intervals $I_1/I_2$ and $z = h$ between the intervals $I_2/I_3$, by satisfying the standard properties of the electrostatic potential, which must be a continuous function, giving

$$\begin{cases} \widetilde{G}_{1k}(0, z') = \widetilde{G}_{2k}(0, z') & \text{for} \quad k = 1, 2, 3 \\ \widetilde{G}_{2k}(h, z') = \widetilde{G}_{3k}(h, z') & \text{for} \quad k = 1, 2, 3 \end{cases} \tag{2.63}$$

### 2.6.3  Electrostatic jump conditions

We assume that there are no free charges localized at the boundaries between different dielectrics, so that we may set $\sigma = 0$ in Eq. (2.26), which then implies that the normal component of the displacement field is continuous at those boundaries. Accordingly, setting $\sigma = 0$ in Eq. (2.27) gives a jump condition for the normal derivative of the electric potential at the boundaries, which must also be imposed on the GF $G(\mathbf{R}, \mathbf{R}')$. In our model the dielectric function $\epsilon(z)$ has finite jumps at the boundaries between the intervals $I_1/I_2$ and $I_2/I_3$, so we obtain from Eq. (2.31)

with $\sigma = 0$ the following electrostatic jump conditions for the normal derivatives of the FTGF at $z = 0$ and $z = h$,

$$\begin{cases} \epsilon_1 \left.\frac{\partial}{\partial z}\widetilde{G}_{1k}(z, z')\right|_{z=0} = \epsilon_2 \left.\frac{\partial}{\partial z}\widetilde{G}_{2k}(z, z')\right|_{z=0}, & \text{for} \quad k = 1, 2, 3 \\ \epsilon_2 \left.\frac{\partial}{\partial z}\widetilde{G}_{2k}(z, z')\right|_{z=h} = \epsilon_3 \left.\frac{\partial}{\partial z}\widetilde{G}_{3k}(z, z')\right|_{z=h}, & \text{for} \quad k = 1, 2, 3 \end{cases} \tag{2.64}$$

### 2.6.4 Continuity and jump conditions for diagonal Green's function

When both $z$ and $z'$ are in the interval $I_j$, one usually defines two components of the corresponding diagonal element of the FTGF as [25]

$$\widetilde{G}_{jj}(z, z') = \begin{cases} \widetilde{G}_{jj}^{<}(z, z'), & z \leq z', \\ \widetilde{G}_{jj}^{>}(z, z'), & z' \leq z, \end{cases} \tag{2.65}$$

which must satisfy the continuity and the jump conditions at $z = z'$,

$$\begin{cases} \widetilde{G}_{jj}^{<}(z', z') = \widetilde{G}_{jj}^{>}(z', z') & \text{for} \quad j = 1, 2, 3 \\ \left.\frac{\partial}{\partial z}\widetilde{G}_{jj}^{>}(z, z')\right|_{z=z'} - \left.\frac{\partial}{\partial z}\widetilde{G}_{jj}^{<}(z, z')\right|_{z=z'} = -\frac{4\pi}{\epsilon_j}, & \text{for} \quad j = 1, 2, 3 \end{cases} \tag{2.66}$$

Note that the condition in the second line of (2.64) can be derived from equation (2.60) with $k = j$, which has to be integrated over an infinitesimally small interval $z \in [z' - 0, z' + 0]$, where the continuity condition (2.66) and the shifting property of the delta function $\delta(z - z')$ are used [25].

## 2.7 Dyson-Schwinger equation for a structure with graphene

Graphene is a 2D material with the thickens of just one carbon atom (of the size $\sim$ Å), which may carry charge that is characterized by the surface density, $\sigma_g$, i.e., the number of unit charges per unit area of graphene. Hence, for the purpose of studying its interaction with the electrostatic field, one may assume that graphene is an infinitesimally thin layer that represents a boundary between two regions, which gives rise to a jump in the normal components of the electric displacement vectors on either side of graphene being equal to $4\pi\sigma_g$ according to Eq. (2.26).

To be specific, assume that a single layer of graphene is placed in the plane $z = z_g$ of a cartesian coordinate system with $\mathbf{R} = (\mathbf{r}, z)$, which is parallel to the boundaries between various

dielectrics in a layered structure. The surface charge density in graphene, $\sigma_g(\mathbf{r}, t)$, is generally a function of both 2D position vector $\mathbf{r} = (x, y)$ and time. As before, we may use the FT with respect to $\mathbf{r}$ and $t$ to obtain the graphene charge density in the FT space as $\widetilde{\sigma}_g(\mathbf{q}, \omega)$. Note that graphene in the space free of external charges and electric fields is neutral, so that $\sigma_g(\mathbf{r}, t) = 0$ in equilibrium. However, if there exists a time dependent electric potential around graphene with the FT $\widetilde{\Phi}(\mathbf{q}, z, \omega)$, then the charge carriers in graphene are polarized by the value of that potential in the plane of graphene, which is evaluated by setting $z = z_g$ in $\widetilde{\Phi}(\mathbf{q}, z, \omega)$. According to the linear response theory for graphene, there exists a constitutive relation between its surface charge density and the surface value of the electrostatic potential, which may be expressed in the FT space as

$$\widetilde{\sigma}_g(\mathbf{q}, \omega) = -e^2 \chi(\mathbf{q}, \omega) \widetilde{\Phi}(\mathbf{q}, z_g, \omega), \tag{2.67}$$

where $e$ is the electron charge and $\chi(\mathbf{q}, \omega)$ is the so-called polarization function of graphene that can be evaluated by using various microscopic models of charge carrier dynamics in graphene [22].

Let us now illustrate how the MCs for the electrostatic potential are modified in the presence of graphene. Assume that the region $z < z_g$ underneath graphene is characterized by a relative dielectric constant $\epsilon_1$ and the potential $\widetilde{\Phi}_1(\mathbf{q}, z, \omega)$, whereas the region $z > z_g$ above graphene is characterized by a relative dielectric constant $\epsilon_2$ and the potential $\widetilde{\Phi}_2(\mathbf{q}, z, \omega)$. Notice that, even when the dielectric constants are equal, $\epsilon_1 = \epsilon_2$, the expressions for the electrostatic potentials $\widetilde{\Phi}_1$ and $\widetilde{\Phi}_2$ may be different due to presence of finite charge density on graphene. One can write the condition for the jump in the normal derivative of the electrostatic potential at the position of graphene by setting $\sigma = \widetilde{\sigma}_g(\mathbf{q}, \omega)$ in Eq. (2.31) and using Eq. (2.67) to get

$$\epsilon_1 \frac{\partial \widetilde{\Phi}_1}{\partial z}(\mathbf{q}, z_g, \omega) - \epsilon_2 \frac{\partial \widetilde{\Phi}_2}{\partial z}(\mathbf{q}, z_g, \omega) = -4\pi e^2 \chi(\mathbf{q}, \omega) \widetilde{\Phi}(\mathbf{q}, z_g, \omega), \tag{2.68}$$

where $\widetilde{\Phi}(\mathbf{q}, z_g, \omega) \equiv \widetilde{\Phi}_1(\mathbf{q}, z_g, \omega) = \widetilde{\Phi}_2(\mathbf{q}, z_g, \omega)$ according to the continuity of the potential. Notice that we have evaluated expressions for the GF in the previous sections when graphene was absent by using a homogenous version of the Neumann-type condition at the boundaries between different dielectrics, which has the form of Eq. (2.68) with the right hand side set to zero. It is now remarkable that, in the presence of graphene, the MC in Eq. (2.68) becomes of the Robin type due to the linear constitutive relation in Eq. (2.67). While it would be possible to repeat calculations from the previous sections to include graphene by using MCs of the form in Eq. (2.68), the algebra would be much more tedious. Therefore, we shall show below how the fact that graphene is an infinitesimally thin layer may be efficiently used within the formalism of a DS equation to obtain the GF $G(\mathbf{R}, \mathbf{R}')$ for the Poisson equation of a layered structure *with* graphene, once the GF $G_0(\mathbf{R}, \mathbf{R}')$ for that same structure *without* graphene is known.

We first consider a more general case of the Poisson equation for a layered structure, where we assume that the 2D FT is performed with respect to the spatial variable $\mathbf{r}$. If $\check{\mathcal{L}}_z$ is a (linear) operator for this equation in the FT space, then the Poisson equation for the FT of the electrostatic potential $\widetilde{\Phi}(z)$ for an arbitrary external charge density $\widetilde{\rho}_{ext}(z)$ may be written generally as

$$\check{\mathcal{L}}_z \widetilde{\Phi}(z) = -4\pi \widetilde{\rho}_{ext}(z), \tag{2.69}$$

where we have dropped the dependence on $\mathbf{q}$ and emphasized that $\check{\mathcal{L}}_z$ only acts on the $z$ dependence of the potential. The associated FTGF for the above equation satisfies the equation of the general from

$$\check{\mathcal{L}}_z \widetilde{G}_0(z, z') = -4\pi \delta(z - z'). \tag{2.70}$$

We assume that the solution $\widetilde{G}_0(z, z')$ of the above "unperturbed" problem in Eq. (2.70) is known, so that the solution of Eq. (2.69) may be written as

$$\widetilde{\Phi}(z) = \int_{-\infty}^{\infty} \widetilde{G}_0(z, z'') \widetilde{\rho}_{ext}(z'') \, dz'', \tag{2.71}$$

where we have renamed the dummy variable of integration to $z''$.

Now, if there is a structural change in the layered structure that may be described by an additional, $z$-dependent term $\check{\mathcal{V}}(z)$ in the operator $\check{\mathcal{L}}_z$, we define a new operator $\check{\mathcal{O}}_z = \check{\mathcal{L}}_z + \check{\mathcal{V}}(z)$, so that the Poisson equation for such "perturbed" structure reads

$$\check{\mathcal{O}}_z \widetilde{\Phi}(z) = -4\pi \widetilde{\rho}_{ext}(z). \tag{2.72}$$

We want to determine the corresponding "perturbed" FTGF $\widetilde{G}(z, z')$, which must satisfy the equation

$$\check{\mathcal{O}}_z \widetilde{G}(z, z') = -4\pi \delta(z - z'). \tag{2.73}$$

We may express $\widetilde{G}(z, z')$ in terms of $\widetilde{G}_0(z, z')$ and $\check{\mathcal{V}}(z)$ by rewriting Eq. (2.73) as

$$\check{\mathcal{L}}_z \widetilde{G}(z, z') = -\check{\mathcal{V}}(z) \widetilde{G}(z, z') - 4\pi \delta(z - z') \tag{2.74}$$

$$= -4\pi \left[ \frac{1}{4\pi} \check{\mathcal{V}}(z) \widetilde{G}(z, z') + \delta(z - z') \right] \tag{2.75}$$

$$\equiv -4\pi \widetilde{\rho}_{ext}^{(*)}(z, z'), \tag{2.76}$$

where we have defined in the last step an effective external charge density $\widetilde{\rho}_{ext}^{(*)}(z, z')$ that only parametrically depends on $z'$. Thus, in view of Eq. (2.69), one may consider $\widetilde{G}(z, z')$ to be the

potential in the unperturbed structure that is induced by the external charge density $\widetilde{\rho}_{ext}^{(*)}(z, z')$, which may be expressed in the integral form by using Eq. (2.71) as

$$
\begin{aligned}
\widetilde{G}(z, z') &= \int_{-\infty}^{\infty} \widetilde{G}_0(z, z'')\widetilde{\rho}_{ext}^{(*)}(z'', z')\, dz'' \\
&= \int_{-\infty}^{\infty} \widetilde{G}_0(z, z'') \left[ \frac{1}{4\pi}\check{\mathcal{V}}(z'')\widetilde{G}(z'', z') + \delta(z'' - z') \right] dz'' \\
&= \widetilde{G}_0(z, z') + \frac{1}{4\pi}\int_{-\infty}^{\infty} \widetilde{G}_0(z, z'')\check{\mathcal{V}}(z'')\widetilde{G}(z'', z')\, dz''.
\end{aligned}
\tag{2.77}
$$

Thus, by equating the left hand side with the last line in Eq. (2.77), we obtain an integral equation for the unknown GF $\widetilde{G}(z, z')$ that includes known functions $\widetilde{G}_0(z, z')$ and $\check{\mathcal{V}}(z)$, which is called DS equation. This equation is widely used in Mathematical Physics in different contexts. For example, considering that the "perturbation" $\check{\mathcal{V}}(z)$ may be small in some sense, one can attempt solving the DS equation (2.77) in a recursive manner giving a systematic solution for $\widetilde{G}(z, z')$ in the form of a series in the "powers" of $\check{\mathcal{V}}(z)$,

$$
\begin{aligned}
\widetilde{G}(z, z') &= \widetilde{G}_0(z, z') + \frac{1}{4\pi}\int_{-\infty}^{\infty} \widetilde{G}_0(z, z'')\check{\mathcal{V}}(z'')\widetilde{G}_0(z'', z')\, dz'' \\
&+ \frac{1}{16\pi^2}\int_{-\infty}^{\infty}\int_{-\infty}^{\infty} \widetilde{G}_0(z, z'')\check{\mathcal{V}}(z'')\widetilde{G}_0(z, z''')\check{\mathcal{V}}(z''')\widetilde{G}_0(z''', z')\, dz'' dz''' + \cdots
\end{aligned}
\tag{2.78}
$$

which may be truncated after a desired number of terms to provide a perturbative solution for $\widetilde{G}(z, z')$. On the other hand, when the $z$ dependence of $\check{\mathcal{V}}(z)$ is sufficiently localized, then the integral over $z''$ in Eq. (2.77) may be evaluated in a local manner. We show next that, for graphene at the plane $z = z_g$, the perturbation $\check{\mathcal{V}}(z)$ is proportional to a Dirac's delta function $\delta(z - z_g)$, which allows an *exact* solution of the DS in Eq. (2.77).

Referring to the 2D constitutive relation in Eq. (2.67), we may express the volume charge density in frequency domain associated with the graphene layer at $z = z_g$ as

$$
\widetilde{\rho}_g(\mathbf{q}, z, \omega) = \widetilde{\sigma}_g(\mathbf{q}, \omega)\delta(z - z_g) = -e^2\chi(\mathbf{q}, \omega)\widetilde{\Phi}(\mathbf{q}, z, \omega)\,\delta(z - z_g),
\tag{2.79}
$$

where the presence of the factor $\delta(z - z_g)$ "sifts" only those values of the potential $\widetilde{\Phi}(\mathbf{q}, z, \omega)$ that are constrained to $z = z_g$. In the presence of both the graphene layer and an arbitrary external charge with density $\widetilde{\rho}_{ext}(z)$, the Poisson equation for the FT of the potential $\widetilde{\Phi}(z)$ reads

$$
\check{\mathcal{L}}_z\widetilde{\Phi}(z) = -4\pi\left[\widetilde{\rho}_g(z) + \widetilde{\rho}_{ext}(z)\right] = 4\pi e^2\chi\widetilde{\Phi}(z)\delta(z - z_g) - 4\pi\widetilde{\rho}_{ext}(z),
\tag{2.80}
$$

33

where we have dropped the variables $\mathbf{q}$ and $\omega$. The above equation may be rearranged so that the potential appears on the left hand side,

$$\left[\check{\mathcal{L}}_z - 4\pi e^2 \chi \delta(z - z_g)\right] \widetilde{\Phi}(z) = -4\pi \widetilde{\rho}_{ext}(z). \tag{2.81}$$

By referring to Eq. (2.72), we see that the operator that represents graphene in the perturbed system is given by $\check{\mathcal{V}}(z) = -4\pi e^2 \chi \delta(z - z_g)$. If we use this expression for $\check{\mathcal{V}}(z)$ in Eq. (2.77), we obtain

$$\widetilde{G}(z, z') = \widetilde{G}_0(z, z') - e^2 \chi \, \widetilde{G}_0(z, z_g) \widetilde{G}(z_g, z'), \tag{2.82}$$

which expresses the unknown function $\widetilde{G}(z, z')$ for an arbitrary $z$ in terms of its value at $z = z_g$. Then, by simply setting $z = z_g$ in Eq. (2.82) we obtain an algebraic equation for the value of $\widetilde{G}(z_g, z')$, which is easily solved to give

$$\widetilde{G}(z_g, z') = \frac{\widetilde{G}_0(z_g, z')}{1 + e^2 \chi \, \widetilde{G}_0(z_g, z_g)}, \tag{2.83}$$

which upon substitution in the right hand side of Eq. (2.82) gives the final expression for a (nonperturbative) solution of the DS in Eq. (2.77) in the presence of a graphene layer at the $z = z_g$ plane as

$$\widetilde{G}(z, z') = \widetilde{G}_0(z, z') - \frac{e^2 \chi \, \widetilde{G}_0(z, z_g) \, \widetilde{G}_0(z_g, z')}{1 + e^2 \chi \widetilde{G}_0(z_g, z_g)}. \tag{2.84}$$

## 2.8 Conclusion

We have outlined in this chapter a detailed derivation of the Poisson equation for the electrostatic potential starting from Maxwell's equation in the quasi-static regime. We argued that the associated equation for the GF must satisfy homogeneous Dirichlet BCs at the closed boundary of a finite region, and may be solved in a piece-wise manner when the dielectric properties exhibit jump-like discontinuities at the boundaries between adjacent regions with fixed dielectric constants. We also argued that the GF must satisfy the same type of MCs at those boundaries as the electrostatic potential. Taking advantage of the translational invariance in a plane for a layered structure, we have converted the PDEs for the potential and the GF into ODEs for the corresponding 2D FTs of those quantities. Moreover, we showed that, depending on the location of the source point and the observation point, the FTGF becomes a tensor. Finally, we have shown that, owing to the the zero-thickness of a graphene sheet in layered structure of dielectrics, one may readily express the FTGF for that structure in terms of the FTGF of the same structure without graphene and the polarization function of graphene.

# Chapter 3

# Results for Green's function for two and three layers of dielectrics

In this Chapter we present detailed derivation of the full expression for the FTGF in the cases of two and three dielectric layers. We use the first, simpler example to illustrate the use of a particular solution of the differential equations for the diagonal elements of the FTGF and make comment on the method of images. In the case of three regions, we present a full derivation of the FTGF by the method of undetermined coefficients, which are fixed by the full set of boundary and matching conditions from the previous chapter.

## 3.1 Particular solution for diagonal Green's function

When both $z$ and $z'$ are in the same interval $I_j$, we set $k = j$ in Eq. (2.60) and obtain non-homogeneous differential equations for the diagonal elements of the FTGF, given by

$$\frac{\partial^2}{\partial z^2}\widetilde{G}_{jj}(\mathbf{q}; z, z') - q^2\widetilde{G}_{jj}(\mathbf{q}; z, z') = -\frac{4\pi}{\epsilon_j}\delta(z - z').\tag{3.1}$$

Recall that an expression for the GF in an *infinite* region with the relative dielectric constant $\epsilon_j$ is given in Eq. (2.39) as the Coulomb potential, which we rewrite here as $G_{jj}^{(\mathrm{inf})}(\mathbf{R}, \mathbf{R}') = 1/\left(\epsilon_j\|\mathbf{R} - \mathbf{R}'\|\right)$. Referring to Eq. (2.43), we may perform an inverse 2DFT of this function to obtain

$$\widetilde{G}_{jj}^{(\mathrm{inf})}(\mathbf{q}; z, z') = \frac{2\pi}{\epsilon_j q}\mathrm{e}^{-q|z-z'|},\tag{3.2}$$

which is easily shown to satisfy Eq. (3.1) for all $z, z' \in \mathbb{R}^3$. Hence, we may use the expression in Eq. (3.2) as a particular solution of the non-homogeneous differential equations (3.1) for $j = 1, 2, 3, \ldots$ and write the components of the FTGF as

$$\widetilde{G}_{jk}(\mathbf{q}; z, z') = \delta_{jk}\, \widetilde{G}_{jj}^{(\mathrm{inf})}(\mathbf{q}; z, z') + \widetilde{G}_{jk}^{(\mathrm{hom})}(\mathbf{q}; z, z'), \tag{3.3}$$

where $\widetilde{G}_{jk}^{(\mathrm{hom})}(\mathbf{q}; z, z')$ are the general solutions of the system of homogeneous differential equations, which follow from Eq. (2.60) as

$$\frac{\partial^2}{\partial z^2}\widetilde{G}_{jk}^{(\mathrm{hom})}(\mathbf{q}; z, z') - q^2\widetilde{G}_{jk}^{(\mathrm{hom})}(\mathbf{q}; z, z') = 0, \quad \text{for} \quad z \in I_j \quad \text{and} \quad z' \in I_k. \tag{3.4}$$

In order to solve this system for $\widetilde{G}_{jk}^{(\mathrm{hom})}(\mathbf{q}; z, z')$ we still need all the MCs at the boundaries between regions with different dielectric constants, but the conditions given in Eq. (2.66) for the diagonal elements of the FTGF are now obsolete, thus reducing the algebraic effort in solving the problem.

## 3.2 Results for the components of Green's function in two regions

In order to illustrate this approach, let us consider a simple problem of two semi-infinite regions with the relative dielectric constants $\epsilon_1$ and $\epsilon_2$, occupying the intervals $I_1 = (-\infty, 0]$ and $I_2 = [0, \infty)$, respectively. To simplify the notation, we shall drop the dependence on $\mathbf{q}$ in the FTGF $\widetilde{G}_{jk}^{(\mathrm{hom})}(\mathbf{q}; z, z')$ from now on.

### 3.2.1 Source point in $I_1$ ($k = 1$)

By using Eqs. (3.2) and (3.3) and assuming that in Eq. (3.4) both $z$ and $z'$ are in the interval $I_1 = (-\infty, 0]$, we can write the FTGF component $\widetilde{G}_{11}(z, z')$ in the form

$$\widetilde{G}_{11}(z, z') = \frac{2\pi}{\epsilon_1 q}\mathrm{e}^{-q|z-z'|} + A\,\mathrm{e}^{qz}, \tag{3.5}$$

where the term containing unknown constant $A$ is the general solution of the homogeneous differential equation Eq. (3.4) with $k = j = 1$, which remains finite when $z \to -\infty$. Similarly,

referring to Eq. (3.3) with $k \neq j$, the FTGF component $\widetilde{G}_{21}(z, z')$ is assumed to only contain the general solution of Eq. (3.4) with $k = 1, j = 2$ that remains finite when $z \to \infty$, given by

$$\widetilde{G}_{21}(z, z') = B\, e^{-qz}. \tag{3.6}$$

The constants $A$ and $B$ are found by applying the continuity and the jump conditions in Eqs. (2.63) and (2.64) at $z = 0$. In applying the condition (2.63), it is worthwhile keeping in mind that the first term in Eq. (3.5), that is, the particular solution in Eq. (3.2) is a continuous function of $z$. On the other hand, in applying the condition (2.64) at $z = 0$, it is worthwhile keeping in mind that $|z - z'| = z - z'$ when $z' < z \to 0$. So, we obtain from Eqs. (2.63) and (2.64) at $z = 0$ for $k = 1$

$$\frac{2\pi}{\epsilon_1 q} e^{qz'} + A = B, \tag{3.7}$$

$$\epsilon_1 \left( -\frac{2\pi}{\epsilon_1 q} e^{qz'} + A \right) = -\epsilon_2 B, \tag{3.8}$$

giving the following expressions for the FTGF components

$$\widetilde{G}_{11}(z, z') = \frac{2\pi}{\epsilon_1 q} \left[ e^{-q|z-z'|} + \frac{\epsilon_1 - \epsilon_2}{\epsilon_1 + \epsilon_2} e^{q(z+z')} \right], \tag{3.9}$$

$$\widetilde{G}_{21}(z, z') = \frac{4\pi}{(\epsilon_1 + \epsilon_2) q} e^{-q(z-z')}. \tag{3.10}$$

### 3.2.2 Source point in $I_2$ $(k = 2)$

In analogy with the procedure above, we may assume that the FTGF components for $z' \in I_2$ have the form

$$\widetilde{G}_{12}(z, z') = C\, e^{qz}, \tag{3.11}$$

$$\widetilde{G}_{22}(z, z') = \frac{2\pi}{\epsilon_2 q} e^{-q|z-z'|} + D\, e^{-qz}, \tag{3.12}$$

where the unknown constants $C$ and $D$ are to be determined from the conditions in Eqs. (2.63) and (2.64) at $z = 0$ for $k = 2$. Since now we have $|z - z'| = -z + z'$ when $z' > z \to 0$, we obtain two equations for $C$ and $D$,

$$C = \frac{2\pi}{\epsilon_2 q} e^{-qz'} + D, \tag{3.13}$$

$$\epsilon_1 C = \epsilon_2 \left( \frac{2\pi}{\epsilon_2 q} e^{qz'} - D \right), \tag{3.14}$$

37

giving the final expressions for the FTGF components

$$\widetilde{G}_{12}(z, z') = \frac{4\pi}{(\epsilon_1 + \epsilon_2)q}e^{q(z-z')}, \tag{3.15}$$

$$\widetilde{G}_{22}(z, z') = \frac{2\pi}{\epsilon_2 q}\left[e^{-q|z-z'|} + \frac{\epsilon_2 - \epsilon_1}{\epsilon_1 + \epsilon_2}e^{-q(z+z')}\right], \tag{3.16}$$

as expected.

### 3.2.3 Method of images

It is interesting to comment on the above results for the GF for two semi-infinite regions. For example, consider the case when the source point is in $I_1$. Performing an inverse 2DFT of the FTGF components in Eq. (3.10) we find the corresponding GF components in configuration space as

$$G_{11}(\mathbf{R}, \mathbf{R}') = \frac{1}{\epsilon_1}\frac{1}{\sqrt{(x-x')^2 + (y-y')^2 + (z-z')^2}} \tag{3.17}$$

$$+ \frac{\epsilon_1 - \epsilon_2}{\epsilon_1(\epsilon_1 + \epsilon_2)}\frac{1}{\sqrt{(x-x')^2 + (y-y')^2 + (z+z')^2}}, \tag{3.18}$$

$$G_{21}(\mathbf{R}, \mathbf{R}') = \frac{2}{(\epsilon_1 + \epsilon_2)}\frac{1}{\sqrt{(x-x')^2 + (y-y')^2 + (z-z')^2}}. \tag{3.19}$$

We notice that these GF components could be obtained by using the method of images [25] for the planar boundary $z = 0$ between the two regions with dielectric constants $\epsilon_1$ and $\epsilon_2$ for $z < 0$ and $z > 0$, respectively. Namely, if we define the source point $\mathbf{R}' = (x', y', z')$ to be in the region $I_1$ with $z' < 0$ and its image through the boundary with the position $\mathbf{R}^* = (x', y', -z')$ to be another source point in the region $I_2$, then we could assume the GF components to be given by

$$G_{11}(\mathbf{R}, \mathbf{R}') = \frac{1}{\epsilon_1}\frac{1}{\|\mathbf{R} - \mathbf{R}'\|} + \frac{\alpha}{\|\mathbf{R} - \mathbf{R}^*\|}, \tag{3.20}$$

$$G_{21}(\mathbf{R}, \mathbf{R}') = \frac{\beta}{\|\mathbf{R} - \mathbf{R}'\|}. \tag{3.21}$$

Here, the unknown constants $\alpha$ and $\beta$ are to be found by imposing the configuration space version of the BCs in Eqs. (2.63) and (2.64) at $z = 0$,

$$G_{11}(\mathbf{R}, \mathbf{R}')|_{z=0} = G_{21}(\mathbf{R}, \mathbf{R}')|_{z=0}, \tag{3.22}$$

$$\epsilon_1 \left.\frac{\partial}{\partial z}G_{11}(\mathbf{R}, \mathbf{R}')\right|_{z=0} = \epsilon_2 \left.\frac{\partial}{\partial z}G_{21}(\mathbf{R}, \mathbf{R}')\right|_{z=0}, \tag{3.23}$$

giving $\alpha = (\epsilon_1 - \epsilon_2)/[\epsilon_1(\epsilon_1 + \epsilon_2)]$ and $\beta = 2/(\epsilon_1 + \epsilon_2)$, which reproduce the result obtained in Eq. (3.19). The image method can be similarly used to find the GF components when the source point is in $I_2$ and its image in the region $I_1$.

## 3.3 Results for the components of Green's function in three regions

We now consider a three-layer structure as in Refs. [7, 8, 26], with dielectric layers occupying the intervals along the $z$ axis defined by $I_1 = (-\infty, 0]$, $I_2 = [0, h]$ and $I_3 = [h, \infty)$, which are characterized by the relative dielectric constants $\epsilon_1$, $\epsilon_2$ and $\epsilon_3$, respectively, as shown in Fig. 2.3. We obtain here expressions for the six components of the FTGF $\widetilde{G}_{jk}(q; z, z')$ with $j \geq k$ by considering different positions of the source point. Unlike the previous case of two regions, we do not use here a particular solution for the diagonal components of the FTGF but rather exploit the conditions given in Eq. (2.66).

### 3.3.1 Source point in $I_1$ ($k = 1$)

By assuming that in Eq. (2.60) both $z$ and $z'$ are in the interval $I_1 = (-\infty, 0]$ but $z \neq z'$, we obtain two homogeneous differential equations for each component for the diagonal element $\widetilde{G}_{11}(z, z')$ in Eq. (2.65), which have the general solutions

$$\widetilde{G}_{11}^<(z, z') = A\,e^{qz}, \tag{3.24}$$
$$\widetilde{G}_{11}^>(z, z') = B\,e^{qz} + C\,e^{-qz}, \tag{3.25}$$

where $A$, $B$ and $C$ are some constants. In order to satisfy the BC in Eq. (2.62) that the FT GF should converge when $z \to -\infty$, a term with $e^{-qz}$ in $\widetilde{G}_{11}^<(z, z')$ has been dropped since it becomes indefinitely large when $z \to -\infty$ .

   Similarly, the homogeneous differential equations for $\widetilde{G}_{21}(z, z')$ and $\widetilde{G}_{31}(z, z')$ in Eq. (2.60) have the general solutions

$$\widetilde{G}_{21}(z, z') = D\,e^{qz} + E\,e^{-qz}, \tag{3.26}$$
$$\widetilde{G}_{31}(z, z') = F\,e^{-qz}, \tag{3.27}$$

where we have dropped a term with $e^{qz}$ in $\widetilde{G}_{31}(z, z')$ which becomes indefinitely large when $z \to \infty$ in order to satisfy the BC in Eq. (2.63). Now, the six constants $A$, $B$, $C$, $D$, $E$ and

$F$ (which can depend on $q$ and $z'$) are determined by imposing the six BCs which follow from Eqs. (2.63), (2.64) and (2.66) for $k = 1$,

$$\widetilde{G}_{11}^{<}(z', z') = \widetilde{G}_{11}^{>}(z', z'), \tag{3.28}$$

$$\frac{\partial}{\partial z}\widetilde{G}_{11}^{>}(z, z')\Big|_{z=z'} - \frac{\partial}{\partial z}\widetilde{G}_{11}^{<}(z, z')\Big|_{z=z'} = -\frac{4\pi}{\epsilon_1}, \tag{3.29}$$

$$\widetilde{G}_{11}(0, z') = \widetilde{G}_{21}(0, z'), \tag{3.30}$$

$$\widetilde{G}_{21}(h, z') = \widetilde{G}_{31}(h, z'), \tag{3.31}$$

$$\epsilon_1 \frac{\partial}{\partial z}\widetilde{G}_{11}(z, z')\Big|_{z=0} = \epsilon_2 \frac{\partial}{\partial z}\widetilde{G}_{21}(z, z')\Big|_{z=0}, \tag{3.32}$$

$$\epsilon_2 \frac{\partial}{\partial z}\widetilde{G}_{21}(z, z')\Big|_{z=h} = \epsilon_3 \frac{\partial}{\partial z}\widetilde{G}_{31}(z, z')\Big|_{z=h}. \tag{3.33}$$

Substituting Eqs. (3.24), (3.25), (3.26), (3.27) into the above conditions gives a non-homogeneous system of six algebraic equations for $A$, $B$, $C$, $D$, $E$ and $F$,

$$B + C = D + E, \tag{3.34}$$

$$D\,\mathrm{e}^{qh} + E\,\mathrm{e}^{-qh} = F\,\mathrm{e}^{-qh}, \tag{3.35}$$

$$\epsilon_1(B - C) = \epsilon_2(D - E), \tag{3.36}$$

$$\epsilon_2\left(D\,\mathrm{e}^{qh} - E\,\mathrm{e}^{-qh}\right) = -\epsilon_3\,F\,\mathrm{e}^{-qh}, \tag{3.37}$$

$$A\,\mathrm{e}^{qz'} = B\,\mathrm{e}^{qz'} + C\,\mathrm{e}^{-qz'}, \tag{3.38}$$

$$B\,\mathrm{e}^{qz'} - C\,\mathrm{e}^{-qz'} - A\,\mathrm{e}^{qz'} = -\frac{4\pi}{q\epsilon_1}. \tag{3.39}$$

The final expressions for $\widetilde{G}_{11}(z, z')$, $\widetilde{G}_{21}(z, z')$ and $\widetilde{G}_{31}(z, z')$ can be written in a compact form if we define auxiliary parameters as

$$\lambda_{\mathrm{b}} = \frac{\epsilon_1 - \epsilon_2}{\epsilon_1 + \epsilon_2}, \tag{3.40}$$

$$\lambda_{\mathrm{t}} = \frac{\epsilon_3 - \epsilon_2}{\epsilon_3 + \epsilon_2}, \tag{3.41}$$

$$\bar{\epsilon}_{12} = \frac{\epsilon_1 + \epsilon_2}{2}, \tag{3.42}$$

$$\bar{\epsilon}_{23} = \frac{\epsilon_3 + \epsilon_2}{2}, \tag{3.43}$$

$$\Delta = \mathrm{e}^{-2qh}. \tag{3.44}$$

The final solution is

40

$$\widetilde{G}_{11} = \frac{2\pi}{q\epsilon_1} \left[ e^{-q|z-z'|} + \frac{\lambda_b - \lambda_t\Delta}{1 - \lambda_b\lambda_t\Delta} e^{q(z+z')} \right], \tag{3.45}$$

$$\widetilde{G}_{21} = \frac{2\pi}{q\bar{\epsilon}_{12}} \frac{e^{-qz} - \lambda_t\Delta e^{qz}}{1 - \lambda_b\lambda_t\Delta} e^{qz'}, \tag{3.46}$$

$$\widetilde{G}_{31} = \frac{2\pi\epsilon_2}{q\bar{\epsilon}_{12}\bar{\epsilon}_{23}} \frac{e^{q(z'-z)}}{1 - \lambda_b\lambda_t\Delta}. \tag{3.47}$$

### 3.3.2 Source point in $I_2$ $(k = 2)$

As in the process in the previous subsection, first the homogeneous differential equations for $\widetilde{G}_{12}(z, z')$ and $\widetilde{G}_{32}(z, z')$ in Eq. (2.60) have the general solutions

$$\widetilde{G}_{12}(z, z') = A\,e^{qz}, \tag{3.48}$$

$$\widetilde{G}_{32}(z, z') = F\,e^{-qz}, \tag{3.49}$$

where we have dropped a term with $e^{-qz}$ in $\widetilde{G}_{12}(z, z')$ which becomes indefinitely large when $z \to -\infty$ and a term with $e^{qz}$ in $\widetilde{G}_{32}(z, z')$ which becomes indefinitely large when $z \to \infty$ to satisfy the BCs in Eq. (2.62). By assuming that in Eq. (2.60) both $z$ and $z'$ are in the interval $I_2 = [0, h]$ but $z \neq z'$, we obtain two homogeneous differential equations for each component for the diagonal element $\widetilde{G}_{22}(z, z')$ in Eq. (2.65), which have the general solutions

$$\widetilde{G}_{22}^<(z, z') = B\,e^{qz} + C\,e^{-qz}, \tag{3.50}$$

$$\widetilde{G}_{22}^>(z, z') = D\,e^{qz} + E\,e^{-qz}. \tag{3.51}$$

Now, the six constants $A$, $B$, $C$, $D$, $E$ and $F$ can be determined by imposing the six MCs which follow from Eqs. (2.63), (2.64) and (2.66) for $k = 2$. We get the system of equations

$$A = B + C, \tag{3.52}$$

$$D\,e^{qh} + E\,e^{-qh} = F\,e^{-qh}, \tag{3.53}$$

$$\epsilon_1 A = \epsilon_2(B - C), \tag{3.54}$$

$$\epsilon_2\left(D\,e^{qh} - E\,e^{-qh}\right) = -\epsilon_3 F\,e^{-qh}, \tag{3.55}$$

$$B\,e^{qz'} + C\,e^{-qz'} = D\,e^{qz'} + E\,e^{-qz'}, \tag{3.56}$$

$$D\,e^{qz'} - E\,e^{-qz'} - B\,e^{qz'} + E\,e^{-qz'} = -\frac{4\pi}{q\epsilon_2}. \tag{3.57}$$

41

So the final solution of those equations may be used to express the components $\widetilde{G}_{22}(z, z')$ and $\widetilde{G}_{32}(z, z')$ in a compact form as

$$\widetilde{G}_{22} = \frac{2\pi}{q\epsilon_2} \left\{ \mathrm{e}^{-q|z-z'|} + \frac{\lambda_\mathrm{b}\lambda_\mathrm{t}\Delta}{1 - \lambda_\mathrm{b}\lambda_\mathrm{t}\Delta} \left[ \mathrm{e}^{q(z-z')} + \mathrm{e}^{-q(z-z')} \right] - \frac{\lambda_\mathrm{b}\,\mathrm{e}^{-q(z+z')} + \lambda_\mathrm{t}\Delta\,\mathrm{e}^{q(z+z')}}{1 - \lambda_\mathrm{b}\lambda_\mathrm{t}\Delta} \right\} \tag{3.58}$$

$$\widetilde{G}_{32} = \frac{2\pi}{q\bar{\epsilon}_{23}} \frac{\mathrm{e}^{-q(h-z')} - \lambda_\mathrm{b}\Delta\,\mathrm{e}^{q(h-z')}}{1 - \lambda_\mathrm{b}\lambda_\mathrm{t}\Delta}\,\mathrm{e}^{-q(z-h)} \equiv \frac{2\pi}{q\bar{\epsilon}_{23}} \frac{\mathrm{e}^{qz'} - \lambda_\mathrm{b}\,\mathrm{e}^{-qz'}}{1 - \lambda_\mathrm{b}\lambda_\mathrm{t}\Delta}\,\mathrm{e}^{-qz}. \tag{3.59}$$

Also, by the Maxwell's symmetric property of the GF, $\widetilde{G}_{12}(z, z') = \widetilde{G}_{21}(z', z)$, which was obtained in the previous subsection.

### 3.3.3  Source point in $I_3$ $(k = 3)$

As in the processes of the previous two subsections, first the homogeneous differential equations for $\widetilde{G}_{13}(z, z')$ and $\widetilde{G}_{23}(z, z')$ in Eq. (2.60) have the general solutions

$$\widetilde{G}_{13}(z, z') = A\,\mathrm{e}^{qz}, \tag{3.60}$$

$$\widetilde{G}_{23}(z, z') = B\,\mathrm{e}^{qz} + C\,\mathrm{e}^{-qz}, \tag{3.61}$$

where we have dropped a term with $\mathrm{e}^{-qz}$ in $\widetilde{G}_{12}(z, z')$ which becomes indefinitely large when $z \to -\infty$ in order to satisfy the BC in Eq. (2.62). By assuming that in Eq. (2.60) both $z$ and $z'$ are in the interval $I_3 = [h, \infty)$ but $z \neq z'$, we obtain two homogeneous differential equations for each component for the diagonal element $\widetilde{G}_{33}(z, z')$ in Eq. (2.65), which have the general solutions

$$\widetilde{G}_{33}^<(z, z') = D\,\mathrm{e}^{qz} + E\,\mathrm{e}^{-qz}, \tag{3.62}$$

$$\widetilde{G}_{33}^>(z, z') = F\,\mathrm{e}^{-qz}, \tag{3.63}$$

where we have dropped a term with $\mathrm{e}^{qz}$ in $\widetilde{G}_{33}^>(z, z')$ which becomes indefinitely large when $z \to \infty$. Now, the six constants $A$, $B$, $C$, $D$, $E$ and $F$ can be determined by imposing the six MCs which follow from Eqs. (2.63), (2.64) and (2.66) for $k = 3$. We get the system of equations

$$A = B + C, \tag{3.64}$$

$$B\,\mathrm{e}^{qh} + C\,\mathrm{e}^{-qh} = D\,\mathrm{e}^{qh} + E\,\mathrm{e}^{qh}, \tag{3.65}$$

$$\epsilon_1 A = \epsilon_2(B - C), \tag{3.66}$$

$$\epsilon_2\left(B\,\mathrm{e}^{qh} - C\,\mathrm{e}^{-qh}\right) = \epsilon_3\left(D\,\mathrm{e}^{qh} - E\,\mathrm{e}^{-qh}\right), \tag{3.67}$$

$$D\,\mathrm{e}^{qz'} + E\,\mathrm{e}^{-qz'} = F\,\mathrm{e}^{-qz'}, \tag{3.68}$$

$$F\,\mathrm{e}^{-qz'} + D\,\mathrm{e}^{qz'} - E\,\mathrm{e}^{-qz'} = -\frac{4\pi}{q\epsilon_3}. \tag{3.69}$$

42

So the final solution of those equations may be used to express the components $\widetilde{G}_{33}^{>}(z, z')$ and $\widetilde{G}_{33}^{<}(z, z')$ in a compact form:

$$\widetilde{G}_{33} = \frac{2\pi}{q\epsilon_3} \left[ e^{-q|z-z'|} + \frac{\lambda_t - \lambda_b \Delta}{1 - \lambda_b \lambda_t \Delta} e^{q(2h-z-z')} \right]. \tag{3.70}$$

Finally, by the Maxwell's symmetric property of the GF, $\widetilde{G}_{13}(z, z') = \widetilde{G}_{31}(z', z)$ and $\widetilde{G}_{23}(z, z') = \widetilde{G}_{32}(z', z)$, which were obtained in the previous subsections, respectively.

## 3.4 Conclusion

By using the translational invariance in directions parallel to the $(x, y)$ plane of a 3D Cartesian coordinate system, we have reduced the PDE for the GF in 3D to a set of ODEs by using a 2D FT. Then the GF is found in a piece-wise manner in the intervals with fixed values of the relative dielectric constants. For that process we used the boundary and MCs for the ODEs, which correspond to the Dirichlet BCs at infinity, the continuity and the electrostatic jump conditions of the GF at the boundary between intervals, and the continuity and the jump conditions when the observation and the source points are inside the same interval. So, solving the former complicated problem is reduced to solving and connecting the solution of a series of ODEs with proper conditions. Finally, after getting all the pieces of the FT of the GF, we can use an inverse 2DFT and the representation theorem for the Poisson equation to get the electric potential. The results for the FTGF were used in recent work on applications of graphene in the field effect devices [7, 8, 26].

# Chapter 4

# Green's function in the presence of rough boundary between two dielectric media

## 4.1  Motivation

Plasmonics is a hot new area in the nano-scale research, which aims at using the collective modes of excitation of charge carriers in metallic nanoparticles in electronics, photonics and bio-chemical sensing [27]. It is well-known that the oscillatory motion of quasi-free electrons in noble metals can be induced under the incidence of electromagnetic radiation upon metal surface [27] or by the passage of fast external charged particles [28]. Such collective motion of metallic electrons is described as plasma oscillations, or plasmons, which are characterized by eigenfrequencies that depend on the electronic density, as well as on the shape and the size of metallic particles. Besides the so-called bulk plasmons, of particular importance in nano-photonics are the so-called surface plasmons that are localized in a thin region of the surface of metal particles.

Having in mind that there exist numerous techniques for producing various assemblies of nano-particles, a question arises as to how smooth can their surfaces be made at the length scale between the atomic size and the full size of the particle. In reality, it is quite likely that metallic surfaces will exhibit various degrees of roughness at the nano-scale, and it is therefore important to explore possible effects of that roughness on the surface plasmon frequencies. In that context, Rahman and Maradudin studied a semi-infinite region occupied by metal with a frequency dependent relative dielectric constant of the form $\epsilon(\omega) = 1 - \omega_p^2/\omega^2$, where $\omega_p$ is the bulk plasma frequency of quasi-free electrons in the metal, which is separated from vacuum (or air) by a

randomly rough interface [29]. It is well known that, in the case of a metal with flat planar surface, such local description of the metal dielectric properties gives rise to the surface plasmon eigenfrequency $\omega_p/\sqrt{2}$, which is a solution of the equation $1 + \epsilon(\omega) = 0$. The work of Rahman and Maradudin attempts to investigate whether there are any changes in that frequency and, in particular, whether any dependence on the plasmon wavenumber may arise in the presence of disorder in the structure of the metal surface.

As a mathematical framework for their model, Rahman and Maradudin consider the GF for the Poisson equation. The latter equations describes electromagnetic fields in structures that contain materials with different dielectric properties in the so-called quasi-static approximation where retardation effects are neglected and the magnetic field can be discarded, which is acceptable for nano-particles with the size much smaller than the typical wavelengths of the external fields. It is well known that the use of the GF in layered nano-structures provides a convenient model for applications in Nanotechnology [7, 8, 26]. Hence, we wish to explore the work of Rahman and Maradudin for possible future use nano-structures including graphene [4].

## 4.2    Formulation of the problem

Rahman and Maradudin studied a randomly rough surface that separates semi-infinite region occupied by metal with a frequency dependent dielectric constant $\epsilon_1 = \epsilon(\omega)$ from semi-infinite region of vacuum or air with $\epsilon_2 = 1$ [29].
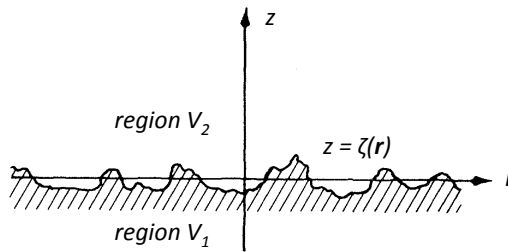


Figure 4.1: Rough surface for the boundary. Adapted from Ref. [29].

Following Rahman and Maradudin [29], we consider two semi-infinite regions with different

dielectric constants that are separated by a boundary surface $S : z = \zeta(\mathbf{r})$, defined by a profile function $\zeta(\mathbf{r})$ for $\mathbf{r} = (x, y) \in \mathbb{R}^2$. Then, $\mathbb{R}^3$ is divided into two regions:

$$
\begin{aligned}
V_1 &= \left\{ (x, y, z) \in \mathbb{R}^3 | z < \zeta(\mathbf{r}) \quad \forall \mathbf{r} = (x, y) \in \mathbb{R}^2 \right\} \\
V_2 &= \left\{ (x, y, z) \in \mathbb{R}^3 | z > \zeta(\mathbf{r}) \quad \forall \mathbf{r} = (x, y) \in \mathbb{R}^2 \right\}.
\end{aligned}
$$

with the relative dielectric constants $\epsilon_1$ in $V_1$ and $\epsilon_2$ in $V_2$, respectively. Assuming that the boundary $S$ is a surface with random roughness, it is reasonable to assume that $\zeta(\mathbf{r})$ is a stationary stochastic function of the coordinates $\mathbf{r} = (x, y)$ in a 3D Cartesian coordinate system, which is determined by the following properties:

$$
\begin{aligned}
\langle \zeta(\mathbf{r}) \rangle &= 0 & (4.1) \\
\langle \zeta(\mathbf{r})\zeta(\mathbf{r}') \rangle &= \sigma^2 W(\mathbf{r} - \mathbf{r}'). & (4.2)
\end{aligned}
$$

Note that Eq. (4.1) and Eq. (4.2) define a general stochastic process with zero mean and translationally invariant correlation function. Specifically, the brackets $\langle \ldots \rangle$ denote the average over the ensemble of realizations of the surface roughness and its deviation from the flatness. In Eq. (4.2) $\sigma$ denotes standard deviation that is defined via the variance,

$$
\sigma^2 = \langle \zeta^2(\mathbf{r}) \rangle - \langle \zeta(\mathbf{r}) \rangle^2 = \langle \zeta^2(\mathbf{r}) \rangle,
$$

which is the correlation function at $\mathbf{r}' = \mathbf{r}$. By that relation, $W(0) = 1$ is required for any model. Moreover, as the correlation should decrease at long distances, $W(\mathbf{r} - \mathbf{r}')$ must also have $\lim_{\|\mathbf{r} - \mathbf{r}'\| \to \infty} W(\mathbf{r} - \mathbf{r}') = 0$. Generally, the choice of the function $W(\mathbf{r} - \mathbf{r}')$ can be different in various models satisfying above conditions.

In addition, for further use we require a 2D Fourier integral representation of the rough boundary, given by the FT pair,

$$
\begin{aligned}
\zeta(\mathbf{r}) &= \int \frac{d^2\mathbf{q}}{(2\pi)^2} e^{i\mathbf{q}\cdot\mathbf{r}} \widetilde{\zeta}(\mathbf{q}), & (4.3) \\
\widetilde{\zeta}(\mathbf{q}) &= \int d^2\mathbf{r} \, e^{-i\mathbf{q}\cdot\mathbf{r}} \zeta(\mathbf{r}). & (4.4)
\end{aligned}
$$

The profile function is characterized by the following stochastic properties in the FT space

$$
\begin{aligned}
\langle \widetilde{\zeta}(\mathbf{q}) \rangle &= 0 & (4.5) \\
\langle \widetilde{\zeta}(\mathbf{q})\widetilde{\zeta}(\mathbf{q}') \rangle &= \sigma^2 (2\pi)^2 \delta(\mathbf{q} + \mathbf{q}') \widetilde{W}(\mathbf{q}), & (4.6)
\end{aligned}
$$

46

where $\widetilde{W}(\mathbf{q})$ is the 2D FT of the function $W(\mathbf{r})$, defined by

$$\widetilde{W}(\mathbf{q}) = \int d^2\mathbf{r}\, e^{-i\mathbf{q}\cdot\mathbf{r}}\, W(\mathbf{r}). \tag{4.7}$$

In the work by Rahman and Maradudin, the Poisson equation is used to find the Green Function (GF) of the electrostatic potential. Depending on region in which the observation and the source points lie, we can decompose the GF into the components $G_{jk}(\mathbf{R}, \mathbf{R}')$, such that the first index ($j = 1, 2$) and the second index ($k = 1, 2$) describe cases when the observation point $\mathbf{R} = (\mathbf{r}, z)$ and the sources point $\mathbf{R}' = (\mathbf{r}', z')$ lie in the regions $V_1$ and $V_2$, respectively. Accordingly, Eq. (2.37) can be decomposed into four equations:

$$\nabla^2 G_{11}(\mathbf{R}, \mathbf{R}') = -\frac{4\pi}{\epsilon_1}\delta(\mathbf{R} - \mathbf{R}'), \qquad z < \zeta(\mathbf{r}), \quad z' < \zeta(\mathbf{r}), \tag{4.8}$$

$$\nabla^2 G_{21}(\mathbf{R}, \mathbf{R}') = 0, \qquad z > \zeta(\mathbf{r}), \quad z' < \zeta(\mathbf{r}), \tag{4.9}$$

$$\nabla^2 G_{12}(\mathbf{R}, \mathbf{R}') = 0, \qquad z < \zeta(\mathbf{r}), \quad z' > \zeta(\mathbf{r}), \tag{4.10}$$

$$\nabla^2 G_{22}(\mathbf{R}, \mathbf{R}') = -\frac{4\pi}{\epsilon_2}\delta(\mathbf{R} - \mathbf{R}'), \qquad z > \zeta(\mathbf{r}), \quad z' > \zeta(\mathbf{r}). \tag{4.11}$$

The proper BCs for the GF are derived from the continuity and jump BCs for the electrostatic potential at the boundary $z = \zeta(\mathbf{r})$. Thus we have the continuity condition for the GF:

$$G_{1k}(\mathbf{R}, \mathbf{R}')|_{z=\zeta(\mathbf{r})} = G_{2k}(\mathbf{R}, \mathbf{R}')|_{z=\zeta(\mathbf{r})} \quad k = 1, 2 \tag{4.12}$$

and the jump condition for normal derivatives of the GF:

$$\epsilon_1 \hat{\mathbf{n}} \cdot \nabla G_{1k}(\mathbf{R}, \mathbf{R}')|_{z=\zeta(\mathbf{r})} = \epsilon_2 \hat{\mathbf{n}} \cdot \nabla G_{2k}(\mathbf{R}, \mathbf{R}')|_{z=\zeta(\mathbf{r})} \quad k = 1, 2 \tag{4.13}$$

where

$$\nabla = \hat{\mathbf{e}}_x \frac{\partial}{\partial x} + \hat{\mathbf{e}}_y \frac{\partial}{\partial y} + \hat{\mathbf{e}}_z \frac{\partial}{\partial z} \equiv \nabla_{\mathbf{r}} + \hat{\mathbf{e}}_z \frac{\partial}{\partial z} \tag{4.14}$$

and the unit vector normal to the boundary $z = \zeta(\mathbf{r})$ is given by

$$\hat{\mathbf{n}}(\mathbf{r}) = \frac{-\nabla_{\mathbf{r}}\zeta(\mathbf{r}) + \hat{\mathbf{e}}_z}{\sqrt{1 + \|\nabla_{\mathbf{r}}\zeta(\mathbf{r})\|^2}}. \tag{4.15}$$

The solution of Eqs. (4.8), (4.9), (4.10) and (4.11), can be obtained by using a 2D FT with respect to $\mathbf{r}$. Thus, defining the FT of the GF by

$$\widetilde{\mathbf{G}}_{jk}(\mathbf{q}, z; \mathbf{r}', z') = \int d^2 \mathbf{r}\, e^{-i\mathbf{q}\cdot\mathbf{r}}\, G_{jk}(\mathbf{r}, z; \mathbf{r}', z'), \qquad (4.16)$$

we can express the equations (4.8), (4.9), (4.10) and (4.11) in a compact form as

$$\frac{\partial^2}{\partial z^2}\widetilde{G}_{jk}(\mathbf{q}, z; \mathbf{r}', z') - q^2\widetilde{G}_{jk}(\mathbf{q}, z; \mathbf{r}', z') = -\frac{4\pi}{\epsilon_j}\, \delta_{jk}\, e^{-i\mathbf{q}\cdot\mathbf{r}'}\delta(z - z'), \qquad (4.17)$$

where $\delta_{jk}$ is a Kronecker delta symbol with indices $j, k = 1, 2$ that correspond to the four cases in Eqs. (4.8), (4.9), (4.10) and (4.11). Then, by using the inverse 2D FT we get the the components of the GF in real space as

$$G_{jk}(\mathbf{R}, \mathbf{R}') = \int \frac{d^2\mathbf{q}}{(2\pi)^2}\, e^{i\mathbf{q}\cdot\mathbf{r}}\widetilde{\mathbf{G}}_{jk}(\mathbf{q}, z; \mathbf{r}', z'). \qquad (4.18)$$

For the homogeneous differential equation in Eq. (4.17) with $j = 2$ and $k = 1$, the general solution is given by $\widetilde{\mathbf{G}}_{21}(\mathbf{q}, z; \mathbf{r}', z') = e^{-qz}A(\mathbf{q})$, where we dropped a term including $e^{qz}$ since it becomes infinite when $z \to \infty$. Thus, for the solution of Eq. (4.9), we find

$$G_{21}(\mathbf{R}, \mathbf{R}') = \int \frac{d^2\mathbf{q}}{(2\pi)^2}e^{i\mathbf{q}\cdot\mathbf{r}}e^{-qz}A(\mathbf{q}). \qquad (4.19)$$

Notice that, in principle, the unknown coefficient $A(\mathbf{q})$ in Eq. (4.20) also depends on coordinates of the source point $\mathbf{R}' = (\mathbf{r}', z')$, which we drop here for brevity.

For the non-homogeneous differential equation in Eq. (4.17) with $j = k = 1$, the general solution is given by

$$\widetilde{\mathbf{G}}_{11}(\mathbf{q}, z; \mathbf{r}', z') = \widetilde{\mathbf{G}}_{11}^{(\text{inf})}(\mathbf{q}, z; \mathbf{r}', z') + \widetilde{\mathbf{G}}_{11}^{(\text{hom})}(\mathbf{q}, z; \mathbf{r}', z'), \qquad (4.20)$$

where $\widetilde{\mathbf{G}}_{11}^{(\text{hom})}(\mathbf{q}, z; \mathbf{r}', z')$ is the general solution of the equivalent homogeneous equation in Eq. (4.8), given by

$$\widetilde{\mathbf{G}}_{11}^{(\text{hom})}(\mathbf{q}, z; \mathbf{r}', z') = e^{qz}B(\mathbf{q}) \qquad (4.21)$$

where we dropped a term including $e^{-qz}$ since it becomes infinite when $z \to -\infty$. On the other hand, $\widetilde{\mathbf{G}}_{11}^{(\text{inf})}(\mathbf{q}, z; \mathbf{r}', z')$ is particular solution of the non-homogeneous equation in Eq. (4.8)

48

defined in an infinite region with the relative dielectric constant $\epsilon_1$. According to Eq. (3.2) we find

$$\widetilde{\mathbf{G}}_{11}^{(\text{inf})}(\mathbf{q}, z; \mathbf{r}', z') = \frac{2\pi}{\epsilon_1 q} e^{-i\mathbf{q}\cdot\mathbf{r}'} e^{-q|z-z'|}. \tag{4.22}$$

Thus, we can write for the solution of Eq. (4.8) in the configuration space as

$$G_{11}(\mathbf{R}, \mathbf{R}') = \int \frac{d^2\mathbf{q}}{(2\pi)^2} e^{i\mathbf{q}\cdot(\mathbf{r}-\mathbf{r}')} \frac{2\pi}{q\epsilon_1} e^{-q|z-z'|} + \int \frac{d^2\mathbf{q}}{(2\pi)^2} e^{i\mathbf{q}\cdot\mathbf{r}} e^{qz} B(\mathbf{q}).$$

## 4.3 Perturbative solution

In order to determine the unknown coefficients $A(\mathbf{q})$ and $B(\mathbf{q})$ in the above two components of the GF, we should implement the BCs in Eqs. (4.12) and (5.99) with $k = 1$. The resulting equations are generally difficult to solve for a profile function $\zeta(\mathbf{r})$ with arbitrarily large amplitude of variation. Assuming that the surface profile function $\zeta(\mathbf{r})$ is small in magnitude, such that $q\sigma \ll 1$, and that its local slope is relative small, such that $|\nabla_{\mathbf{r}}\zeta(\mathbf{r})| \ll 1$, we may use a perturbative approach to obtain average values for those coefficients. If we further assume that $\zeta(\mathbf{r})$ is a stationary Gaussian process with zero mean, it suffices to find expressions for the coefficients to the second order in $\zeta(\mathbf{r})$. We formally expand $A(\mathbf{q})$ and $B(\mathbf{q})$ up to the second order in $\zeta(\mathbf{q})$:

$$A(\mathbf{q}) = A^{(0)}(\mathbf{q}) + A^{(1)}(\mathbf{q}) + A^{(2)}(\mathbf{q}) + \cdots \tag{4.23}$$
$$B(\mathbf{q}) = B^{(0)}(\mathbf{q}) + B^{(1)}(\mathbf{q}) + B^{(2)}(\mathbf{q}) + \cdots \tag{4.24}$$

where the superscript denotes the order of each term in $\zeta(\mathbf{q})$. Then, by substituting the above representation of the coefficients into BCs Eq. (4.12) and Eq. (5.99) and making equal terms of same order in both sides of the resulting equations, we obtain the results for each order of the coefficients.

Let us first implement this procedure to the BCs in Eq. (4.12),

$$G_{11}(\mathbf{r}, z)|_{z=\zeta(\mathbf{r})} = G_{21}(\mathbf{r}, z)|_{z=\zeta(\mathbf{r})}. \tag{4.25}$$

For the LHS of Eq. (4.25), we assume that the source point is always below the boundary, $z' < \zeta(\mathbf{r})$ for all $\mathbf{r}$, so that we may write $|\zeta(\mathbf{r}) - z'| = \zeta(\mathbf{r}) - z'$ in $G_{11}$. Next, we use the expansion $e^{\pm q\zeta(\mathbf{r})} = 1 \pm q\zeta(\mathbf{r}) + \frac{1}{2}q^2\zeta^2(\mathbf{r}) + o(\zeta^2)$. Note that it retains only terms of up to $O(\zeta^2(\mathbf{r}))$ under the assumption that the surface roughness is treated as a small perturbation to the plane surface.

Now the LHS becomes:

$$L_{11}(\mathbf{r}) \cong \int \frac{d^2\mathbf{q}}{(2\pi)^2} e^{i\mathbf{q}\cdot(\mathbf{r}-\mathbf{r}')}\frac{2\pi}{\epsilon_1 q}e^{qz'}[1 - q\zeta(\mathbf{r}) + \frac{1}{2}q^2\zeta^2(\mathbf{r})]$$

$$+ \int \frac{d^2\mathbf{q}}{(2\pi)^2} e^{-i\mathbf{q}\cdot\mathbf{r}}B(\mathbf{q})[1 + q\zeta(\mathbf{r}) + \frac{1}{2}q^2\zeta^2(\mathbf{r})]. \qquad (4.26)$$

In the next step, we multiply both sides in Eq. (4.26) by $e^{-i\mathbf{k}\cdot\mathbf{r}}$ and integrate over $\mathbf{r}$ in order to write the 2D FT of $L_{11}(\mathbf{r})$ as:

$$\widetilde{L}_{11}(\mathbf{k}) = \int \frac{d^2\mathbf{q}}{(2\pi)^2}\left[\frac{2\pi}{\epsilon_1 q}e^{qz'}e^{-i\mathbf{q}\cdot\mathbf{r}'} + B(\mathbf{q})\right]\int d^2\mathbf{r}\, e^{-i(\mathbf{k}-\mathbf{q})\cdot\mathbf{r}}$$

$$- \int \frac{d^2\mathbf{q}}{(2\pi)^2}q\left[\frac{2\pi}{\epsilon_1 q}e^{qz'}e^{-i\mathbf{q}\cdot\mathbf{r}'} - B(\mathbf{q})\right]\int d^2\mathbf{r}\, \zeta(\mathbf{r})e^{-i(\mathbf{k}-\mathbf{q})\cdot\mathbf{r}}$$

$$+ \frac{1}{2}q^2\int \frac{d^2\mathbf{q}}{(2\pi)^2}\left[\frac{2\pi}{\epsilon_1 q}e^{qz'}e^{-i\mathbf{q}\cdot\mathbf{r}'} + B(\mathbf{q})\right]\int d^2\mathbf{r}\, \zeta^2(\mathbf{r})e^{-i(\mathbf{k}-\mathbf{q})\cdot\mathbf{r}}. \qquad (4.27)$$

Similarly, for the RHS of Eq. (4.25), we do the same expansion of the exponential factor containing $\zeta(\mathbf{r})$ and express the 2D FT of the RHS as:

$$\widetilde{R}_{21}(\mathbf{k}) = \int \frac{d^2\mathbf{q}}{(2\pi)^2}A(\mathbf{q})\left[\int d^2\mathbf{r}\, e^{-i(\mathbf{k}-\mathbf{q})\cdot\mathbf{r}} - q\int d^2\mathbf{r}\, e^{-i(\mathbf{k}-\mathbf{q})\cdot\mathbf{r}}\zeta(\mathbf{r}) + \frac{q^2}{2}\int d^2\mathbf{r}\, e^{-i(\mathbf{k}-\mathbf{q})\cdot\mathbf{r}}\zeta^2(\mathbf{r})\right] \qquad (4.28)$$

Noting that

$$\int d^2\mathbf{r}\, e^{-i(\mathbf{k}-\mathbf{q})\cdot\mathbf{r}} = (2\pi)^2\delta(\mathbf{k} - \mathbf{q}),$$

$$\int d^2\mathbf{r}\, e^{-i(\mathbf{k}-\mathbf{q})\cdot\mathbf{r}}\zeta(\mathbf{r}) = \widetilde{\zeta}(\mathbf{k} - \mathbf{q}),$$

we denote $\alpha(\mathbf{k} - \mathbf{q}) = \int d^2\mathbf{r}\, e^{-i(\mathbf{k}-\mathbf{q})\cdot\mathbf{r}}\zeta^2(\mathbf{r})$ and use the convolution theorem of inverse FT to write:

$$\alpha(\mathbf{k} - \mathbf{q}) \equiv \int d^2\mathbf{r}\, e^{-i(\mathbf{k}-\mathbf{q})\cdot\mathbf{r}}\zeta^2(\mathbf{r})$$

$$= \int \frac{d^2\mathbf{Q}}{(2\pi)^2}\widetilde{\zeta}(\mathbf{Q})\widetilde{\zeta}(\mathbf{k} - \mathbf{q} - \mathbf{Q}). \qquad (4.29)$$

50

Substituting the above expressions into Eq. (4.25), we get from the first BC:

$$\int \frac{d^2\mathbf{q}}{(2\pi)^2} \left\{ \frac{2\pi}{\epsilon_1 q} e^{-i\mathbf{q}\cdot\mathbf{r}'+qz'} \left[ -(2\pi)^2\delta(\mathbf{k}-\mathbf{q}) + q\widetilde{\zeta}(\mathbf{k}-\mathbf{q}) - \frac{q^2}{2}\alpha(\mathbf{k}-\mathbf{q}) \right] \right.$$

$$+A(\mathbf{q})\left[ (2\pi)^2\delta(\mathbf{k}-\mathbf{q}) - q\widetilde{\zeta}(\mathbf{k}-\mathbf{q}) + \frac{q^2}{2}\alpha(\mathbf{k}-\mathbf{q}) \right]$$

$$\left. -B(\mathbf{q})\left[ (2\pi)^2\delta(\mathbf{k}-\mathbf{q}) + q\widetilde{\zeta}(\mathbf{k}-\mathbf{q}) + \frac{q^2}{2}\alpha(\mathbf{k}-\mathbf{q}) \right] \right\} = 0, \tag{4.30}$$

where $\alpha$ is defined in Eq. (4.29).

Similarly, second equation for the coefficients $A(\mathbf{q})$ and $B(\mathbf{q})$ is obtained from the jump BC as:

$$\epsilon_1 \hat{\mathbf{n}} \cdot \nabla G_{11}(\mathbf{R}, \mathbf{R}')|_{z=\zeta(\mathbf{r})} = \epsilon_2 \hat{\mathbf{n}} \cdot \nabla G_{21}(\mathbf{R}, \mathbf{R}')|_{z=\zeta(\mathbf{r})} \tag{4.31}$$

In order to collect all terms of different orders in $\zeta(\mathbf{q})$ that appear in Eq. (4.31), we do the expansion to the operator $\hat{\mathbf{n}} \cdot \nabla$ as:

$$\hat{\mathbf{n}} \cdot \nabla = \left[1 + (\nabla_\mathbf{r}\zeta(\mathbf{r}))^2\right]^{-\frac{1}{2}} \left[ -(\nabla_\mathbf{r}\zeta(\mathbf{r})) \cdot \nabla_\mathbf{r} + \frac{\partial}{\partial z} \right] \tag{4.32}$$

$$\cong \frac{\partial}{\partial z} - (\nabla_\mathbf{r}\zeta(\mathbf{r})) \cdot \nabla_\mathbf{r} - \frac{1}{2}(\nabla_\mathbf{r}\zeta(\mathbf{r}))^2\frac{\partial}{\partial z} + \cdots$$

Now Eq. (4.31) becomes:

$$0 = \hat{\mathbf{n}} \cdot \nabla \left. (\epsilon_1 G_{11} - \epsilon_2 G_{21}) \right|_{z=\zeta(\mathbf{r})}$$

$$= \left\{ \frac{\partial}{\partial z} - (\nabla_\mathbf{r}\zeta(\mathbf{r})) \cdot \nabla_\mathbf{r} - \frac{1}{2}(\nabla_\mathbf{r}\zeta(\mathbf{r}))^2\frac{\partial}{\partial z} \right\}$$

$$\times \left. \int \frac{d^2\mathbf{q}}{(2\pi)^2} e^{i\mathbf{q}\cdot\mathbf{r}} \left[ \epsilon_1 \left( \frac{2\pi}{q\epsilon_1} e^{-i\mathbf{q}\cdot\mathbf{r}} e^{-q|z-z'|} + B(\mathbf{q})e^{qz} \right) - \epsilon_2 e^{-qz} A(\mathbf{q}) \right] \right|_{z=\zeta(\mathbf{r})}.$$

As in the case of the BC in Eq. (4.12), by doing the expansions of the factors containing the exponentials $e^{\pm q\zeta(\mathbf{r})}$ and performing the 2D FT with respect to $\mathbf{r}$, we get several terms involving different orders of $\widetilde{\zeta}(\mathbf{k})$, since by the convolution theorem for FT, we have:

$$\int d^2\mathbf{r}\, e^{-i(\mathbf{q}-\mathbf{k})\cdot\mathbf{r}} \|\nabla_\mathbf{r}\zeta(\mathbf{r})\|^2 = -\int \frac{d^2\mathbf{Q}}{(2\pi)^2} \mathbf{Q} \cdot (\mathbf{k}-\mathbf{q}-\mathbf{Q})\widetilde{\zeta}(\mathbf{Q})\widetilde{\zeta}(\mathbf{k}-\mathbf{q}-\mathbf{Q}),$$

$$i\mathbf{q} \cdot \int d^2\mathbf{r}\, e^{-i(\mathbf{q}-\mathbf{k})\cdot\mathbf{r}} \zeta(\mathbf{r})\nabla_\mathbf{r}\zeta(\mathbf{r}) = -\int \frac{d^2\mathbf{q}}{(2\pi)^2} \mathbf{q} \cdot \mathbf{Q}\, \widetilde{\zeta}(\mathbf{Q})\widetilde{\zeta}(\mathbf{k}-\mathbf{q}-\mathbf{Q}),$$

$$i\mathbf{q} \cdot \int d^2\mathbf{r}\, e^{-i(\mathbf{q}-\mathbf{k})\cdot\mathbf{r}} \nabla_\mathbf{r}\zeta(\mathbf{r}) = -\mathbf{q} \cdot (\mathbf{k}-\mathbf{q})\, \widetilde{\zeta}(\mathbf{k}-\mathbf{q}).$$

51

Substituting those expressions into the jump BC, we have the second equation for $A(\mathbf{q})$ and $B(\mathbf{q})$:

$$\int \frac{d^2\mathbf{q}}{(2\pi)^2} \left\{ 2\pi e^{-i\mathbf{q}\cdot\mathbf{r}'+qz'} \left[ -(2\pi)^2\delta(\mathbf{k}-\mathbf{q}) + (q+\hat{\mathbf{q}}\cdot(\mathbf{k}-\mathbf{q}))\widetilde{\zeta}(\mathbf{k}-\mathbf{q}) - \beta(\mathbf{k}-\mathbf{q}) \right] \right.$$
$$+\epsilon_1 q B(\mathbf{q}) \left[ (2\pi)^2\delta(\mathbf{k}-\mathbf{q}) + (q+\hat{\mathbf{q}}\cdot(\mathbf{k}-\mathbf{q}))\widetilde{\zeta}(\mathbf{k}-\mathbf{q}) + \beta(\mathbf{k}-\mathbf{q}) \right]$$
$$\left. -\epsilon_2 q A(\mathbf{q}) \left[ -(2\pi)^2\delta(\mathbf{k}-\mathbf{q}) + (q+\hat{\mathbf{q}}\cdot(\mathbf{k}-\mathbf{q}))\widetilde{\zeta}(\mathbf{k}-\mathbf{q}) - \beta(\mathbf{k}-\mathbf{q}) \right] \right\} = 0, \quad (4.33)$$

where $\beta(\mathbf{k}-\mathbf{q})$ is defined as:

$$\beta(\mathbf{k}-\mathbf{q}) = \int \frac{d^2\mathbf{Q}}{(2\pi)^2}\widetilde{\zeta}(\mathbf{Q})\widetilde{\zeta}(\mathbf{k}-\mathbf{q}-\mathbf{Q}) \left( \frac{q^2}{2} + \mathbf{q}\cdot\mathbf{Q} + \frac{1}{2}\mathbf{Q}\cdot(\mathbf{k}-\mathbf{q}-\mathbf{Q}) \right). \quad (4.34)$$

Finally, from Eqs. (4.30) and (4.33) the solutions for each order of $A(\mathbf{k})$ and $B(\mathbf{k})$ are:

$$\begin{bmatrix} A^{(0)}(\mathbf{k}) \\ B^{(0)}(\mathbf{k}) \end{bmatrix} = \frac{2\pi}{k}\frac{1}{(\epsilon_1+\epsilon_2)}e^{-i\mathbf{k}\cdot\mathbf{r}'+kz'} \begin{bmatrix} 2 \\ \frac{\epsilon_1-\epsilon_2}{\epsilon_1} \end{bmatrix} \quad (4.35)$$

$$\begin{bmatrix} A^{(1)}(\mathbf{k}) \\ B^{(1)}(\mathbf{k}) \end{bmatrix} = -4\pi\frac{\epsilon_2-\epsilon_1}{(\epsilon_1+\epsilon_2)^2}\int \frac{d^2\mathbf{q}}{(2\pi)^2}e^{-i\mathbf{q}\cdot\mathbf{r}'+qz'}\widetilde{\zeta}(\mathbf{k}-\mathbf{q}) \begin{bmatrix} \hat{\mathbf{k}}\cdot\hat{\mathbf{q}} - 1 \\ \frac{\epsilon_2}{\epsilon_1} + \hat{\mathbf{k}}\cdot\hat{\mathbf{q}} \end{bmatrix} \quad (4.36)$$

$$\begin{bmatrix} A^{(2)}(\mathbf{k}) \\ B^{(2)}(\mathbf{k}) \end{bmatrix} = -4\pi\frac{\epsilon_2-\epsilon_1}{(\epsilon_1+\epsilon_2)^3}\int \frac{d^2\mathbf{q}}{(2\pi)^2}\int \frac{d^2\mathbf{Q}}{(2\pi)^2}e^{-i\mathbf{Q}\cdot\mathbf{r}'+Qz'}\widetilde{\zeta}(\mathbf{k}-\mathbf{q})\widetilde{\zeta}(\mathbf{q}-\mathbf{Q}) \quad (4.37)$$
$$\times \begin{bmatrix} -(\epsilon_1-\epsilon_2)(\hat{\mathbf{k}}\cdot\hat{\mathbf{q}})(\hat{\mathbf{q}}\cdot\hat{\mathbf{Q}}) + 2\hat{\mathbf{q}}\cdot(\epsilon_1\hat{\mathbf{Q}}-\epsilon_2\hat{\mathbf{k}}) - (\epsilon_1-\epsilon_2) \\ -(\epsilon_1-\epsilon_2)(\hat{\mathbf{k}}\cdot\hat{\mathbf{q}})(\hat{\mathbf{q}}\cdot\hat{\mathbf{Q}}) + 2\epsilon_2\hat{\mathbf{q}}\cdot(\hat{\mathbf{Q}}+\hat{\mathbf{k}}) + (\epsilon_2-\frac{\epsilon_2^2}{\epsilon_1}) \end{bmatrix},$$

where $\hat{\mathbf{k}}$, $\hat{\mathbf{q}}$ and $\hat{\mathbf{Q}}$ are the unit vectors in the direction of the vectors $\mathbf{k}$, $\mathbf{q}$ and $\mathbf{Q}$, respectively.

## 4.4  Averaged results to the second order

For a randomly rough surface we calculate the averaged values of the perturbative solution for $A(\mathbf{k})$ and $B(\mathbf{k})$ by using the stochastic properties of $\zeta(\mathbf{r})$:

$$\langle A(\mathbf{k}) \rangle = \langle A^{(0)}(\mathbf{k}) \rangle + \langle A^{(1)}(\mathbf{k}) \rangle + \langle A^{(2)}(\mathbf{k}) \rangle, \quad (4.38)$$
$$\langle B(\mathbf{k}) \rangle = \langle B^{(0)}(\mathbf{k}) \rangle + \langle B^{(1)}(\mathbf{k}) \rangle + \langle B^{(2)}(\mathbf{k}) \rangle. \quad (4.39)$$

Before calculating each order above, we introduce Gaussian model for the 2-point correlation function of roughness in Eq. (4.2), where the $W(\mathbf{r})$ is defined as:

$$W(\mathbf{r}) = e^{-\frac{r^2}{a^2}}.$$

In addition, as the results for each order of $A(\mathbf{k})$ and $B(\mathbf{k})$ is represented in Fourier space, we also need the FT of the Gaussian form $\widetilde{W}(\mathbf{k})$ as:

$$\widetilde{W}(\mathbf{k}) = \int d^2\mathbf{r} e^{-i\mathbf{k}\cdot\mathbf{r}} W(\mathbf{r}) = \pi a^2 e^{-\frac{a^2 k^2}{4}}. \tag{4.40}$$

In addition, we may assume that the roughness of the surface $\zeta(\mathbf{r})$ is a Gaussian process. It is worth noting the properties of auto-correlation functions for such process taken at multiple points $\mathbf{r}, \mathbf{r}'', \mathbf{r}''', \ldots$. Namely, such auto-correlation functions vanish for odd number of points, whereas for the even number of points auto-correlation function may be decomposed into a linear combination of the products of 2-points correlation functions defined in Eq. (4.2), e.g.,

$$\begin{aligned}
\langle \zeta(\mathbf{r}) \rangle &= 0 \\
\langle \zeta(\mathbf{r})\zeta(\mathbf{r}')\zeta(\mathbf{r}'') \rangle &= 0 \\
\langle \zeta(\mathbf{r})\zeta(\mathbf{r}')\zeta(\mathbf{r}'')\zeta(\mathbf{r}''') \rangle &= \langle \zeta(\mathbf{r})\zeta(\mathbf{r}') \rangle \langle \zeta(\mathbf{r}'')\zeta(\mathbf{r}''') \rangle + \langle \zeta(\mathbf{r})\zeta(\mathbf{r}'') \rangle \langle \zeta(\mathbf{r}')\zeta(\mathbf{r}''') \rangle \\
&+ \langle \zeta(\mathbf{r})\zeta(\mathbf{r}''') \rangle \langle \zeta(\mathbf{r}')\zeta(\mathbf{r}'') \rangle.
\end{aligned}$$

$$\ldots$$

This property is very useful when higher orders perturbative solutions of $A(\mathbf{k})$ and $B(\mathbf{k})$ are needed. This also shows that the error in our perturbative solution to the order $A^{(2)}(\mathbf{k})$ and $B^{(2)}(\mathbf{k})$ is in fact of the fourth order, $\propto \sigma^4$.

Now, for the 0th order of $A(\mathbf{k})$ and $B(\mathbf{k})$, because there is no stochastic term $\zeta(\mathbf{q})$ in them by Eq. (4.35), the averages stay the same:

$$\langle A^{(0)}(\mathbf{k}) \rangle = A^{(0)}(\mathbf{k}) = \frac{4\pi}{k} \frac{1}{(\epsilon_1 + \epsilon_2)} e^{-i\mathbf{k}\cdot\mathbf{r}' + kz'}, \tag{4.41}$$

$$\langle B^{(0)}(\mathbf{k}) \rangle = B^{(0)}(\mathbf{k}) = \frac{2\pi}{k} \frac{\epsilon_1 - \epsilon_2}{\epsilon_1(\epsilon_1 + \epsilon_2)} e^{-i\mathbf{k}\cdot\mathbf{r}' + kz'}. \tag{4.42}$$

As for the 1st order of $A(\mathbf{k})$ and $B(\mathbf{k})$, since the average of $\zeta(\mathbf{q})$ over the ensemble of realizations of the surface roughness $\langle \zeta(\mathbf{q}) \rangle = 0$, we have:

$$\langle A^{(1)}(\mathbf{k}) \rangle = 0, \tag{4.43}$$

$$\langle B^{(1)}(\mathbf{k}) \rangle = 0. \tag{4.44}$$

For the 2nd order of $A(\mathbf{k})$ and $B(\mathbf{k})$, first we use Eq. (4.6) in the product $\widetilde{\zeta}(\mathbf{k} - \mathbf{q})\widetilde{\zeta}(\mathbf{q} - \mathbf{Q})$ that appears in the RHS of Eq. (4.37) giving:

$$\langle \widetilde{\zeta}(\mathbf{k} - \mathbf{q})\widetilde{\zeta}(\mathbf{q} - \mathbf{Q})\rangle = (2\pi)^2 \sigma^2 \delta(\mathbf{k} - \mathbf{Q})\widetilde{W}(\mathbf{k} - \mathbf{q}). \tag{4.45}$$

Using the delta function $\delta(\mathbf{k} - \mathbf{Q})$ to perform the integration over $\mathbf{Q}$ in the averaged Eq. (4.37), the 2nd order expressions become:

$$\langle A^{(2)}(\mathbf{k})\rangle = -4\pi\sigma^2 \frac{(\epsilon_2 - \epsilon_1)^2}{(\epsilon_1 + \epsilon_2)^3} e^{-i\mathbf{k}\cdot\mathbf{r}' + kz'} \int \frac{d^2\mathbf{q}}{(2\pi)^2} \widetilde{W}(\mathbf{k} - \mathbf{q})\,(1 - \hat{\mathbf{k}}\cdot\hat{\mathbf{q}})^2 \tag{4.46}$$

$$\langle B^{(2)}(\mathbf{k})\rangle = -4\pi\sigma^2 \frac{(\epsilon_2 - \epsilon_1)^2}{(\epsilon_1 + \epsilon_2)^3} e^{-i\mathbf{k}\cdot\mathbf{r}' + kz'} \int \frac{d^2\mathbf{q}}{(2\pi)^2} \widetilde{W}(\mathbf{k} - \mathbf{q}) \tag{4.47}$$

$$\times \left[(\hat{\mathbf{k}}\cdot\hat{\mathbf{q}})^2 + \frac{4\epsilon_2}{\epsilon_2 - \epsilon_1}\hat{\mathbf{k}}\cdot\hat{\mathbf{q}} + \frac{\epsilon_2}{\epsilon_1}\right].$$

While these expressions give the second order solutions for the coefficients $A(\mathbf{k})$ and $B(\mathbf{k})$ in terms of the FT of the 2-point correlation function $\widetilde{W}(\mathbf{k})$ of an arbitrary, translationally invariant stochastic process $\zeta(\mathbf{r})$, it is worth mentioning that using the Gaussian model in Eq. (4.40) permits analytical solution of the integrals over $\mathbf{q}$ in Eqs. (4.46) and (4.47).

Finally, we can similarly write the solutions for Eqs. (4.10) and (4.11) as:

$$G_{12}(\mathbf{R}, \mathbf{R}') = \int \frac{d^2\mathbf{q}}{(2\pi)^2} e^{i\mathbf{q}\cdot\mathbf{r}} e^{qz} C(\mathbf{q}), \tag{4.48}$$

$$G_{22}(\mathbf{R}, \mathbf{R}') = \int \frac{d^2\mathbf{q}}{(2\pi)^2} e^{i\mathbf{q}(\mathbf{r}-\mathbf{r}')} \frac{2\pi}{q\epsilon_2} e^{-q|z-z'|} + \int \frac{d^2\mathbf{q}}{(2\pi)^2} e^{i\mathbf{q}\cdot\mathbf{r}} e^{-qz} D(\mathbf{q}), \tag{4.49}$$

and determine perturbative solutions for the coefficients $C(\mathbf{k})$ and $D(\mathbf{k})$ by implementing the BCs in Eqs. (4.12) and (5.99) with $k = 2$. However, unlike Rahman and Maradudin, we assume general values of the dielectric constants on either side of the boundary, so that the results for $G_{12}$ and $G_{22}$ may be obtained from those for $G_{21}$ and $G_{11}$, respectively, by simply switching the indices of the dielectric constants $\epsilon_1$ and $\epsilon_2$.

## 4.5 Conclusion

We have derived a perturbative solution for the GF of the Poisson equation for electrostatic potential in the presence of two semi-infinite regions with different relative dielectric constants

that are separated by a randomly rough boundary. The profile function of the boundary surface was assumed to be a stochastic function with zero mean that depends of the position coordinates $(x, y)$ in the plane $z = 0$ of a Cartesian coordinate system. This 2D stochastic process is assumed to be stationary in order to reflect the translational invariance of the random surface, giving rise to a 2-point correlation function that depends on the vector distance $\mathbf{r} - \mathbf{r}'$ between the points $\mathbf{r}$ and $\mathbf{r}'$ in the mean plane $z = 0$. Moreover, assuming that the 2-point correlation function only depends on the magnitude of the distance $\|\mathbf{r} - \mathbf{r}'\|$, but not on the direction between the two points, we can describe an isotropic rough boundary. In general, the decrease of the 2-point correlation function with increasing distance $\|\mathbf{r} - \mathbf{r}'\| \rightarrow 0$ is characterized by the so-called correlation length $a$.

Our perturbative solution for the GF is accurate to the second order in the size of the random boundary fluctuation, that is, to the order of its variance $\sigma^2$. In addition, our solution for the GF accurately describes electrostatic interactions at distances $\gtrsim a$ in the directions parallel to a randomly rough surface with the correlation length $a$. Our results may be used to, e.g., estimate the effects of roughness on the image potential of individual charges, or the screened interaction energy between multiple charges, in the vicinity of a rough metal surface. Furthermore, by allowing the dielectric constants of the regions on either side of a rough boundary to be frequency dependent, we may investigate the effects of roughness on the plasmon or phonon frequencies in the materials occupying those regions.

# Chapter 5

# Hydrodynamic model of electron gas in metal layer

In most studies on mathematical modeling of plasmonic devices, a region occupied by a metal was treated locally by simply assigning frequency dependence to its dielectric constant, using either empirical data or simple models like Drude dielectric function. As discussed in the section 2.1, our form of the GF therefore makes it easy to include a metallic region within such local approach by considering the corresponding parameter $\epsilon_j$ to be a function of $\omega$. However, in recent years there has been increasing interest to include nonlocal effects in the description of the dielectric response of mobile electrons in metallic regions using the so-called hydrodynamic model [18, 19, 20, 21]. Hence, we study here this model in various approximations and describe how it can be treated by the GF method.

We consider a structure containing closed region $V$ that is occupied by a metal and is surrounded by a dielectric material with the relative dielectric constant $\epsilon_r$ that may depend on the position vector $\mathbf{R}$. Suppose that the metallic region $V$ is composed of quasi-free electrons and motionless ions with equilibrium volume densities $n_{e0} = n_{i0} = n_0$. We want to determine the electrostatic response of the metal due to polarization of its EG by an external charged particle with the charge density $\rho_{\text{ext}}(\mathbf{R}, t)$. By defining $n(\mathbf{R}, t)$ as the number density per unit volume of electrons with charge $-e < 0$, and $\mathbf{v}(\mathbf{R}, t) = (v_x, v_y, v_z)$ as the velocity field of electrons, the

QHD model for electronic excitations inside the metallic region may be expressed as:

$$\frac{\partial}{\partial t} n + \nabla \cdot (n\,\mathbf{v}) = 0 \tag{5.1}$$

$$m\left(\frac{\partial}{\partial t} + \mathbf{v} \cdot \nabla\right) \cdot \mathbf{v} = -\nabla U(\mathbf{R}, t) - m\gamma\,\mathbf{v} \tag{5.2}$$

$$U(\mathbf{R}, t) = -e\,\Phi(\mathbf{R}, t) + \frac{\hbar^2}{2m}(3\pi^2)^{\frac{2}{3}}\, n^{\frac{2}{3}} - \frac{\hbar^2}{2m}\frac{\nabla^2\sqrt{n}}{\sqrt{n}} \tag{5.3}$$

$$\nabla \cdot [\epsilon_r(\mathbf{R})\nabla\Phi(\mathbf{R}, t)] = 4\pi e\, n(\mathbf{R}, t)\,\Theta_V(\mathbf{R}) - 4\pi\rho_{\text{ext}}(\mathbf{R}, t), \tag{5.4}$$

where $m$ and $\gamma$ are electron mass and phenomenological damping rate due to electron friction on the background ions, respectively. Note that Eq. (5.1) is the continuity equation, which describes the conservation of electron number, whereas Eq. (5.2) is the Euler equation, or Navier-Stokes equation describing the balance of momentum in the EG. As for the potential energy per electron, which is defined in Eq. (5.3), the first term in the right hand side corresponds to the electron energy in the total electric potential $\Phi(\mathbf{R}, t)$, the second term is related to the so-called "Thomas-Fermi (TF) pressure" in the EG, whereas the last term describes quantum effects due to the "Bohm potential" [30, 31]. The last two terms in Eq. (5.3) are of quantum mechanical origin, as indicate by the presence of the Planck's constat $\hbar$. They are related to the familiar concepts in the Density Functional Theory (DFT) of many-electron systems where electron-electron interactions are treated at the level of a local density approximation (LDA) and the gradient correction(s) to it, respectively. Finally, Eq. (5.4) is the Poisson equation for the total electrostatic potential $\Phi(\mathbf{R}, t)$ in the presence of the external charge density and the induced charge density due to polarization of the EG in the metal slab region, which is indicated by the function $\Theta_V(\mathbf{R})$ that takes the value $\Theta_V(\mathbf{R}) = 1$ when $\mathbf{R} \in V$ and $\Theta_V(\mathbf{R}) = 0$ otherwise.

In order to linearize the above system of equations, the value of the density $n(\mathbf{R}, t)$, the velocity $\mathbf{v}(\mathbf{R}, t)$ and the potential $\Phi(\mathbf{R}, t)$ can be represented as perturbed from their values in equilibrium due to the presence of the external charge, which is considered to be a small perturbation of the system. So, we define: $n(\mathbf{R}, t) = n_{eq} + n_1(\mathbf{R}, t) + \cdots$, $\mathbf{v}(\mathbf{R}, t) = \mathbf{v}_{eq} + \mathbf{v}_1(\mathbf{R}, t) + \cdots$, $\Phi(\mathbf{R}, t) = \Phi_{eq} + \Phi_1(\mathbf{R}, t) + \cdots$. Since in equilibrium state we have $n_{eq} = n_0 = \text{const}$, $\mathbf{v}_{eq} = 0$ and $\Phi_{eq} = 0$, we may write $\mathbf{v}_1(\mathbf{R}, t) = \mathbf{v}(\mathbf{R}, t)$ and $\Phi_1(\mathbf{R}, t) = \Phi(\mathbf{R}, t)$ to the first order. Now the linearized system of equations for the first order perturbations $n_1(\mathbf{R}, t)$, $\mathbf{v}(\mathbf{R}, t)$, $\Phi(\mathbf{R}, t)$ is

given by:

$$\frac{\partial}{\partial t}n_1(\mathbf{R},t) \; + \; n_0\nabla \cdot \mathbf{v}(\mathbf{R},t) = 0, \tag{5.5}$$

$$\frac{\partial}{\partial t}\mathbf{v}(\mathbf{R},t) \; = \; -\frac{1}{m}\nabla U_1(\mathbf{R},t) - \gamma\,\mathbf{v}(\mathbf{R},t), \tag{5.6}$$

$$U_1(\mathbf{R},t) \; = \; -e\,\Phi(\mathbf{R},t) + \frac{1}{3}\,(3\pi^2)^{\frac{2}{3}}\,\frac{\hbar^2}{mn_0^{\frac{1}{3}}}n_1(\mathbf{R},t) - \frac{\hbar^2}{4mn_0}\,\nabla^2 n_1(\mathbf{R},t), \tag{5.7}$$

$$\nabla \cdot [\epsilon_r(\mathbf{R})\nabla\Phi(\mathbf{R},t)] \; = \; 4\pi e\,n_1(\mathbf{R},t)\,\Theta_V(\mathbf{R}) - 4\pi\rho_{\text{ext}}(\mathbf{R},t). \tag{5.8}$$

We may express the last two terms in Eq. (5.7) together as $\frac{m}{n_0}\beta^2(1 - l_c^2\,\nabla^2)n_1(\mathbf{R},t)$ so as to transform the equation as:

$$U_1(\mathbf{R},t) = -e\,\Phi(\mathbf{R},t) + \frac{m}{n_0}\beta^2(1 - l_c^2\,\nabla^2)n_1(\mathbf{R},t), \tag{5.9}$$

where we define two parameters that characterize the QHD model, $\beta$ and $l_c$. Here, $\beta = v_F/\sqrt{3}$ is a characteristic velocity that represents the speed of propagation of the density disturbances in the EG due to restoring effect of pressure, where $v_F = \frac{\hbar}{m}(3\pi^2 n_0)^{\frac{1}{3}}$ is the Fermi speed of the EG. Notice that this definition of the parameter $\beta$ is often corrected in simulations of the EG dynamics at high frequencies so that $\beta = v_F\sqrt{3/5}$. [32] On the other hand, the parameter $l_c$ provides a characteristic length scale for the density variations in the EG for which the effects of the Bohm potential become important, and is defined as $l_c = \hbar/(2m\beta)$. Using the definition $\beta = v_F/\sqrt{3}$, we may also express this parameter in terms of the inverse Fermi wavenumber $\lambda_F \equiv k_F^{-1} = \hbar/(mv_F)$ of the EG via $l_c = \sqrt{3}\,\lambda_F/2$.

Next, we eliminate the velocity field $\mathbf{v}$ from the above system of equations and obtain the following fourth-order PDE for the induced charge density $\rho(\mathbf{R},t)$ in the EG,

$$\left(\gamma + \frac{\partial}{\partial t}\right)\frac{\partial\rho(\mathbf{R},t)}{\partial t} = -\omega_p{}^2\rho(\mathbf{R},t) + \beta^2(1 - l_c^2\,\nabla^2)\nabla^2\rho(\mathbf{R},t) - \omega_p{}^2\rho_{\text{ext}}(\mathbf{R},t), \tag{5.10}$$

where we have defined $\rho(\mathbf{R},t) = -e\,n_1(\mathbf{R},t)$ and introduced the plasma frequency in the bulk of the EG, $\omega_p = \sqrt{4\pi e^2 n_0/m}$.

We now specify $V$ to be a region defined by $|z| \leq a$ in a cartesian coordinate system where $\mathbf{R} = (x, y, z)$, representing a metal slab with an infinite area and finite thickness of $2a$, which is surrounded by a dielectric material with the relative dielectric constant that only depends on the position $z$, as in Fig. 1.1. Then, the solution of the Poisson equation Eq. (5.8), which is written in the slab geometry as

$$\nabla \cdot [\epsilon_r(z)\nabla\Phi(\mathbf{R},t)] \; = \; -4\pi\rho(\mathbf{R},t)H(a - |z|) - 4\pi\rho_{\text{ext}}(\mathbf{R},t), \tag{5.11}$$

58

with $H$ being the Heaviside unit step function, may be sought for in a piece-wise manner as

$$\Phi(\mathbf{R}, t) = \begin{cases} \Phi^{(m)}(\mathbf{R}, t) & \text{for} \quad |z| < a, \\ \Phi^{(d)}(\mathbf{R}, t) & \text{for} \quad |z| > a, \end{cases} \tag{5.12}$$

where $\Phi^{(m)}$ is the electric potential inside the metal slab and $\Phi^{(d)}$ is the potential in the nearby dielectric(s).


## 5.1   Local hydrodynamic model

We can describe the dynamic polarization of a metal in a purely classical manner, which gives rise to a nondispersive, or local description of the EG, commonly referred as the local response model, or Drude model of the EG. The mathematical formulation of such LHD model is achieved by setting $l_c = 0$ and $\beta = 0$ in Eq. (5.10). Physically, this is based on the assumption that the spatial variations in the electron density are small enough such that $l_c^2 |\nabla^2 \rho| \ll |\rho|$, and $|\nabla^2 \rho| \ll k_s^2 |\rho|$ where $k_s \equiv \omega_p / \beta$ is the inverse TF screening length of the EG. So, the equation for the induced charge density $\rho(\mathbf{R}, t)$ becomes

$$\left( \gamma + \frac{\partial}{\partial t} \right) \frac{\partial \rho(\mathbf{R}, t)}{\partial t} = -\omega_p{}^2 \rho(\mathbf{R}, t) - \omega_p{}^2 \rho_{\text{ext}}(\mathbf{R}, t). \tag{5.13}$$

We define a FT of the induced charge density in the EG with respect to time $t$ as

$$\hat{\rho}(\mathbf{R}, \omega) = \int_{-\infty}^{\infty} dt \, e^{i\omega t} \rho(\mathbf{R}, t), \tag{5.14}$$

with similar definitions for the total potential $\Phi(\mathbf{R}, t)$ and the external charge density $\rho_{\text{ext}}(\mathbf{R}, t)$ yielding the corresponding functions $\hat{\Phi}(\mathbf{R}, \omega)$ and $\hat{\rho}_{\text{ext}}(\mathbf{R}, \omega)$ in the FT space. By Fourier transforming Eq. (5.10) we obtain a simple algebraic equation for $\hat{\rho}$,

$$-i(\gamma - i\omega)\omega \hat{\rho}(\mathbf{R}, \omega) + \omega_p{}^2 \hat{\rho}(\mathbf{R}, \omega) = -\omega_p{}^2 \hat{\rho}_{\text{ext}}(\mathbf{R}, \omega), \tag{5.15}$$

which gives

$$\hat{\rho}(\mathbf{R}, \omega) = \frac{-\omega_p{}^2}{\omega_p{}^2 - \omega(\omega + i\gamma)} \, \hat{\rho}_{\text{ext}}(\mathbf{R}, \omega), \tag{5.16}$$

representing a local relation between the induced and external charge densities in the FT space.

We next consider the Poisson equation (5.8) for the position vector $\mathbf{R}$ inside the metal slab where the background dielectric constant is assumed to be $\epsilon_r = 1$. Performing the FT of that equation with respect to time and using the results from Eq. (5.16) we find

$$\nabla^2 \hat{\Phi}(\mathbf{R}, \omega) = -4\pi \left[ \frac{-\omega_p{}^2}{\omega_p{}^2 - \omega(\omega + i\gamma)} \hat{\rho}_{\text{ext}}(\mathbf{R}, \omega) + \hat{\rho}_{\text{ext}}(\mathbf{R}, \omega) \right]. \tag{5.17}$$

This equation may be rearranged into the form that is isomorphic with the Poisson equation in Eq. (2.14) for the total electric potential in an infinite homogeneous region with a frequency dependent constant $\epsilon(\omega)$

$$\epsilon(\omega) \nabla^2 \hat{\Phi}(\mathbf{R}, \omega) = -4\pi \hat{\rho}_{\text{ext}}(\mathbf{R}, \omega), \tag{5.18}$$

where we define

$$\epsilon(\omega) = 1 - \frac{\omega_p{}^2}{\omega(\omega + i\gamma)}. \tag{5.19}$$

This form of the dielectric constant, or rather function is known as the Drude dielectric function, which describes the dynamic response of the EG in a metal within the LHD model. Note that this result is obtained in the classical limit of the hydrodynamic model by letting $\hbar \to 0$ in Eq. (5.7), which indicates that all the non-local effects in the Poisson equation (5.4) are of quantum mechanical nature.

## 5.1.1  Dispersion relation for local hydrodynamic model

It is worth discussing whether there exists a nontrivial solution for the total potential in Eq. (2.61) in the case that the external charges are absent for a layered structure of dielectrics that contains a metal slab. Assume that the metal slab occupies the region $I_2 : z \in [0, h]$ and is described by the local model using the Drude dielectric function in Eq. (5.19) so that

$$\epsilon_2(\omega) = 1 - \frac{\omega_p{}^2}{\omega(\omega + i\gamma)}. \tag{5.20}$$

Further assume that the metal slab is surrounded by semi-infinite regions $I_1 : z \in (-\infty, 0)$ and $I_3 : z \in (h, \infty)$ consisting of the dielectric materials with dielectric constants $\epsilon_1$ and $\epsilon_3$, respectively. In order to obtain the total potential throughout the entire space, we may consider the three layer structure studied in section 3.3 and use the expressions obtained there for the tensorial components of the GF for the Poisson equation. However, we work here in an extended FT space, where we take both the 2D FT with respect to the spatial variable $\mathbf{r}$, as in Eq. (2.47), and the FT with respect to time $t$, as in Eq. (5.14). Thus, from Eq. (2.61) written in the extended

FT space, the total potential in the region $I_j$ (for $j = 1, 2, 3$) is expressed in the presence of an arbitrary external charge density $\tilde{\rho}_{\text{ext}}(\mathbf{q}, z, \omega)$ as

$$\widetilde{\Phi}_j(\mathbf{q}, z, \omega) = \sum_{k=1}^{3} \int_{I_k} \widetilde{G}_{jk}(\mathbf{q}; z, z', \omega) \, \tilde{\rho}_{\text{ext}}^{(k)}(\mathbf{q}, z', \omega) \, dz', \tag{5.21}$$

where we have restored the dependence on $\mathbf{q}$ and indicated that the FTGF components are now also dependent on frequency via the assignment in Eq. (5.20), where we set $\gamma = 0$. To ensure that a nontrivial solution for $\hat{\Phi}_j(\mathbf{q}, z, \omega)$ exists in any region $j$ when $\tilde{\rho}_{\text{ext}}^{(k)}(\mathbf{q}, z, \omega) \to 0$ in all regions $k$, we need to find conditions that will make the components of the GF $\widetilde{G}_{jk}(\mathbf{q}; z, z', \omega)$ singular in the extended FT space regardless of the location of the points $z$ and $z'$. An inspection of the expressions found for the FTGF components in section 3.1. shows that they all contain a factor

$$\widetilde{G}_{jk}(\mathbf{q}, z, z', \omega) \sim \frac{1}{1 - \lambda_{\text{b}} \lambda_{\text{t}} \Delta}, \tag{5.22}$$

implying that the desired condition for the nontrivial solution may be written as $1 - \lambda_{\text{b}} \lambda_{\text{t}} \Delta = 0$, or equivalently

$$1 - \frac{\epsilon_1 - \epsilon_2}{\epsilon_1 + \epsilon_2} \frac{\epsilon_3 - \epsilon_2}{\epsilon_3 + \epsilon_2} \, \mathrm{e}^{-2qh} = 0. \tag{5.23}$$

If we use $\epsilon_2 \equiv \epsilon_2(\omega)$ given in Eq. (5.20) with $\gamma = 0$ and assume $\epsilon_1 = \epsilon_3 = 1$ for simplicity, we obtain two solutions for the frequency as a function of the wavenumber $q$ as

$$\omega = \frac{\omega_p}{\sqrt{1 + \coth(qa)}}, \tag{5.24}$$

$$\omega = \frac{\omega_p}{\sqrt{1 + \tanh(qa)}}, \tag{5.25}$$

where $a = h/2$ is half of the thickness of the metal slab. Thus, we have shown that there exists a source-free, steady-state response of the EG in a metal slab described by a local model, which is characterized by the eigenmodes called plasma oscillations (or plasmons) of the electron charge density. The resulting expressions for the eigenfrequency $\omega$ as a function of the wavenumber $q$ in Eqs. (5.24) and (5.25) are called even and odd plasmon dispersion relations because they correspond to oscillations of the induced charge density, which are symmetric and antisymmetric functions of the position $z$ with respect to the slab center, respectively.

## 5.2 Standard hydrodynamic model

In the literature on the HD model, the nonlocal effects in a metal are usually treated by keeping the TF pressure term in Eq. (5.10) (i.e., keeping finite $\beta$), while neglecting the quantum effects

due to the Bohm potential. So, by setting $l_c = 0$ in Eq. (5.10) under the assumption $l_c^2|\nabla^2\rho| \ll |\rho|$, we recover the SHD model. In this case the induced charge density $\rho(\mathbf{R}, t)$ in the metal is governed by the equation

$$\left[\left(\gamma + \frac{\partial}{\partial t}\right)\frac{\partial}{\partial t} + {\omega_p}^2 - \beta^2\nabla^2\right]\rho(\mathbf{R}, t) = -{\omega_p}^2\rho_{\text{ext}}(\mathbf{R}, t), \qquad (5.26)$$

which as a second order PDE in the spatial variable and hence needs to be supplemented by the appropriate BCs. Notice that Eq.(5.26) is a nonhomogeneous wave equation for the EG in the metal layer, which upon Fourier transforming its time dependence becomes the Helmholtz equation.

### 5.2.1 Boundary conditions for standard hydrodynamic model

We need to solve Eq. (5.26) for points $\mathbf{R} \in V$ by imposing proper BCs on the induced charge density $\rho(\mathbf{R}, t)$ when $\mathbf{R} \in \partial V$, where $\partial V$ is the interior surface of the boundary of the region $V$. On the other hand, the Poisson equation in Eq. (5.8) needs to be solved in the entire 3D space, so that the potential $\Phi(\mathbf{R}, t)$ vanishes when $\|\mathbf{R}\| \to \infty$ and satisfies the usual electrostatic MCs when $\mathbf{R} \in \partial V$. Those MCs are deduced from the full set of Maxwell's BCs in the quasi-static regime, giving two requirements at a metal-dielectric boundary: the continuity of the electrostatic potential and the continuity of the normal component of the displacement vector field. We notice that, while Eq. (5.26) appears to be decoupled from the Poisson equation Eq. (5.8), a coupling between $\rho(\mathbf{R}, t)$ and $\Phi(\mathbf{R}, t)$ does occur within the BCs for the equation Eq. (5.26).

Clearly, the LHD model does not require any BCs. And in the limit of a SHD, when $l_c = 0$ but $\beta \neq 0$ in Eq. (5.10), we only need one BC for $\rho(\mathbf{R}, t)$ on $\partial V$, which may be motivated by a physical requirement that the normal component of the electron velocity field $\mathbf{v}$ should vanish at an impenetrable boundary $\partial V$, consistent with the specular reflection model (SRM) of a metal surface. [33, 34] Assuming an impenetrable boundary, it is physically plausible to assume that the normal component of the electron velocity vanishes at the boundary,

$$\hat{\mathbf{n}} \cdot \mathbf{v}(\mathbf{R}, t)|_{\mathbf{R}\in\partial V} = 0, \qquad (5.27)$$

where $\hat{\mathbf{n}}$ is a unit vector perpendicular to the surface $\partial V$ at the point $\mathbf{R} \in \partial V$, which points outside the domain $V$, by definition. Then, taking the gradient of Eq. (5.9) and making a scalar product of both sides with $\hat{\mathbf{n}}$, the Eq. (5.27) becomes equivalent to

$$\frac{\partial}{\partial n}U_1(\mathbf{R}, t)\bigg|_{\mathbf{R}\in\partial V} = 0, \qquad (5.28)$$

62

where we have defined the normal derivative by $\frac{\partial}{\partial n} \equiv \hat{\mathbf{n}} \cdot \nabla$. So, the BC for the induced charge density $\rho(\mathbf{R}, t) = -e \, n_1(\mathbf{R}, t)$ in SHD model becomes

$$\frac{\partial}{\partial n} \rho(\mathbf{R}, t) \bigg|_{\mathbf{R} \in \partial V} + \frac{k_s^2}{4\pi} \frac{\partial}{\partial n} \Phi(\mathbf{R}, t) \bigg|_{\mathbf{R} \in \partial V} = 0, \tag{5.29}$$

where $k_s \equiv \omega_p / \beta$. Note that this parameter is known as the inverse screening length in the TF model of an EG, which may be conveniently expressed in terms of the dimensionless electron-electron distance in the EG, defined as $r_s = (4\pi a_B^3 n_0 / 3)^{-1/3}$ with $a_B = \hbar^2 / (me^2)$ being the Bohr radius for electron, as $k_s = \frac{3}{a_B \sqrt{r_s}} \left(\frac{4}{9\pi}\right)^{1/3}$.

## 5.2.2 Method of Green's function for induced charge density and electric potential

Referring to the layer structure described at the beginning of this chapter, we take advantage of the slab geometry and define the extended FT of the induced charge density in the EG with respect to the 2D position vector $\mathbf{r} = (x, y)$ and time $t$ as:

$$\tilde{\rho}(\mathbf{q}, z, \omega) = \int d^2 \mathbf{r} \, e^{-i\mathbf{q} \cdot \mathbf{r}} \int_{-\infty}^{\infty} dt \, e^{i\omega t} \rho(\mathbf{r}, z, t), \tag{5.30}$$

where $\mathbf{q} = (q_x, q_y)$, with a similar definition for the external charge density. Similarly, the FT of the potential $\Phi(\mathbf{R}, t)$ is defined as:

$$\widetilde{\Phi}(\mathbf{q}, z, \omega) = \int d^2 \mathbf{r} \, e^{-i\mathbf{q} \cdot \mathbf{r}} \int_{-\infty}^{\infty} dt \, e^{i\omega t} \Phi(\mathbf{r}, z, t). \tag{5.31}$$

As a result, we get from Eq. (5.26) a second-order PDE for induced charge density as

$$\left(\frac{\partial^2}{\partial z^2} - q_s^2\right) \tilde{\rho}(z) = k_s{}^2 \tilde{\rho}_{\text{ext}}(z), \quad -a \leq x \leq a, \tag{5.32}$$

where we have dropped the variables $\mathbf{q}$ and $\omega$ and defined the parameter

$$q_s = \sqrt{q^2 - \frac{\omega(\omega + i\gamma) - \omega_p{}^2}{\beta^2}}. \tag{5.33}$$

Due to the layer structure the BCs for $\tilde{\rho}(z)$ in Eq. (5.29) become in the FT space

$$\frac{\partial \tilde{\rho}(z)}{\partial z} \bigg|_{z = \pm a} = \frac{k_s^2}{4\pi} E_{\pm}, \tag{5.34}$$

where $E_\pm$ are the normal components of the electric field evaluated at the upper and lower interior boundary points of the metal layer,

$$E_+ = -\left.\frac{\partial \widetilde{\Phi}}{\partial z}\right|_{z=a^{-0}} \quad \text{and} \quad E_- = -\left.\frac{\partial \widetilde{\Phi}}{\partial z}\right|_{z=-a^{+0}}. \tag{5.35}$$

**Generating the two Green's functions**

Before solving Eq. (5.32) for the induced charge density subject to the BCs in Eq. (5.34), we need to determine $E_\pm$. This is achieved by means of the Poisson equation in the FT space for the potential inside the slab Eq. (5.11), where we assume $\epsilon_r = 1$,

$$\left(\frac{\partial^2}{\partial z^2} - q^2\right)\widetilde{\Phi}(z) = -4\pi\left[\widetilde{\rho}(z)H(a - |z|) + \tilde{\rho}_{\text{ext}}(z)\right], \tag{5.36}$$

which gives an expression for the potential in terms of the GF $\widetilde{G}(z, z')$ as

$$\widetilde{\Phi}(z) = \int_{-a}^{a} \widetilde{G}(z, z')\tilde{\rho}(z')\mathrm{d}z' + \int_{-\infty}^{\infty} \widetilde{G}(z, z')\tilde{\rho}_{\text{ext}}(z')\mathrm{d}z', \tag{5.37}$$

that may be used in the in Eq. (5.35).

Notice that we consider a layered structure with three regions such that $z$-dependent dielectric constant has a general form

$$\epsilon(z) = \begin{cases} \epsilon_3, & z \geq a, \\ \epsilon_2, & -a < z < a, \\ \epsilon_1, & z \leq -a. \end{cases} \tag{5.38}$$

Hence, we may use for the GF $\widetilde{G}(z, z')$ in Eq. (5.37) all the results found in section 3.3 where the metal slab occupied the interval $z \in [0, h]$. Denoting the GF in Eq. (5.37) by $\widetilde{G}_{new}(z, z')$ and the GF in section 3.3 by $\widetilde{G}_{old}(z, z'; h)$, we only need to write $h = 2a$ and make the following substitutions

$$\widetilde{G}_{new}(z, z') = \widetilde{G}_{old}(z + a, z' + a; 2a) \tag{5.39}$$

to be able to use the results of section 3.3.

We also wish to solve Eq. (5.32) for the induced charge density by means of the GF method. Note that the BCs at $z = \pm a$ in Eq. (5.34) are of the nonhomogeneous Neumann type. Thus, we need a GF for Eq. (5.32), denoted $D(z, z')$, which satisfies homogeneous Neumann BCs at

$z = \pm a$. Then, we may express the solution of Eq. (5.32) for $\widetilde{\rho}$ subject to the nonhomogeneous BCs in Eq. (5.34) as

$$\widetilde{\rho}(z, z') = \int_{-a}^{a} D(z, z') \widetilde{\rho}_{\text{ext}}(z') \mathrm{d}z' - D(z, a) \frac{E_+}{4\pi} + D(z, -a) \frac{E_-}{4\pi}. \tag{5.40}$$

Here, the GF $D(z, z')$ is a solution of the nonhomogeneous boundary value problem when the source point is inside the metal slab $-a < z' < a$, given by

$$\left( \frac{\partial^2}{\partial z^2} - q_s^2 \right) D(z, z') = k_s{}^2 \delta(z - z'), \tag{5.41}$$

$$\left. \frac{\partial D}{\partial z}(z, z') \right|_{z=-a} = 0 \quad \text{and} \quad \left. \frac{\partial D}{\partial z}(z, z') \right|_{z=a} = 0. \tag{5.42}$$

As before, we assume $D(z, z')$ in the form

$$D(z, z') = \begin{cases} D_> = A \, e^{q_s z} + B \, e^{-q_s z}, & -a \le z' < z \le a, \\ D_< = C \, e^{q_s z} + D \, e^{-q_s z}, & -a \le z < z' \le a, \end{cases} \tag{5.43}$$

where $A, B, C, D$ are to be determined from the homogeneous Neumann BCs and the usual continuity and jump conditions at $z = z'$,

$$\begin{cases} D_>(z', z') = D_<(z', z'), \\ \left. \frac{\partial D_>}{\partial z}(z, z') \right|_{z=z'} - \left. \frac{\partial D_<}{\partial z} \right|_{z=z'} (z, z') = k_s{}^2. \end{cases} \tag{5.44}$$

The final answer is

$$D(z, z') = -\frac{k_s{}^2}{q_s \sinh(2q_s a)} \begin{cases} \cosh[q_s(z + a)] \, \cosh[q_s(z' - a)], & z < z', \\ \cosh[q_s(z - a)] \, \cosh[q_s(z' + a')], & z > z'. \end{cases} \tag{5.45}$$

Alternatively, a compact form using the absolute value is:

$$D(z, z') = -\frac{k_s{}^2}{2q_s \sinh(2q_s a)} \left\{ \cosh[q_s(z + z')] + \cosh[q_s(2a - |z - z'|)] \right\}. \tag{5.46}$$

**Results for $E_-$ and $E_+$**

Before applying the specific GFs for $\widetilde{G}(z, z)$ and $D(z, z')$, we first obtain a general expression for the density $\widetilde{\rho}$ by substituting the expression for $\widetilde{\rho}$ in Eq. (5.40) into Eq. (5.37):

$$\begin{aligned}
\widetilde{\Phi}(z) &= \int_{-\infty}^{\infty} \widetilde{G}(z, z') \widetilde{\rho}_{\text{ext}}(z') \mathrm{d}z' + \int_{-a}^{a} \widetilde{G}(z, z') \int_{-a}^{a} D(z', z'') \widetilde{\rho}_{\text{ext}}(z'') \mathrm{d}z'' \mathrm{d}z' \\
&\quad - \frac{E_+}{4\pi} \int_{-a}^{a} \widetilde{G}(z, z') D(z', a) \mathrm{d}z' + \frac{E_-}{4\pi} \int_{-a}^{a} \widetilde{G}(z, z') D(z', -a) \mathrm{d}z'
\end{aligned} \tag{5.47}$$

65

By differentiating Eq. (5.47) with respect to $z$ and setting $z = -a$, $z = a$, we obtain two coupled algebraic equations for $E_+ = -\left.\frac{d\widetilde{\Phi}}{dz}\right|_{z=a^{-0}}$ and $E_- = -\left.\frac{d\widetilde{\Phi}}{dz}\right|_{z=-a^{+0}}$ as:

$$
E_+ \left[ 1 - \frac{1}{4\pi} \int_{-a}^{a} \left.\frac{\partial \widetilde{G}_{22}}{\partial z}\right|_{z=a} D(z', a) dz' \right] + E_- \frac{1}{4\pi} \int_{-a}^{a} \left.\frac{\partial \widetilde{G}_{22}}{\partial z}\right|_{z=a} D(z', -a) dz'
$$

$$
= -\int_{-\infty}^{\infty} \left.\frac{\partial \widetilde{G}}{\partial z}\right|_{z=a^{-0}} \tilde{\rho}_{\text{ext}}(z') dz' - \int_{-a}^{a} \left.\frac{\partial \widetilde{G}_{22}}{\partial z}\right|_{z=a} \int_{-a}^{a} D(z', z'') \tilde{\rho}_{\text{ext}}(z'') dz'' dz', \qquad (5.48)
$$

$$
E_- \left[ 1 + \frac{1}{4\pi} \int_{-a}^{a} \left.\frac{\partial \widetilde{G}_{22}}{\partial z}\right|_{z=-a} D(z', a) dz' \right] - E_- \frac{1}{4\pi} \int_{-a}^{a} \left.\frac{\partial \widetilde{G}_{22}}{\partial z}\right|_{z=-a} D(z', -a) dz'
$$

$$
= -\int_{-\infty}^{\infty} \left.\frac{\partial \widetilde{G}}{\partial z}\right|_{z=-a^{+0}} \tilde{\rho}_{\text{ext}}(z') dz' - \int_{-a}^{a} \left.\frac{\partial \widetilde{G}_{22}}{\partial z}\right|_{z=-a} \int_{-a}^{a} D(z', z'') \tilde{\rho}_{\text{ext}}(z'') dz'' dz', \qquad (5.49)
$$

where we have indicated that the diagonal component of the GF should be used when both $z$ and $z'$ are in the region 2 occupied by the metal slab.

### 5.2.3   Dispersion relation for standard hydrodynamic model

When the external charge is absent, $\tilde{\rho}_{\text{ext}}(z) = 0$, the first two terms on the right hand side of Eq. (5.47) vanish, but the resulting electrostatic potential may remain finite if the coefficients $E_-$ and $E_+$ are not both zero. Noticing that the system of equations (5.48) and (5.49) for $E_-$ and $E_+$ becomes homogeneous when $\tilde{\rho}_{\text{ext}}(z) = 0$, one may seek a relation between the frequency $\omega$ and the wavenumber $q = \|\mathbf{q}\|$ that gives rise to a nontrivial solution for $E_-$ and $E_+$, and hence to a finite $\widetilde{\Phi}(z)$ in Eq. (5.47). As in the case of the LHD, assuming $\gamma = 0$ this relation will give us the plasmon dispersion curves for the SHD.

For purpose of finding the plasmon dispersion, we assume that $\epsilon_1 = \epsilon_2 = \epsilon_3 = 1$, which leads to the free-space Poisson GF as:

$$
\widetilde{G}(z, z') = -\frac{2\pi}{q} e^{-q|z-z'|}. \qquad (5.50)
$$

Naturally, after obtaining the results for the two GF $\widetilde{G}(z, z')$ and $D(z, z')$, we can solve for two unknown $E_-$ and $E_+$ by equation set Eq. (5.48) and Eq. (5.49). In order to ensure that

the solution is nontrivial, the determinant of the matrix defining the system of equations should vanish. If we denote

$$C_{--} = -\frac{1}{4\pi} \int_{-a}^{a} \frac{\partial \widetilde{G}}{\partial z}(z, z') \bigg|_{z=-a} D(z', -a), \tag{5.51}$$

$$C_{-+} = -\frac{1}{4\pi} \int_{-a}^{a} \frac{\partial \widetilde{G}}{\partial z}(z, z') \bigg|_{z=-a} D(z', a), \tag{5.52}$$

$$C_{++} = \frac{1}{4\pi} \int_{-a}^{a} \frac{\partial \widetilde{G}}{\partial z}(z, z') \bigg|_{z=a} D(z', a), \tag{5.53}$$

$$C_{+-} = \frac{1}{4\pi} \int_{-a}^{a} \frac{\partial \widetilde{G}}{\partial z}(z, z') \bigg|_{z=a} D(z', -a), \tag{5.54}$$

we can show that $C_{++} = C_{--} \equiv M$ and $C_{+-} = C_{-+} \equiv N$, where by implementing the two GFs in Eq. (5.50) and Eq. (5.46) we find

$$M = \frac{1}{2q_s \sinh(2q_s a)} \frac{1}{q^2 - q_s^2} \left[ -q \, e^{-2qa} + q \cosh(2q_s a) - q_s \sinh(2q_s a) \right], \tag{5.55}$$

$$N = \frac{1}{2q_s \sinh(2q_s a)} \frac{1}{q^2 - q_s^2} e^{-2qa} \left[ q \, e^{2qa} - q_s \cosh(2q_s a) - q_s \sinh(2q_s a) \right]. \tag{5.56}$$

Finally, when $\tilde{\rho}_{\text{ext}}(z) = 0$ the Eqs. (5.48) and (5.49) become

$$\begin{cases} (1 - M) \, E_+ + N \, E_- = 0, \\ N \, E_+ + (1 - M) \, E_- = 0, \end{cases} \tag{5.57}$$

which gives rise to a nontrivial solution if and only if the the determinant of the coefficients defining this system vanishes, i.e.,

$$(1 - M)^2 - N^2 = 0, \tag{5.58}$$

giving two equations that need to be solved for the frequency $\omega$ as a function of $q$,

$$\begin{cases} 1 - M - N = 0, \\ 1 - M + N = 0. \end{cases} \tag{5.59}$$

If we set $\gamma = 0$ and define the reduced frequency as $\Omega = \omega/\omega_p$, after some algebra we find that the plasmon dispersion relations for the even and odd modes in the SHD may be obtained by

solving the following two equations, respectively

$$\Omega^2 = e^{-qa} \sinh(qa) \left[ 1 + \frac{q}{q_s} \coth(q_s a) \right], \tag{5.60}$$

$$\Omega^2 = e^{-qa} \cosh(qa) \left[ 1 + \frac{q}{q_s} \tanh(q_s a) \right]. \tag{5.61}$$

In Fig. 5.1, we show the results of solving Eqs. (5.60) and (5.61) for the reduced frequency $\Omega$ as a function of the reduced wavenumber $qa$ by choosing the screening parameter in the nonlocal SHD model such that $k_s a = 10$. Those results are compared with the plasmon dispersion relations for the even and odd modes in the EG described by the local model, given in Eqs. (5.24) and (5.25), respectively. It is noteworthy that there are only one even and one odd plasmon dispersion relations in the local model, which do not exceed the bulk plasma frequency $\omega_p$. The even and odd eigenfrequencies approach the values $\omega = \omega_p$ and $\omega = 0$ in the limit of long wavelengths, $qa \to 0$, respectively, while they both converge to a common value $\omega = \omega_p/\sqrt{2}$ at short wavelengths, $qa \gg 1$, which is characteristic of the so-called surface plasmon in a thick metal slab within the local model.

On the other hand, one notices that the results for the SHD model give rise to multiple plasmon dispersion relations for both even and odd modes, labeled by $n = 0, 1, 2, \ldots$. The modes labeled $n = 0$ seem to be derived from the even and odd modes of the local model as they converge to their respective dispersion relations in the limit of long wavelengths, or for a thin metal slab with $qa \ll 1$. In particular, it appears that the reduced frequency for the $n = 0$ modes is bounded by $\Omega < \sqrt{1 + q^2/k_s{}^2}$, which makes the parameter $q_s$ in Eq. (5.33) with $\gamma = 0$ real and positive, so that the corresponding solutions of Eq. (5.32) for the SHD model are localized near the surfaces of the metal slab. Hence the $n = 0$ modes are associated with the surface plasmons, which are of interest in the nanoplasmonic applications.

On the other hand, the plasmon dispersion relations for the higher harmonics in the SHD model, labeled $n = 1, 2, 3 \ldots$, have reduced frequencies higher than $\Omega = \sqrt{1 + q^2/k_s{}^2}$, so that the corresponding values of $q_s$ in Eq. (5.33) with $\gamma = 0$ are purely imaginary, giving rise to oscillatory solutions of Eq. (5.32) throughout the metal slab, which are related to the bulk plasmon modes. One can see that in the SHD model all the bulk plasmon modes and the even surface plasmon mode exhibit positive dispersion characterized by an increase in frequency with increasing wavenumber $q$. This is not true, however, for the odd surface mode, which has a negative dispersion for small $q$ that passes through a minimum and joins the even surface mode at higher $q$ values. Finally, one notices that all the plasmon dispersion relations in the SHD model become approximately linear functions of the wavenumber for sufficiently large values of $qa$.
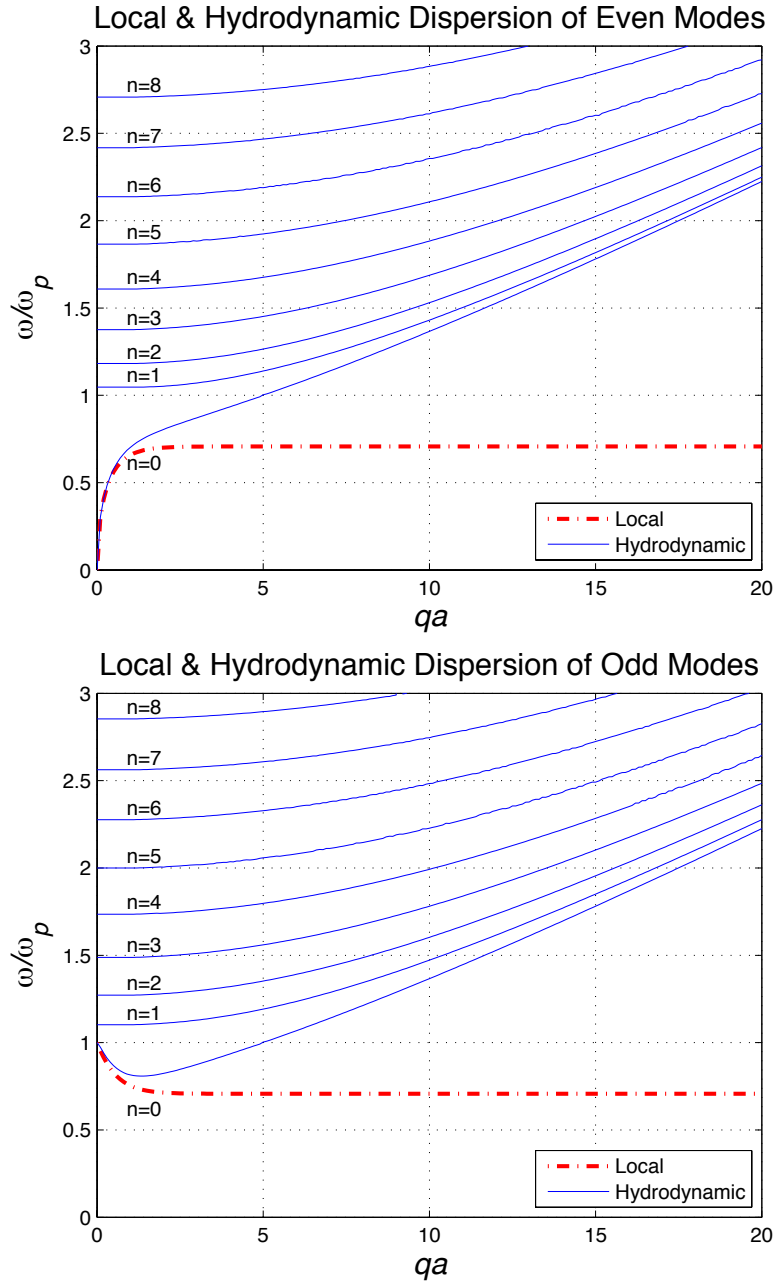
Figure 5.1: Dispersion relations for both the (a) even and (b) odd plasmon modes in a metal slab of thickness $a$. The results are shown for both the hydrodynamic model with nonlocal effects (blue solid lines) and the local model (red dashed lines) of the EG with the density parameter fixed at $r_s = 3$. The TF screening length in the EG is chosen so that $k_s a = 10$.

## 5.3 Quantum hydrodynamic model

If we want to fully retain quantum effects which give rise to a QHD model, we have to keep both $\beta$ and $l_c$ finite. As a consequence, the equation for the induced charge density in the metal slab, Eq. (5.10), remains a fourth-order PDE in the spatial variables and hence requires ABCs in comparison to the equation Eq. (5.26) for the SHD model. It is physically justified to retain here the SRM-motivated requirement of vanishing normal component of the electron velocity at the metal-dielectric boundary, which gives the BC in Eq. (5.28), as one of the BCs for Eq. (5.10) in the QHD model. However, since it is not obvious how one can choose the other condition, we search here for an ABC to be imposed on the induced charge density $\rho(\mathbf{R}, t)$ when the point $\mathbf{R}$ approaches the *interior* surface of the boundary $\partial V$ of the closed region $V$ occupied by the EG.

By using the FT with respect to time as in Eq. (5.14), we deduce an equation for the FT of the induced charge density in the EG from Eq. (5.10) as:

$$\left[ \nabla^2 \nabla^2 - k_c^2 \nabla^2 - k_c^2 \frac{\omega(\omega + i\gamma) - \omega_p^2}{\beta^2} \right] \hat{\rho}(\mathbf{R}, \omega) = - (k_c k_s)^2 \hat{\rho}_{\text{ext}}(\mathbf{R}, \omega), \tag{5.62}$$

where we define $k_c \equiv l_c^{-1}$. Note that this parameter may be conveniently expressed in terms of the electron density parameter as $k_c = \frac{2}{\sqrt{3}\, r_s a_B} \left( \frac{9\pi}{4} \right)^{1/3}$. One may further deduce from the linearized potential energy in Eq. (5.9) and the general formulation of the SRM condition in Eq. (5.28) that $\hat{\rho}(\mathbf{R}, \omega)$ has to satisfy the following physical BC

$$\frac{\partial}{\partial n}(k_c^2 - \nabla^2)\hat{\rho}(\mathbf{R}, \omega)\bigg|_{\mathbf{R} \in \partial V} = - \frac{(k_c k_s)^2}{4\pi} \frac{\partial \hat{\Phi}}{\partial n}(\mathbf{R}, \omega)\bigg|_{\mathbf{R} \in \partial V}. \tag{5.63}$$

Noting that Eq. (5.62) is a fourth-order PDE, we have to find an ABC for $\hat{\rho}(\mathbf{R}, \omega)$ on $\partial V$.

### 5.3.1 Additional boundary condition for quantum hydrodynamic model

In order to search for ABCs properly, we consider the eigenvalue problem associated with Eq. (5.62). Specifically, if we define the operator $\check{\mathcal{L}}$ appearing on the LHS of that equation as

$$\check{\mathcal{L}} = \nabla^2 \nabla^2 - k_c^2 \nabla^2 + Q, \tag{5.64}$$

where $Q \equiv k_c^2 \left( \omega_p^2 - \omega^2 \right) / \beta^2$, then we need to find nontrivial solutions of the associated homogeneous equation $\check{\mathcal{L}}[\hat{\rho}] = 0$, which are subject to suitable *homogeneous* BCs on $\partial V$ that will make $\check{\mathcal{L}}$ a Hermitian, or self-adjoint operator. Let us assume that $u(\mathbf{R})$ and $v(\mathbf{R})$ are any two

scalar functions of the position $\mathbf{R}$ that satisfy the same homogeneous equation, $\check{\mathcal{L}}[u] = 0$ and $\check{\mathcal{L}}[v] = 0$, for $\mathbf{R} \in V$, as well as the same set of homogeneous BCs for $\mathbf{R} \in \partial V$. Since we must ensure that

$$\int_V u \, \check{\mathcal{L}}[v] \, \mathrm{d}^3 \mathbf{R} = \int_V v \, \check{\mathcal{L}}[u] \, \mathrm{d}^3 \mathbf{R}, \tag{5.65}$$

for all such functions, we integrate the difference $u \, \check{\mathcal{L}}[v] - v \, \check{\mathcal{L}}[u]$ over the region $V$ and use twice the Green's 2nd identity,

$$\int_V \left( u \nabla^2 v - v \nabla^2 u \right) \mathrm{d}^3 \mathbf{R} = \oint_{\partial V} \left( u \frac{\partial v}{\partial n} - v \frac{\partial u}{\partial n} \right) \mathrm{d}S, \tag{5.66}$$

to obtain

$$\begin{aligned}
\int_V \left( u \, \check{\mathcal{L}}[v] - v \, \check{\mathcal{L}}[u] \right) \mathrm{d}^3 \mathbf{R} &= \oint_{\partial V} \left[ u \frac{\partial}{\partial n} \nabla^2 v - \nabla^2 v \frac{\partial u}{\partial n} + \nabla^2 u \frac{\partial v}{\partial n} - v \frac{\partial}{\partial n} \nabla^2 u \right. \\
&\quad - \left. k_c^2 \left( u \frac{\partial v}{\partial n} - v \frac{\partial u}{\partial n} \right) \right] \mathrm{d}S,
\end{aligned} \tag{5.67}$$

We can ensure that Eq. (5.65) will be true if the integral in the right-hand side of Eq. (5.67) is zero, which will be guaranteed by making its integrand vanish on the boundary,

$$\left[ u \frac{\partial}{\partial n} \nabla^2 v - \nabla^2 v \frac{\partial u}{\partial n} + \nabla^2 u \frac{\partial v}{\partial n} - v \frac{\partial}{\partial n} \nabla^2 u - k_c^2 \left( u \frac{\partial v}{\partial n} - v \frac{\partial u}{\partial n} \right) \right]\Bigg|_{\mathbf{R} \in \partial V} = 0, \tag{5.68}$$

Since we wish to make one of the homogeneous BCs for the functions $u$ and $v$ to be associated with the physical BC in Eq. (5.63), so that $\frac{\partial}{\partial n}(k_c^2 - \nabla^2)u\big|_{\mathbf{R} \in \partial V} = 0$ and $\frac{\partial}{\partial n}(k_c^2 - \nabla^2)v\big|_{\mathbf{R} \in \partial V} = 0$, we also rewrite the condition in Eq. (5.68) as

$$\begin{aligned}
[(k_c^2 - \nabla^2)v] \frac{\partial}{\partial n}[(k_c^2 - \nabla^2)u] &- [(k_c^2 - \nabla^2)u] \frac{\partial}{\partial n}[(k_c^2 - \nabla^2)v] \\
&+ \nabla^2 u \frac{\partial}{\partial n} \nabla^2 v - \nabla^2 v \frac{\partial}{\partial n} \nabla^2 u = 0,
\end{aligned} \tag{5.69}$$

for all $\mathbf{R} \in \partial V$. A careful analysis of Eqs. (5.68) and (5.69) shows that there are five sets of homogeneous BCs to be satisfied by the functions $u$ and $v$ on $\partial V$ that will make the right-hand

71

side in Eq. (5.65) vanish:

$$\frac{\partial u}{\partial n} = 0 \qquad \text{and} \qquad u = 0 \tag{5.70}$$

$$\frac{\partial u}{\partial n} = 0 \qquad \text{and} \qquad \frac{\partial}{\partial n}\left(\nabla^2 u\right) = 0 \tag{5.71}$$

$$(k_c{}^2 - \nabla^2)u = 0 \qquad \text{and} \qquad u = 0 \tag{5.72}$$

$$(k_c{}^2 - \nabla^2)u = 0 \qquad \text{and} \qquad \frac{\partial}{\partial n}\left(\nabla^2 u\right) = 0 \tag{5.73}$$

$$\frac{\partial}{\partial n}\left[\left(k_c{}^2 - \nabla^2\right)u\right] = 0 \qquad \text{and} \qquad \nabla^2 u = 0, \tag{5.74}$$

with the BCs for the function $v$ having the same form. However, the only two conditions that are consistent with the physical requirement in Eq. (5.63) are given in Eqs. (5.71) and (5.74). So, we assert that the proper sets of BCs to be imposed on the solution $\hat{\rho}(\mathbf{R}, \omega)$ of Eq. (5.62) on the boundary $\partial V$ are given by

$$\frac{\partial \hat{\rho}}{\partial n} = -\frac{k_s^2}{4\pi}\frac{\partial \hat{\Phi}}{\partial n} \qquad \text{and} \qquad \frac{\partial}{\partial n}\left(\nabla^2 \hat{\rho}\right) = 0, \tag{5.75}$$

$$\frac{\partial}{\partial n}\left[\left(k_c{}^2 - \nabla^2\right)\hat{\rho}\right] = -\frac{(k_c k_s)^2}{4\pi}\frac{\partial \hat{\Phi}}{\partial n} \qquad \text{and} \qquad \nabla^2 \hat{\rho} = 0. \tag{5.76}$$

where we refer to Eq. (5.75) as the set 1 and Eq. (5.76) as the set 2 of the BCs. For the slab geometry of the main text we have $\frac{\partial}{\partial n} = \frac{\partial}{\partial z}$ and, performing an additional FT over the 2D position vector $\mathbf{r} = (x, y)$ in Eqs. (5.75) and (5.76), we may deduce the BCs given in Eqs. (5.87) and (5.88) below.

Thus we have found that, in addition to the physical requirement that the normal component of the electron velocity (or the corresponding electron flux) should vanish at the impenetrable boundary $\partial V$, also required are conditions to be imposed on the values of either the Bohm quantum potential, which is proportional to $\nabla^2 \hat{\rho}$, or on the associated quantum flux, $\frac{\partial}{\partial n}\nabla^2 \hat{\rho}$, on the boundary $\partial V$. We assume that both these additional conditions are homogeneous, which is in accord with the common practice in using the so-called quantum drift-diffusion model in computer simulations of semiconductor devices. [35, 36, 37]

We find that, interestingly, there are two ABCs that are consistent with the vanishing normal component of the electron velocity. Those ABCs are found to require that either the Bohm potential, which is proportional to $\nabla^2 \rho$ according to Eq. (5.7), or the normal component of the associated Bohm force should vanish on $\partial V$. It is gratifying to recognize that the same types of ABCs often arise in the computational schemes that use variations of the QHD model in computer simulations of semiconductor devices. [36, 37]

### 5.3.2 Induced charge density in metal

Taking advantage of the slab geometry, we define the FT with respect to the 2D position vector $\mathbf{r}$ and time $t$ for the induced charge density in the EG, external charge density and the total electric potential as in Eqs. (5.30), (5.78), and (5.31), respectively. Then, from Eq. (5.10) we obtain a fourth-order ODE for the induced charge density

$$\left[\left(\frac{\partial^2}{\partial z^2} - q^2\right)^2 - k_c{}^2\left(\frac{\partial^2}{\partial z^2} - q^2\right) + k_c{}^2\frac{\omega_p{}^2 - \omega(\omega + i\gamma)}{\beta^2}\right]\tilde{\rho}(z) = -\left(k_c k_s\right)^2\tilde{\rho}_{\text{ext}}(z), \quad (5.77)$$

where we have dropped the explicit dependencies of $\tilde{\rho}$ and $\tilde{\rho}_{\text{ext}}$ on $\mathbf{q}$ and $\omega$, and let $q^2 = q_x^2 + q_y^2$.

To make progress, we limit our considerations to external charge density that represents a point charge that moves parallel to the metal layer at distance $z_0$ inside that layer, $-a < z_0 < a$, with the FT written as

$$\tilde{\rho}_{\text{ext}}(z) = \tilde{\rho}_0\,\delta(z - z_0). \quad (5.78)$$

It is further convenient to rewrite Eq. (5.77) in a factored form,

$$\left(\frac{\partial^2}{\partial z^2} - q_-^2\right)\left(\frac{\partial^2}{\partial z^2} - q_+^2\right)\tilde{\rho}(z) = -\left(k_c k_s\right)^2\tilde{\rho}_0\,\delta(z - z_0), \quad (5.79)$$

where we defined the wavenumbers $q_\pm$ as

$$q_\pm = \sqrt{q^2 + \frac{1}{2}k_c{}^2\left\{1 \pm \sqrt{1 + 4\left(\frac{k_s}{k_c}\right)^2\left[\frac{\omega(\omega + i\gamma)}{\omega_p{}^2} - 1\right]}\right\}}. \quad (5.80)$$

It is worthwhile mentioning that, for frequencies close to the bulk plasma frequency, $\omega \approx \omega_p$ with $\gamma \approx 0$, one finds from Eq (5.80) that $q_+ \approx \sqrt{q^2 + k_c{}^2}$ and $q_- \approx q_s$ with the parameter $q_s$ defined in Eq. (5.33) for the SHD model. The same limiting expressions for $q_\pm$ are obtained for arbitrary frequencies if one considers formally the case $k_s \ll k_c$, or $l_c k_s \ll 1$, corresponding to the neglect of the gradient correction in Eq. (5.7). One may recognize that the above limiting expression for $q_-$ corresponds to the wavenumber that was introduced in Ref. 15 to discuss the plasmon dispersion relations in a metal slab described by the SHD model. On the other hand, taking the formal limit of $k_c \to \infty$ gives $q_+ \approx k_c$ and allows the reduction of Eq. (5.79) to a second-order differential equation commensurate with the SHD model, as discussed in Ref. 39.

We may write the general solution of Eq. (5.79) as a sum of the general solution of the associated homogeneous equation, $\tilde{\rho}_h$, and a particular solution, $\tilde{\rho}_p$, for the specific form of the external charge density,

$$\tilde{\rho}(z) = \tilde{\rho}_h(z) + \tilde{\rho}_p(z), \quad (5.81)$$

73

Thus, we find from Eq. (5.79)

$$\tilde{\rho}_h(z) = \sum_{j=1}^{4} A_j \, f_j(z), \tag{5.82}$$

where $f_1(z) = \cosh(q_+z)$, $f_2(z) = \cosh(q_-z)$, $f_3(z) = \sinh(q_+z)$, and $f_4(z) = \sinh(q_-z)$, with $A_j$ (for $j = 1, 2, 3, 4$) being arbitrary constants.

For the particular solution of the fourth-order equation in Eq. (5.79) one may use GFs $D_\pm(x, x_0)$ for the associated second-order equations,

$$\left( \frac{\partial^2}{\partial z^2} - q_\pm^2 \right) D_\pm(z, z_0) = \delta(z - z_0), \tag{5.83}$$

whence it may be easily verified that

$$\tilde{\rho}_p(z) = -\tilde{\rho}_0 \frac{(k_c k_s)^2}{q_+^2 - q_-^2} [D_+(z, z_0) - D_-(z, z_0)]. \tag{5.84}$$

Referring to the BC we discussed before, Eq. (5.77) needs to be solved on the interval $|z| \leq a$ subject to BCs, which include the gradients of the electronic charge density at $z = \pm a$, see Eqs. (5.87) and (5.88) below. Hence, it is convenient to use the GFs for Eq. (5.83) that are defined on the interval $-a \leq z \leq a$ and satisfy the homogeneous Neumann BCs at its endpoints

$$\left. \frac{\partial D_\pm}{\partial z}(z, z_0) \right|_{z=\pm a} = 0, \tag{5.85}$$

as in Eqs. (5.41) and (5.42). Thus, from Eqs. (5.83) and (5.85) we find

$$D_\pm(z, z_0) = -\frac{\cosh[q_\pm(a + z_<)] \, \cosh[q_\pm(a - z_>)]}{q_\pm \sinh(2q_\pm a)}, \tag{5.86}$$

where $z_> = \max(z, z_0)$ and $z_< = \min(z, z_0)$.

Finally, having found the general solution of Eq. (5.79) for the FT of the induced charge density, we invoke the results obtained before for the BCs. Namely, the solution given in Eqs. (5.81), (5.82) and (5.84) needs to satisfy either the set 1 or set 2 of BCs at $z = \pm a$, which follow from Eqs. (5.75) and (5.76) as

$$\left. \frac{\partial \tilde{\rho}}{\partial z} \right|_{z=\pm a} = -\frac{k_s^2}{4\pi} \left. \frac{\partial \tilde{\Phi}^{(m)}}{\partial z} \right|_{z=\pm a} \quad \text{and} \quad \left( \frac{\partial^2}{\partial z^2} - q^2 \right) \left. \frac{\partial \tilde{\rho}}{\partial z} \right|_{z=\pm a} = 0, \tag{5.87}$$

$$\left(k_c{}^2 + q^2 - \frac{\partial^2}{\partial z^2}\right)\frac{\partial\tilde{\rho}}{\partial z}\bigg|_{z=\pm a} = -\frac{(k_c k_s)^2}{4\pi}\frac{\partial\tilde{\Phi}^{(m)}}{\partial z}\bigg|_{z=\pm a} \quad\text{and}\quad \left(\frac{\partial^2}{\partial z^2} - q^2\right)\tilde{\rho}\bigg|_{z=\pm a} = 0. \quad (5.88)$$

where $\tilde{\Phi}^{(m)}(\mathbf{q}, z, \omega)$ is the FT of the electric potential inside the metal slab. Note that the first condition in Eq. (5.87) is the only BC that is needed for solving the SHD model. Recall that taking the formal limit $k_c \to \infty$ converts Eq. (5.79) into a second-order differential equation for the SHD model. We now see that taking the same limit in the first condition in Eq. (5.88) reproduces the first condition in Eq. (5.87) and, since the additional conditions in those two equations are not needed for the SHD model, the ambiguity of having two sets of BCs is removed for that model.

### 5.3.3 Electric potential

Assuming that the background relative dielectric constant in the metal slab is $\epsilon_r = 1$, we obtain from Eq. (5.11) an equation for the FT of the electric potential $\tilde{\Phi}^{(m)}(\mathbf{q}, z, \omega)$ in that region, given by

$$\left(\frac{\partial^2}{\partial z^2} - q^2\right)\tilde{\Phi}^{(m)}(z) = -4\pi\tilde{\rho}(z) - 4\pi\tilde{\rho}_0\,\delta(z - z_0), \quad (5.89)$$

where we have dropped the explicit dependencies of $\tilde{\Phi}^{(m)}$, the induced charge density $\tilde{\rho}$ and the external charge magnitude $\tilde{\rho}_0$ on $\mathbf{q}$ and $\omega$. A general solution of Eq. (5.89) may be written as the sum $\tilde{\Phi}^{(m)} = \tilde{\Phi}_h^{(m)} + \tilde{\Phi}_p^{(m)}$, which consists of a general solution of the associated homogeneous equation,

$$\tilde{\Phi}_h^{(m)}(z) = B_1\cosh(qz) + B_2\sinh(qz), \quad (5.90)$$

where $B_1$ and $B_2$ are arbitrary constants, and a particular solution of Eq. (5.89),

$$\tilde{\Phi}_p^{(m)}(z) = \int_{-a}^{a}\widetilde{G}(z, z')\left[\tilde{\rho}_h(z') + \tilde{\rho}_p(z')\right]\,dz' + \tilde{\rho}_0\widetilde{G}(z, z_0). \quad (5.91)$$

Here, we have used the expression for the induced charge density in Eq. (5.81) and the expression for the external charge in Eq. (5.78), with $\widetilde{G}(z, z')$ being the free-space GF for the equation in Eq. (5.89), given by

$$\widetilde{G}(z, z') = \frac{2\pi}{q}\,e^{-q|z-z'|}. \quad (5.92)$$

A comment is due regarding the two terms in the particular solution $\tilde{\Phi}_p^{(m)}(z)$, which arise from the integrals in Eq. (5.91). Even though those integrals are well defined in terms of

75

Eqs. (5.82), (5.84), (5.86), and (5.92), their computation may be tedious for arbitrary values of $z$ and $z_0$. However, those computations may be aided by noticing that the first term is given by

$$\int_{-a}^{a} \widetilde{G}(z,z')\tilde{\rho}_h(z')\,dz' = \sum_{j=1}^{4} A_j\,F_j(z),$$

(5.93)

where

$$
\begin{aligned}
F_j(z) &\equiv \int_{-a}^{a} \widetilde{G}(z,z')f_j(z')\,dz' \\
&= \frac{1}{q_j^2 - q^2}[-4\pi f_j(z) + \widetilde{G}(z,a)f_j'(a) - \widetilde{G}(z,-a)f_j'(-a)] \\
&\quad + \frac{1}{q_j^2 - q^2}\left[ -\left.\frac{\partial}{\partial z'}\widetilde{G}(z,z')\right|_{z'=a} f_j(a) + \left.\frac{\partial}{\partial z'}\widetilde{G}(x,x')\right|_{x'=-a} f_j(-a)\right],
\end{aligned}
$$

(5.94)

with $q_1 = q_3 = q_+$, $q_2 = q_4 = q_-$, and $f_j'(z) = df_j/dz$ denoting the derivatives of the functions $f_j(z)$ defined in Eq. (5.82) for $j = 1, 2, 3, 4$, whereas the second term is given by

$$\int_{-a}^{a} \widetilde{G}(z,z')\tilde{\rho}_p(z')\,dz' = -(k_c k_s)^2 \frac{\tilde{\rho}_0}{q_+^2 - q_-^2}\left[\Delta_+(z,z_0) - \Delta_-(z,z_0)\right],$$

(5.95)

where

$$
\begin{aligned}
\Delta_{\pm}(z,z_0) &\equiv \int_{-a}^{a} \widetilde{G}(z,z')D_{\pm}(z',z_0)\,dz' \\
&= -\frac{1}{q_{\pm}^2 - q^2}[\widetilde{G}(z,z_0) + 4\pi D_{\pm}(z,z_0)] \\
&\quad - \frac{1}{q_{\pm}^2 - q^2}\left[\left.\frac{\partial}{\partial z'}\widetilde{G}(z,z')\right|_{z'=a} D_{\pm}(a,z_0) - \left.\frac{\partial}{\partial z'}\widetilde{G}(z,z')\right|_{z'=-a} D_{\pm}(-a,z_0)\right]
\end{aligned}
$$

(5.96)

On the other hand, with no sources of charge outside the metal slab, the Poisson equation in Eq. (5.11) becomes the Laplace equation for the potential $\Phi^{(d)}(\mathbf{R}, t)$ in the dielectrics. Assuming that the dielectrics are homogeneous semi-infinite regions on either side of the metal slab, a general solution of the Laplace equation that vanishes as $|z| \to \infty$ gives for the FT of the electric potential $\tilde{\Phi}^{(d)}(\mathbf{q}, z, \omega)$ outside the metal slab

$$\tilde{\Phi}^{(d)}(z) = \begin{cases} C_1\,e^{qz} & \text{for } z \leq -a, \\ C_2\,e^{-qz} & \text{for } z \geq a, \end{cases}$$

(5.97)

where we have dropped explicit dependence on $\mathbf{q}$ and $\omega$.

A connection between the solutions of the Poisson equation in Eqs. (5.11) and (5.12) for the regions outside and inside the metal slab is established by imposing the usual electrostatic MCs, which require the continuity of the potential in the FT space at the points $z = \pm a$,

$$\tilde{\Phi}^{(d)}(\pm a) = \tilde{\Phi}^{(m)}(\pm a), \tag{5.98}$$

and the continuity of the dielectric displacements at those points,

$$\epsilon_{\pm} \left. \frac{\partial \tilde{\Phi}^{(d)}}{\partial z} \right|_{z=\pm a} = \left. \frac{\partial \tilde{\Phi}^{(m)}}{\partial z} \right|_{z=\pm a}, \tag{5.99}$$

where we assumed that the two semi-infinite regions for $z \gtrless \pm a$ are filled with the materials having the relative dielectric constants $\epsilon_{\pm}$, respectively.

Thus, together with the BCs in Eqs. (5.87) or (5.88) for the induced charge density, the BCs for the potential in Eqs. (5.98) and (5.99) constitute eight conditions that may be used to determine the eight coefficients, $A_j$ (for $j = 1, 2, 3, 4$), $B_1$, $B_2$, $C_1$, and $C_2$ in terms of the parameter $\tilde{\rho}_0$ that characterizes the magnitude of the external charge.

### 5.3.4 Dispersion relation for quantum hydrodynamic model

In this section we want to continue the discussion of the dispersion relation by implementing two different ABCs. To simplify the calculation, we assume that the metal is surrounded by vacuum such that $\epsilon_{\pm} = 1$, and also that there is no external charge, $\tilde{\rho}_{\text{ext}}(z) = 0$. By implementing one of the two sets of BCs for $\rho(\mathbf{R}, t)$ and $\Phi(\mathbf{R}, t)$ in Eqs. (5.87) and (5.88), coupled with the continuity BCs for the potential and the dielectric displacement, Eqs. (5.98) or (5.99), respectively, we construct a well-posed problem for $\rho(\mathbf{R}, t)$ and $\Phi(\mathbf{R}, t)$. Then we seek the dispersion relation which gives rise to a nontrivial solution for the volume density of induced charge $\rho(\mathbf{R}, t)$. This will be done separately for the BCs in Eq. (5.87), which we call BC1, and the BCs in Eq. (5.88), which we call BC2.

Recall that we have found two sets of dispersion relations in the SHD model, one corresponding to so-called even plasmon modes where $\rho(\mathbf{R}, t)$ and $\Phi(\mathbf{R}, t)$ are symmetric functions of the position $z$ relative to the slab center, and the other corresponding to odd plasmon modes, where $\rho(\mathbf{R}, t)$ and $\Phi(\mathbf{R}, t)$ are antisymmetric functions of the position $z$. Since the dispersion relations of the QHD and SHD are solved in the same symmetrical slab geometry, in the absence of the external charge, $\tilde{\rho}_0(z) = 0$, it is desirable to seek the dispersion relation for the QHD by solving for the even modes and the odd modes separately.

By applying the first set BC1, Eq. (5.87), for the even modes, we obtain two equations for coefficients $A_1$ and $A_2$ as

$$A_1 (q_+^2 - q^2) \sinh(q_+ a) + A_2 (q_-^2 - q^2) \sinh(q_- a) = 0, \tag{5.100}$$

$$A_1 q_+ \sinh(q_+ a) + A_2 q_- \sinh(q_- a) = -k_s^2 e^{-qa}(A_1 \lambda_+ + A_2 \lambda_-), \tag{5.101}$$

where $\lambda_\pm = [-q_\pm \sinh(q_\pm a) \cosh(qa) + q \cosh(q_\pm a) \sinh(qa)]/(q_\pm^2 - q^2)$. Note that the equations for $A_1$ and $A_2$ are deduced by the symmetry property of the even modes. Specifically, for the coefficients $A_j$ (for $j = 1, 2, 3, 4$) in the induced charge density in Eq. (5.82) and for $B_1$ and $B_2$ in the electric potential inside the metal in Eq. (5.90), it is necessary that all the odd functions in the expression should vanish. This means the coefficients for the odd functions $\sinh$ should be equal to zero, that is $A_3 = 0$, $A_4 = 0$ and $B_2 = 0$. As for $C_1$ and $C_2$, to ensure that the potential in Eq. (5.97) is an even function, we impose a relation between them as $C_2 = C_1$. Then, an elimination of the coefficients $B_1$ and $C_1$ yields a homogeneous system of equations for $A_1$ and $A_2$ given in Eqs. (5.100) and (5.100).

Next, by setting the determinant of the matrix defining the left-hand sides in Eqs. (5.100) and (5.100) to zero, we arrive at the dispersion relation for even modes, which give rise to nontrivial solutions for the plasmon oscillations $\rho(\mathbf{R}, t)$ that are even functions of $z$,

$$\frac{1}{q_+^2 - q^2} \left\{ 1 + k_s^2 \frac{e^{-qa}}{q_+^2 - q^2} \left[ -\cosh(qa) + \frac{q \sinh(qa)}{q_+ \tanh(q_+ a)} \right] \right\}$$
$$= \frac{1}{q_-^2 - q^2} \left\{ 1 + k_s^2 \frac{e^{-qa}}{q_-^2 - q^2} \left[ -\cosh(qa) + \frac{q \sinh(qa)}{q_- \tanh(q_- a)} \right] \right\}. \tag{5.102}$$

Analogously, to solve the dispersion relation for odd plasmon modes with the set BC1, Eq. (5.87), one may reduce the unknown coefficients by the antisymmetrical property of the odd modes. By eliminating the even functions $\cosh$ in Eqs. (5.82) and (5.90), we have $A_1 = 0$, $A_2 = 0$ and $B_1 = 0$, as well as the relation $C_1 = -C_2$ by constructing Eq. (5.97) as an odd function. So, the dispersion relation for odd plasmon modes under the set BC1 becomes

$$\frac{1}{q_+^2 - q^2} \left\{ 1 + k_s^2 \frac{e^{-qa}}{q_+^2 - q^2} \left[ -\sinh(qa) + \frac{q \cosh(qa)}{q_+ \coth(q_+ a)} \right] \right\}$$
$$= \frac{1}{q_-^2 - q^2} \left\{ 1 + k_s^2 \frac{e^{-qa}}{q_-^2 - q^2} \left[ -\sinh(qa) + \frac{q \cosh(qa)}{q_- \coth(q_- a)} \right] \right\}. \tag{5.103}$$

For the set BC2, Eq. (5.88), we follow the same procedure for even and odd plasmon modes by eliminating the coefficients with functions of the opposite parity. So, the corresponding equations for the coefficients $A_1$ and $A_2$ for even modes with the set BC2 are

$$A_1 q_+ (q_+^2 - q^2) \cosh(q_+ a) + A_2 q_- (q_-^2 - q^2) \cosh(q_- a) = 0, \tag{5.104}$$

$$A_1 Q_+ \sinh(q_+ a) + A_2 Q_- \sinh(q_- a) = -(k_c k_s)^2 e^{-qa}(A_1 \lambda_+ + A_2 \lambda_-), \tag{5.105}$$

where $Q_\pm = q_\pm(k_c^2 + q^2 - q_\pm^2)$ and $\lambda_\pm$ has the same definition as that following Eqs. (5.100) and (5.101) for the set BC1. Accordingly, we find the dispersion relation for even plasmon modes with the set BC2 as

$$\frac{q_+ \tanh(q_+ a)}{q_+^2 - q^2} \left\{ k_c^2 + q^2 - q_+^2 + (k_c k_s)^2 \frac{e^{-qa}}{q_+^2 - q^2} \left[ -\cosh(qa) + \frac{q \sinh(qa)}{q_+ \tanh(q_+ a)} \right] \right\}$$
$$= \frac{q_- \tanh(q_- a)}{q_-^2 - q^2} \left\{ k_c^2 + q^2 - q_-^2 + (k_c k_s)^2 \frac{e^{-qa}}{q_-^2 - q^2} \left[ -\cosh(qa) + \frac{q \sinh(qa)}{q_- \tanh(q_- a)} \right] \right\}, \quad (5.106)$$

whereas analogous procedure gives the dispersion for the odd plasmon modes with the set BC2 as

$$\frac{q_+ \coth(q_+ a)}{q_+^2 - q^2} \left\{ k_c^2 + q^2 - q_+^2 + (k_c k_s)^2 \frac{e^{-qa}}{q_+^2 - q^2} \left[ -\sinh(qa) + \frac{q \cosh(qa)}{q_+ \coth(q_+ a)} \right] \right\}$$
$$= \frac{q_- \coth(q_- a)}{q_-^2 - q^2} \left\{ k_c^2 + q^2 - q_-^2 + (k_c k_s)^2 \frac{e^{-qa}}{q_-^2 - q^2} \left[ -\sinh(qa) + \frac{q \cosh(qa)}{q_- \coth(q_- a)} \right] \right\}. \quad (5.107)$$

It is worth mentioning that, if one takes the limit $k_c \to \infty$, the wavenumbers become $q_+ \approx \sqrt{q^2 + k_c^2}$ and $q_- \approx q_s$ with the parameter $q_s$ defined in Eq. (5.33) for the SHD model. By using this approximation for the wavenumbers $q_\pm$, one finds that the dispersion relations from BC2 given in Eqs. (5.106) and (5.107) can be reduced to the dispersion relation for the SHD model, given in Eqs. (5.60) and (5.61). The physical interpretation for this results is found by recalling that the limit $k_c \to \infty$ corresponds to the limit $l_c \to 0$, which is the length scale for the density variations in the EG that characterize the effects from Bohm potential. Accordingly, when the influence of the Bohm quantum term is neglected, the forth order PDE for induced charge density $\rho(\mathbf{R}, t)$ is reduced to second order PDE, which characterizes the SHD model.

In Fig. 5.2, we present both the SHD and QHD dispersion relations for comparison by choosing $r_s = 3$ and $k_s a = 10$, accompanied by the dispersion relation of the local model illustrated by the green dashed line. As can be seen, compared with the local model, which only has one even and one odd plasmon dispersion relations, multiple dispersion relation curves are seen for both the SHD and QHD models. First, if we look at the surface plasmon for both local and nonlocal models, which are labeled by $n = 0$, we see that in the limit of long wavelengths, $qa \ll 1$, both local and non-local models show the same relation between reduced frequency $\Omega$ and the reduced wavenumber $qa$. On the other hand, as the wavelength increases, while the surface plasmons for the local model in both even and odd mode converge to a common value $\omega = \omega_p \sqrt{2}$, it is interesting to notice that the surface plasmon dispersions for both the SHD and QHD increase and continue to behave in highly similar manner when $\omega < \omega_p$. This phenomenon indicates that the Bohm quantum potential does not exert much influence when the value of eigenfrequency $\omega$ is below the bulk plasma frequency $\omega_p$. However, for $\omega > \omega_p$ in the limit of short wavelengths, one can easily see that the reduced frequency for surface plasmon
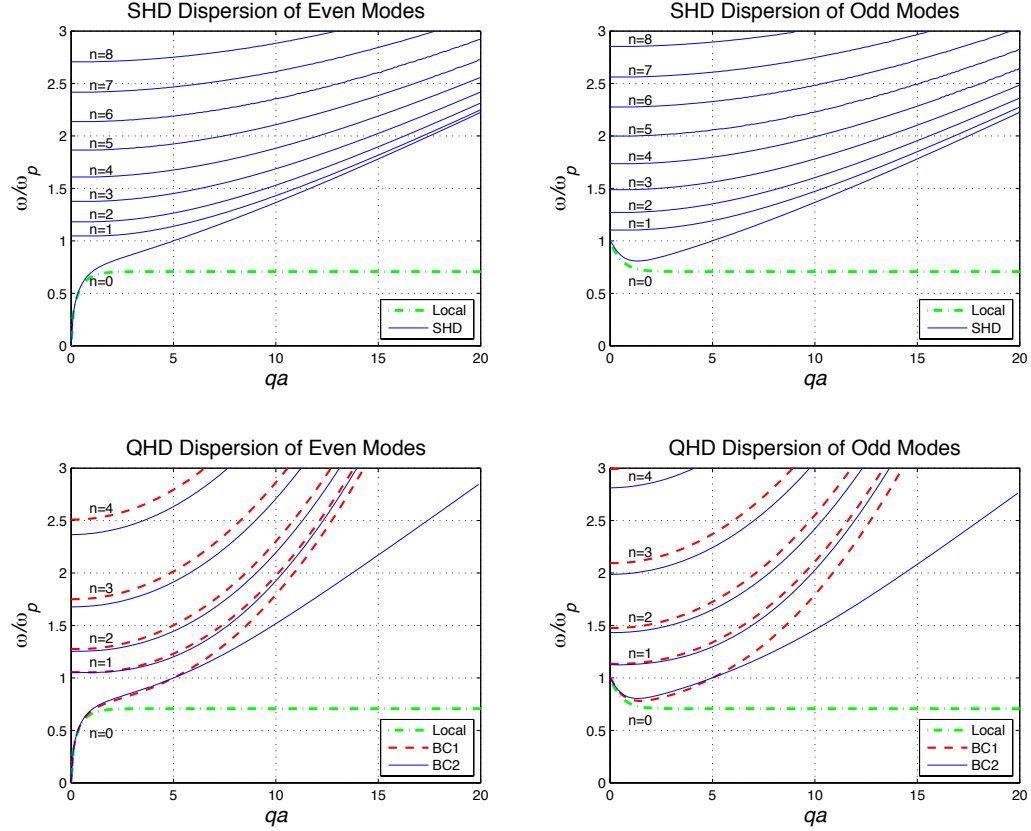
Figure 5.2: Dispersion relations for both the even and odd plasmon modes in a metal slab of thickness $a$, where we show the reduced frequency $\Omega$ as a function of the wavenumber $qa$. The results are shown for both the SHD model and QHD model, while for the QHD model two sets of dispersion relations are presented by utilizing the sets of BC1 and BC2, given in in Eqs. (5.87) and (5.88), respectively. The green dash and dot line presents the LHD model. The surface plasmon modes are labeled by $n = 0$ while the bulk plasmon modes are characterized by $n = 1, 2, 3, \ldots$ with the density parameter of the EG fixed at $r_s = 3$. The Thomas-Fermi screening length in the EG is chosen so that $k_s a = 10$.
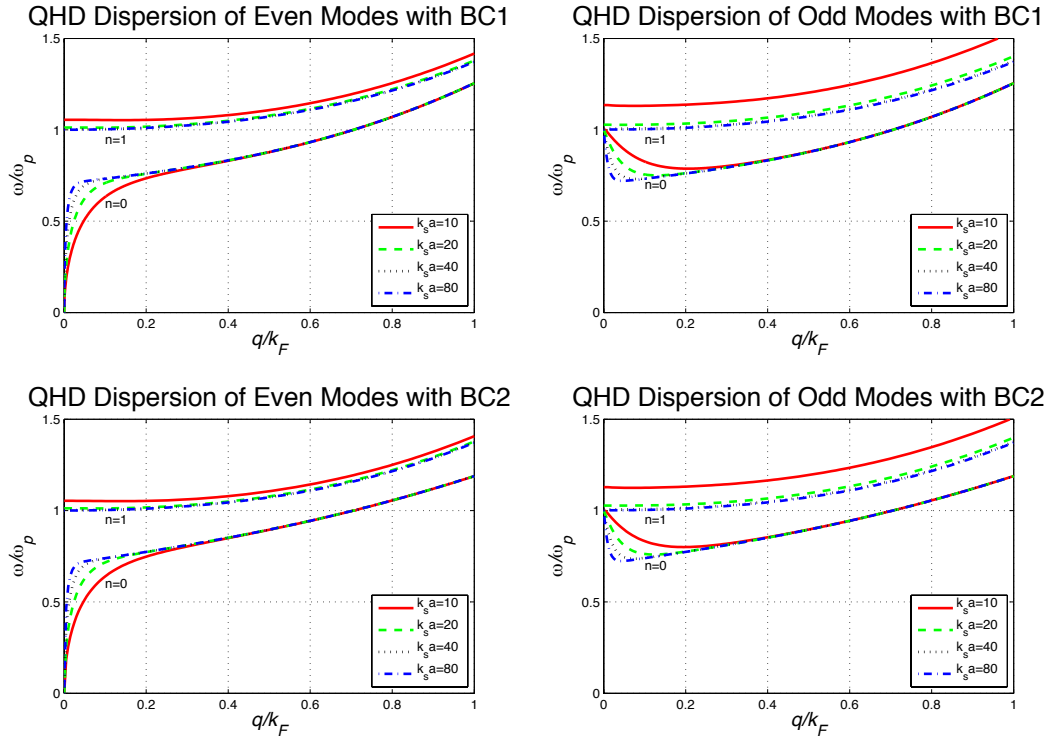
Figure 5.3: Dispersion relations for both the even and odd plasmon modes of the QHD model for BC1 and BC2, where we show the reduced frequency $\Omega$ as a function of the reduced wavenumber $q/k_F$, with $k_F$ being the Fermi wavenumber in the EG. The surface plasmons with $n = 0$ and the first bulk plasmons with $n = 1$ are presented for different metallic slab thicknesses, $k_s a = 10, 20, 40, 80$, with the density parameter fixed at $r_s = 3$.

mode reveals different short wavelength behaviors (large $qa$). For the SHD model, the reduced frequency is bounded by $\Omega < \sqrt{1 + \frac{q^2}{k_s^2}}$, which corresponding to the real and positive value for $q_s$ with $\gamma = 0$. For QHD model, both BC1 and BC2 are bounded by $\Omega < \sqrt{1 + \frac{(2q^2 + k_c^2)^2}{4k_s^2 k_c^2} - \frac{k_c^2}{4k_s^2}}$, which leads to the real and positive value for both wavenumber $q_{\pm}$ when $\gamma = 0$. Another notable result for the short wavelength behavior of the QHD model is that, for BC2, as $qa \to \infty$, we find a linear relationship between $\Omega$ and $qa$ for both even and odd modes as $\Omega = \sqrt{2}\, qa/k_s a$, whereas the surface plasmons for BC1 are obviously quadratic curves when $qa$ is sufficiently large, which is a consequence of different conditions for the electric potential and induced charge density on the boundary.

Moreover, according to Fig. 5.2, it is worthwhile to point out that, for the so-called bulk plasmons in the nonlocal models, which are labeled by $n = 1, 2, 3, ...$, there are significant differences between the SHD and QHD models. One of them lies in the dispersion behavior at the limit of the short wavelengths. As can be seen, when $qa$ increases, the increase of the reduced frequency $\Omega$ in SHD is slower than that of both QHD models for $n = 1, 2, 3, ...$. It is also worth to note that in the QHD model, the bulk plasmons are characterized by the reduced frequencies that are larger than $\Omega = \sqrt{1 + \frac{(2q^2 + k_c^2)^2}{4k_s^2 k_c^2} - \frac{k_c^2}{4k_s^2}}$. This indicates that for bulk plasmons, the wavenumber $q_+$ is real and positive while $q_-$ is imaginary, which is attributed to the infinitely many solutions of Eq. (5.102) to Eq. (5.107). By fixing an arbitrary value for wavenumber $qa$, one can observe that for each bulk plasmon mode in the nonlocal models, the values of $\Omega$ for QHD are greater than those in SHD model for both even and odd modes, and the curves are sparser for bulk plasmons in the QHD model. If one continues this comparison between the QHD bulk dispersions for BC1 and BC2, the figures reveal that the value of $\Omega$ for BC2 is slightly lower than that of BC1, and the difference increases while the value of the mode $n$ increases. Those differences between the SHD model and the QHD models arise due to the gradient correction from the Bohm quantum potential as a result of quantum effect.

In order to observe how the thickness of slab affects plasmon dispersions, we present Fig. 5.3 where the dependence on the new variable are $q/k_F$ is shown, where $k_F = mv_F/\hbar$ is the Fermi wavenumber in the EG. By using the new variable $q/k_F$, we avoid the influence of the thickness in the variable $qa$ used for Fig. 5.2. From the dispersion relation we can see that as the slab thickness increases, the surface plasmon of QHD will tend asymptotically to the surface plasmon of SHD. It is physically feasible because, as the metal slab thickness increases to a size which is much larger than $l_c$, the Bohm potential quantum effect can be ignored thus giving rise to the SHD model.

## 5.4 Conclusion

The study of the dynamic response of a metallic slab due to the polarization by the passage of external charged particles has been attracting attention for a long time. The discussion of the dispersion relation for plasmon polarization has arisen for various of metallic structures under nonlocal description, where the authors treated the EG inside the metal within the hydrodynamic approximation [38, 39]. Based on the local description of the metal, if we introduce the so-called TF form of the pressure in the equation of potential energy for electrons, the resulting expression for the dispersion relations of SHD model reveals that both the surface and bulk (or volume) plasmons can be excited directly by the external charges. An extensive review of the SHD model was given in Ref. [40]. In our recent study for SHD model [41], we introduced the GF technique for the mathematical model resulting from the SHD model, which give rise to multiple plasmon dispersion for both surface and volume plasmon.

In order to deduce the dispersion relation from the excitation of the collective oscillation in the thin metal layer, we have presented in this chapter a QHD model of the EG in metallic structures, which exerts better performance than the SHD model in recognizing the spatially nonlocal effects of electron excitation in nanometer-sized structures. This formulation of the hydrodynamic model was recently used to study the energy loss and dynamic polarization of a thin metal slab by a fast moving external point charge [42].

# Chapter 6

# Green's function for Poisson equation in the presence of aqueous electrolyte

Carbon nanostructures, and graphene in particular, have been studied in recent years for a wide range of applications for biological and chemical sensors [9, 10, 11]. While experimental investigation of graphene based biochemical sensors is rapidly accelerating area, theoretical modeling of electrochemistry of graphene is still in its infancy. Graphene operates in such applications in the configuration of a FET with its surface exposed to an electrolyte containing mobile ions, as in Fig. 1.3. By applying a gate potential through the electrolyte gives rise to the so-called EDL near graphene, which may improve the control of graphene's electrical conductivity making it extremely sensitive to the presence of adsorbed molecules, ion concentration, or the pH in an aqueous solution. In addition, graphene is usually supported by an insulating substrate, such as $SiO_2$, which may contain large density of charged impurities that also affect graphene's conductivity.

In a recent study [8], the ability of mobile ions in the solution to screen the effects of charged impurities was studied in the regime of a low potential drop across EDL by using a linearized PB model, or the Debye-Hückel (DH) approximation for the electrolyte. However, typical applications of graphene FETs require high doping densities of charge carriers that are achieved by applying relatively large electrolytic gate potentials, which render the linearized PB model insufficient. To remedy this situation, we develop a partially-linearized PB model for ionic screening of charged impurities underneath graphene, which is based on the GF approach. In order to include the effect of finite ion size, at least at a qualitative level, we derive a GF for the partially-linearized PB model that also includes a Stern layer at the interface with graphene and allows modeling of ionic screening in the regime of a dually-gated single-layer graphene FET.

# 6.1 Poisson-Boltzmann equation in the electrolyte

## 6.1.1 Boltzmann distribution of mobile ions

In electrochemistry, one considers thermodynamic interactions of a liquid solvent with added salt. In the presence of water, the molecules of salt dissociate into positive ions with charge $eZ_+$ and negative ions with charge $-eZ_-$, where $e > 0$ is the proton charge and $Z_\pm$ is the ion valence. We consider here a symmetric aqueous electrolyte with $Z_+ = Z_- = Z$ [43, 8, 26]. In the Boltzmann approach, the ions are considered to be explicit point electric charges obeying the Poisson equation. If the electrostatic potential at a position $\mathbf{R}$ is $\Phi(\mathbf{R})$, then the local potential energy of the positively and negatively charged ions is given by $V_\pm = \pm eZ_\pm\Phi(\mathbf{R})$. In the ground state, the electrostatic potential in the bulk region of electrolyte is constant and may be defined as a zero reference potential. Under those conditions, the concentrations (or the number densities) of the positively and negatively charged ions are also constant and equal to each other, $c_+ = c_- = c$, where $c$ is the salt concentration. However, if the electrostatic potential is not constant, e.g., due to immersion of a charged electrode or graphene into the electrolyte, the salt ions will rearrange their positions so that their densities will be provided by the probability distribution, which has the Boltzmann form under equilibrium conditions at a thermodynamic temperature $T$ (in Kelvin), given by

$$c_+(\mathbf{R}) \;=\; c\,e^{-\frac{Z_+e\Phi(\mathbf{R})}{k_BT}}, \tag{6.1}$$

$$c_-(\mathbf{R}) \;=\; c\,e^{\frac{Z_-e\Phi(\mathbf{R})}{k_BT}}, \tag{6.2}$$

where $k_B$ is the Boltzmann constant. Now the expression for the electric charge density due to the mobile ions in the electrolyte becomes

$$\rho_{\mathrm{ion}} = e(c_+ - c_-) = Zec\left[e^{-\frac{Z_+e\Phi(\mathbf{R})}{k_BT}} - e^{\frac{Z_-e\Phi(\mathbf{R})}{k_BT}}\right]. \tag{6.3}$$

## 6.1.2 Nonlinear Poisson-Boltzmann equation

When a charged electrode is immersed in an ionic solution, then a redistribution of the electrostatic potential and the concentrations of the salt ions will occur in the electrolyte, giving rise to the so-called EDL in a region of the electrolyte adjacent to that electrode. The distribution of the electrostatic potential in the electrolyte may be found by substituting the local electric charge density based on the Boltzmann distribution, Eq. (6.3), into the Poisson equation, giving rise to

the PB model of EDL. If we further assume that there is a distribution of some external charge, such as charged bio-molecules in the electrolyte, with the charge density $\rho_{\text{ext}}(\mathbf{R})$ that is a given function of the position $\mathbf{R}$, then the PB equation may be written as

$$\nabla \cdot [\epsilon \nabla \Phi(\mathbf{R})] = -4\pi \rho(\mathbf{R}), \tag{6.4}$$

where $\epsilon$ is the dielectric constant of solvent (water) in the electrolyte, and the total charge density $\rho(\mathbf{R})$ is given by

$$
\begin{aligned}
\rho(\mathbf{R}) &= \rho_{\text{ion}}(\mathbf{R}) + \rho_{\text{ext}}(\mathbf{R}) \\
&= Zec \left[ e^{-\frac{Z_+ e\Phi(\mathbf{R})}{k_B T}} - e^{\frac{Z_- e\Phi(\mathbf{R})}{k_B T}} \right] + \rho_{\text{ext}}(\mathbf{R}) \\
&= -2Zec \sinh\left[ \frac{Ze\Phi(\mathbf{R})}{k_B T} \right] + \rho_{\text{ext}}(\mathbf{R}).
\end{aligned}
\tag{6.5}
$$

Equivalently, when $\epsilon$ is constant throughout the electrolyte, the nonlinear PB equation arrives in a more compact form as

$$\nabla^2 \Phi(\mathbf{R}) = \frac{8\pi Zec}{\epsilon} \sinh\left[ \frac{Ze\Phi(\mathbf{R})}{k_B T} \right] - \frac{4\pi}{\epsilon} \rho_{\text{ext}}(\mathbf{R}). \tag{6.6}$$

Solving Eq. (6.6) subject to the standard electrostatic BCs at the electrode surface will then yield the spatial dependencies of the potential, as well as the ion concentrations in the EDL according to Eq. (6.1) and (6.2). If the layer of electrolyte is thick enough, then deep in its bulk region, far from the electrode, the electrolyte will be overall neutral with $c_+ = c_- = c$, while the electrostatic potential will be constant and determined by the so-called reference electrode, see Fig. 1.3. Usually, the value of the potential in the bilk electrolyte is taken as a zero reference potential.

### 6.1.3 Nonlinear Poisson-Boltzmann equation in one dimension

If the area of an electrode, or the area $A$ of graphene sheet immersed in the electrolyte is large enough and if there are no lateral fluctuations of electrostatic potential in directions parallel to graphene, then the spatial distribution of the potential will only depend on the distance from graphene. Adopting a 3D Cartesian coordinate system with the position vector $\mathbf{R} = (\mathbf{r}, z)$, where $\mathbf{r} = (x, y)$ is the position in a plane parallel to graphene, then it is justifiable to assume

that the potential $\Phi(\mathbf{R})$ can be written as $\Phi(z)$. With the assumption that $\rho_{\text{ext}}(\mathbf{R}) = 0$, the PB equation becomes:

$$\frac{\partial^2}{\partial z^2}\Phi(z) = \frac{8\pi Zec}{\epsilon}\sinh\left[\frac{Ze\Phi(z)}{k_B T}\right].\tag{6.7}$$

If we denote $\psi = \frac{Ze\Phi(z)}{k_B T}$ as a non-dimensional electrostatic potential, then the PB equation for $\psi$ becomes:

$$\frac{d^2\psi(z)}{dz^2} = \kappa^2\sinh[\psi(z)],\tag{6.8}$$

where we define parameter

$$\kappa = \sqrt{c\frac{8\pi Z^2 e^2}{\epsilon k_B T}},$$

corresponding to the so-called Debye screening length in electrolyte, given by $\lambda_D = 1/\kappa$.

Equation (6.8) is a second-order nonlinear ODE. By denoting a non-dimensional electric field as $E(z) = E(\psi(z)) = -\frac{d\psi}{dz}$, the above equation for $\psi(z)$ may be reduced to a first-order ODE for $E$ as a function of $\psi$, giving the so-called first integral. From there, one can find an exact solution $\psi(z)$, subject to the electrostatic BC at the edge of the EDL and assuming $\psi(z) \to 0$ as $z \to \infty$ [43].

## 6.2 Green's function for Poisson-Boltzmann equation in Debye-Hückel approximation

Our previous derivations of the GF in layered structures can be easily adapted to include a layer of electrolyte in the so-called DH approximation, which is based on a linearization of the non-linear PB equation in Eq. (6.6). Namely, if the temperature $T$ is high enough and/or potential variation from its reference value in the bulk electrolyte is small, one may assume $|Ze\Phi(\mathbf{R})| \ll k_B T$. Then we can introduce the approximation $\sinh(\frac{Ze\Phi(\mathbf{R})}{k_B T}) \approx \frac{Ze\Phi(\mathbf{R})}{k_B T}$ for the charge density due to mobile ions in the solution into the PB equation in Eq. (6.6). As a result, we obtain a linear PDE of the Helmholtz type for the electrostatic potential in the EDL,

$$\nabla^2\Phi(\mathbf{R}) - \kappa^2\Phi(\mathbf{R}) = -\frac{4\pi}{\epsilon}\rho_{\text{ext}}(\mathbf{R}).\tag{6.9}$$

We are interested here in a three-layered structure shown in Fig. 2.3, where the region $I_1$ is defined by $-\infty \leq z \leq 0$ with relative dielectric constant $\epsilon_1$ corresponding to a thick layer

of insulating oxide, while the region $I_2$ is defined by $0 \le z \le h$ with dielectric constant $\epsilon_2$ and it corresponds to the so-called Stern layer in electrochemistry, which is free of charges and separates the EDL in the electrolyte from the electrode (graphene) surface [43]. Finally, the region $I_3$ is defined as the semi-infinite domain $z \ge h$, which models the EDL as the so-called diffuse layer containing mobile ions, with dielectric constant of the background solvent being $\epsilon_3$.

For the electrical potential, first we rewrite the potential in a piecewise manner as $\Phi_j$ when $z \in I_j$. As for $j = 1, 2$ without mobile ions, the potential satisfies the previously discussed Poisson equation as

$$\nabla^2 \Phi_j(\mathbf{R}) = -\frac{4\pi}{\epsilon_j} \rho_{\text{ext}}(\mathbf{R}), \tag{6.10}$$

whereas for region $I_3$ the potential $\Phi_3$ satisfies the Helmholtz equation due to the mobile ions,

$$\nabla^2 \Phi_3(\mathbf{R}) - \kappa^2 \Phi_3(\mathbf{R}) = -\frac{4\pi}{\epsilon} \rho_{\text{ext}}(\mathbf{R}). \tag{6.11}$$

Instead of deriving the GF $G_j$ for layer $I_j$ in 3D space directly, we take advantage of translational invariance in the $(x, y)$ plane and perform the 2D FT as

$$\Phi(\mathbf{r}, z) = \int \frac{d^2\mathbf{q}}{(2\pi)^2} e^{i\mathbf{q}\cdot\mathbf{r}} \tilde{\Phi}(\mathbf{q}, z). \tag{6.12}$$

By analogy with the procedure used in section 2.5, we need to specify the GF for different observation points $\mathbf{R}$, as well as the source points $\mathbf{R}'$. So, we introduce the FTGF $\widetilde{G}_{jk}(z, z')$ with double index, where the index $j$ corresponds to the specific location of the observation point, $z \in I_j$, while $k$ indicates that the source point satisfies $z' \in I_k$, with $j, k = 1, 2, 3$. Now, the nine components of the FTGF are fully determined from the system of ODEs written in a compact form as

$$\frac{\partial^2}{\partial z^2} \widetilde{G}_{jk}(\mathbf{q}; z, z') - q_j^2 \widetilde{G}_{jk}(\mathbf{q}; z, z') = -\frac{4\pi}{\epsilon_j} \delta_{jk} \delta(z - z'), \text{ for } z \in I_j \text{ and } z' \in I_k \tag{6.13}$$

where

$$q_j^2 = \left\{ \begin{array}{cc} q^2 & \text{for } j = 1, 2 \\ q^2 + \kappa^2 & \text{for } j = 3. \end{array} \right. \tag{6.14}$$

Before diving into the tedious works, there is one thing worth noticing. Recall that the set of ODEs for FTGF without electrolyte in section 2.5 is

$$\frac{\partial^2}{\partial z^2} \widetilde{G}_{jk}(\mathbf{q}; z, z') - q^2 \widetilde{G}_{jk}(\mathbf{q}; z, z') = -\frac{4\pi}{\epsilon_j} \delta_{jk} \delta(z - z'), \text{ for } z \in I_j \text{ and } z' \in I_k. \tag{6.15}$$

88

Comparing to the new set of ODEs for the FTGF with electrolyte in Eq. (6.13), the only difference in the old set of ODEs in Eq. (6.15) is the value of the coefficient $q_j$ when $j = 3$. This means that during the process of solving for $G_{jk}$ when $j, k = 1, 2, 3$, the only difference would be in the general solutions for $G_{3k}$ for all $k = 1, 2, 3$. To be more specific, the general solutions for $G_{3k}$ has the form

$$\widetilde{G}_{31}(z, z') = Ae^{-\sqrt{q^2+\kappa^2}z}, \tag{6.16}$$

$$\widetilde{G}_{32}(z, z') = Be^{-\sqrt{q^2+\kappa^2}z}, \tag{6.17}$$

$$\widetilde{G}_{33}^{<}(z, z') = Ce^{\sqrt{q^2+\kappa^2}z} + De^{-\sqrt{q^2+\kappa^2}z}, \tag{6.18}$$

$$\widetilde{G}_{33}^{>}(z, z') = Ee^{-\sqrt{q^2+\kappa^2}z}. \tag{6.19}$$

where $A, B, C, D$ and $E$ are just arbitrary constants that need to be determined by the MCs and the BCs listed in section 2.6. As for the general solution of $\widetilde{G}_{jk}$ for all $j = 1, 2, 3$ with $k = 1, 2$, they have the same form as in the section 2.5.

Now, after obtaining the general form for all components of the FTGF, we apply the same sets of MCs and BCs, i.e., the continuity, jump condition, and condition at infinity, to obtain the final expressions for the FTGF. As a result, the expressions for $\widetilde{G}_{jk}$ can be written in a compact form if we define auxiliary parameters as

$$\lambda_{\text{b}} = \frac{\epsilon_1 - \epsilon_2}{\epsilon_1 + \epsilon_2}, \tag{6.20}$$

$$\bar{\epsilon}_{12} = \frac{\epsilon_1 + \epsilon_2}{2}, \tag{6.21}$$

$$\bar{\epsilon}_{23} = \frac{\epsilon_3 + \epsilon_2}{2}, \tag{6.22}$$

$$\Delta = e^{-2qh}, \tag{6.23}$$

$$\lambda_{\text{T}} = \frac{\epsilon_3\sqrt{q^2 + \kappa^2} - \epsilon_2 q}{\epsilon_3\sqrt{q^2 + \kappa^2} + \epsilon_2 q}. \tag{6.24}$$

The final solutions are

$$\widetilde{G}_{11} = \frac{2\pi}{q\epsilon_1}\left[\mathrm{e}^{-q|z-z'|} + \frac{\lambda_\mathrm{b} - \lambda_\mathrm{T}\Delta}{1 - \lambda_\mathrm{b}\lambda_\mathrm{T}\Delta}\,\mathrm{e}^{q(z+z')}\right], \tag{6.25}$$

$$\widetilde{G}_{21} = \frac{2\pi}{q\bar{\epsilon}_{12}}\frac{\mathrm{e}^{-qz} - \lambda_\mathrm{T}\Delta\,\mathrm{e}^{qz}}{1 - \lambda_\mathrm{b}\lambda_\mathrm{T}\Delta}\,\mathrm{e}^{qz'}, \tag{6.26}$$

$$\widetilde{G}_{31} = \frac{2\pi}{q\bar{\epsilon}_{12}}\frac{1 - \lambda_\mathrm{T}}{1 - \lambda_\mathrm{b}\lambda_\mathrm{T}\Delta}\mathrm{e}^{\sqrt{q^2+\kappa^2}(h-z)+q(z'-h)}, \tag{6.27}$$

$$\widetilde{G}_{22} = \frac{2\pi}{q\epsilon_2}\left\{\mathrm{e}^{-q|z-z'|} + \frac{\lambda_\mathrm{b}\lambda_\mathrm{T}\Delta}{1 - \lambda_\mathrm{b}\lambda_\mathrm{T}\Delta}\left[\mathrm{e}^{q(z-z')} + \mathrm{e}^{-q(z-z')}\right]\right\}$$
$$\quad - \frac{2\pi}{q\epsilon_2}\frac{\lambda_\mathrm{b}\,\mathrm{e}^{-q(z+z')} + \lambda_\mathrm{T}\Delta\,\mathrm{e}^{q(z+z')}}{1 - \lambda_\mathrm{b}\lambda_\mathrm{T}\Delta}, \tag{6.28}$$

$$\widetilde{G}_{32} = \frac{2\pi}{q\epsilon_2}\frac{(\mathrm{e}^{qz'} - \lambda_\mathrm{b}\mathrm{e}^{-qz'})(1 - \lambda_\mathrm{T})}{1 - \lambda_\mathrm{b}\lambda_\mathrm{T}\Delta}\,\mathrm{e}^{\sqrt{q^2+\kappa^2}(h-z)-qh}, \tag{6.29}$$

$$\widetilde{G}_{33} = \frac{2\pi}{\sqrt{q^2+\kappa^2}\epsilon_3}\left[\mathrm{e}^{-\sqrt{q^2+\kappa^2}|z-z'|} + \frac{\lambda_\mathrm{T} - \lambda_\mathrm{b}\Delta}{1 - \lambda_\mathrm{b}\lambda_\mathrm{T}\Delta}\,\mathrm{e}^{\sqrt{q^2+\kappa^2}(2h-z-z')}\right], \tag{6.30}$$

where the nine components of the FTGF system are reduced to six components owing to the Maxwell's symmetry property of GF.

## 6.3 Green's function for partially linearized Poisson-Boltzmann equation

We now want to model a dual-gated graphene with a large potential drop across the EDL in the electrolyte, which invalidates the DH approximation. Unlike the structure shown in Fig. 2.3, we consider here the insulating oxide underneath graphene to have finite thickness $t$, as shown in Fig. 6.1. So, using the same Cartesian coordinate system as in section 6.2, we see that the region $I_1$ is defined here by $-t \leq z \leq 0$, whereas the other two regions retain the same definitions. We assume that the region $I_1$ contains a distribution of fixed charged impurities, whereas the region $I_3$ contains salt ions in the electrolyte, which form the EDL, and possibly some small amounts of charged bio-molecules. In addition, we introduce explicitly in Fig. 6.1 a single layer of graphene in the plane $z = 0$ and assume that it carries a surface charge density $\sigma_g$. Noting that the charge carriers in graphene (electrons and holes) are also mobile, we expect that both the charge carriers in graphene and the mobile ions in the electrolyte will redistribute themselves so as to screen any spatial fluctuation in the electrostatic potential arising from the fixed charged impurities in the

oxide substrate or from the charged bio-molecules in the electrolyte adjacent to the surface of graphene.

Similarly to the procedure of how we dealt with the electrostatic potential in layered structures in previous chapters, we first rewrite the potential in a piecewise manner as $\Phi_j(\mathbf{R})$ for $z \in I_j$, satisfying the following equations for $j = 1, 2, 3$

$$\epsilon_j \nabla^2 \Phi_j(\mathbf{R}) = -4\pi[\rho_j^{(\text{ion})}(\Phi_j(\mathbf{R})) + \rho_j^{(\text{ext})}(\mathbf{R})], \tag{6.31}$$

where $\rho_j^{(\text{ion})}$ is the local charge density due to mobile ions, defined as

$$\rho_j^{(\text{ion})}(\Phi_j(\mathbf{R})) = \begin{cases} 0 & \text{for} \quad j = 1, 2 \\ -2Zec \sinh\{\beta Ze[\Phi_3(\mathbf{R}) - \Phi_3(\infty)]\} & \text{for} \quad j = 3, \end{cases} \tag{6.32}$$

with $\beta = \frac{1}{k_B T}$ and $\Phi_3(\infty)$ being the (constant) value of the potential deep in the bulk of the electrolyte, $z \to \infty$, determined by a top gate. Moreover, we assume that the external charge density in Eq. (6.31) may be decomposed into the density of charged impurities $\rho_{\text{imp}}(\mathbf{R})$ in the region $I_1$ occupied by oxide and the density of charged bio-molecules $\rho_{\text{bio}}(\mathbf{R})$ in the region $I_3$ occupied by electrolyte, so that

$$\rho_j^{(\text{ext})}(\mathbf{R}) = \begin{cases} \rho_{\text{imp}}(\mathbf{R}) & \text{for} \quad j = 1, \\ 0 & \text{for} \quad j = 2, \\ \rho_{\text{bio}}(\mathbf{R}) & \text{for} \quad j = 3. \end{cases} \tag{6.33}$$

The equations (6.31) should be solved subject to the BCs at $z = -t$ and $z \to \infty$, such that

$$\Phi_1(\mathbf{R})|_{z=-t} = \phi_{bg}, \tag{6.34}$$

$$\Phi_3(\mathbf{R})|_{z\to\infty} \equiv \Phi_3(\infty) = \phi_{tg}, \tag{6.35}$$

where $\phi_{bg}$ and $\phi_{tg}$ are the (constant) electrostatic potentials at the back gate at $z = -t$ and at the top gate deep in the electrolyte, respectively. In addition, the electrostatic potential has to satisfy the following MCs at $z = 0$ and $z = h$,

$$\Phi_1(\mathbf{R})|_{z=0} = \Phi_2(\mathbf{R})|_{z=0} \equiv \phi_0(\mathbf{r}) \tag{6.36}$$

$$\Phi_2(\mathbf{R})|_{z=h} = \Phi_3(\mathbf{R})|_{z=h} \tag{6.37}$$

$$-\epsilon_2 \frac{\partial \Phi_2(\mathbf{R})}{\partial z}\bigg|_{z=0} + \epsilon_1 \frac{\partial \Phi_1(\mathbf{R})}{\partial z}\bigg|_{z=0} = 4\pi\sigma_g[\phi_0(\mathbf{r})] \tag{6.38}$$

$$\epsilon_2 \frac{\partial \Phi_2(\mathbf{R})}{\partial z}\bigg|_{z=h} = \epsilon_3 \frac{\partial \Phi_3(\mathbf{R})}{\partial z}\bigg|_{z=h}. \tag{6.39}$$
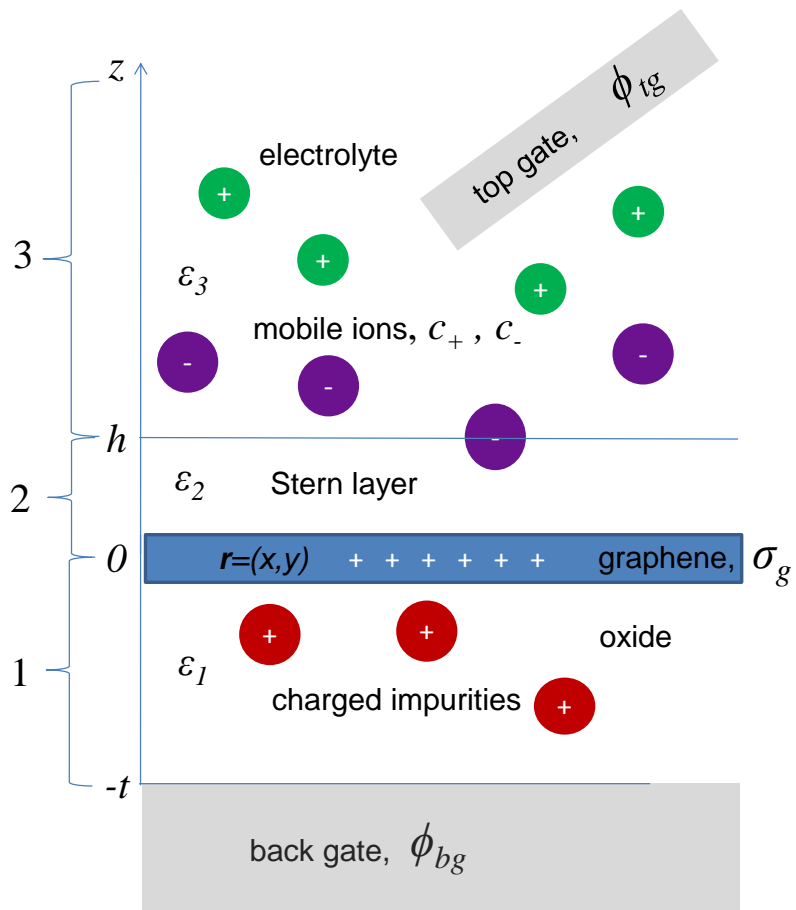
Figure 6.1: Schematic diagram for the three regions in a dual-gated graphene transistor with electrolyte containing mobile salt ions and with an oxide substrate containing charged impurities. Adapted from Ref. [8].

We have defined in Eq. (6.36) the value of the electrostatic potential $\phi_0(\mathbf{r})$ in the plane $z = 0$, which only depends on the lateral position $\mathbf{r} = (x, y)$ and we have indicated in Eq. (6.38) the charge density on graphene is a functional $\sigma_g[\phi_0(\mathbf{r})]$ of that potential.

We now assume that all quantities may be written as the sum of their average value taken over the large area $A$ of graphene plus a small fluctuating part. So, for the electrostatic potential and the external charge components in the regions $I_1$ and $I_3$ we write

$$\Phi_j(\mathbf{R}) = \bar{\Phi}_j(z) + \delta\Phi_j(\mathbf{R}), \tag{6.40}$$

$$\rho_{\text{imp}}(\mathbf{R}) = \bar{\rho}_{\text{imp}}(z) + \delta\rho_{\text{imp}}(\mathbf{R}), \tag{6.41}$$

$$\rho_{\text{bio}}(\mathbf{R}) = \bar{\rho}_{\text{bio}}(z) + \delta\rho_{\text{bio}}(\mathbf{R}), \tag{6.42}$$

where

$$\bar{\Phi}_j(z) = \frac{1}{A} \int_A \Phi_j(\mathbf{r}, z) \, d^2\mathbf{r}, \tag{6.43}$$

$$\bar{\rho}_{\text{imp}}(z) = \frac{1}{A} \int_A \rho_{\text{imp}}(\mathbf{r}, z) \, d^2\mathbf{r}. \tag{6.44}$$

For the sake of simplicity, we shall assume that the average density of charged bio-molecules vanishes in the region $I_3$, $\bar{\rho}_{\text{bio}}(z) = 0$, even though its fluctuating part $\delta\rho_{\text{bio}}(\mathbf{R})$ may be nonzero in that region.

For the charge density on graphene, we first write the electrostatic potential in the plane of graphene as

$$\phi_0(\mathbf{r}) = \bar{\phi}_0 + \delta\phi_0(\mathbf{r}), \tag{6.45}$$

where $\bar{\phi}_0$ is the (constant) surface average of that potential that defines the equilibrium charge density on graphene $\sigma_0(\bar{\phi}_0)$ (see Eq. (6.48) below) and $\delta\phi_0(\mathbf{r})$ is the fluctuating part of that potential. We further assume a linear-response type constitutive relation akin to those for the electric and magnetic fields in Eqs. (2.6) and (2.7), which relates the charge density fluctuation on graphene $\delta\sigma_g = \sigma_g - \sigma_0$ to the fluctuation of the in-graphene potential as

$$\delta\sigma_g(\mathbf{r}) = -e^2 \int \mathcal{X}(\mathbf{r} - \mathbf{r}')\delta\phi_0(\mathbf{r}') \, d^2\mathbf{r}'. \tag{6.46}$$

Taking a 2DFT of this relation and comparing the result with that in Eq. (2.67), we conclude that the response function $\mathcal{X}(\mathbf{r})$ is an inverse 2DFT of the static polarizability of graphene $\chi(\mathbf{q})$. Hence, we may write the total surface charge density on graphene as a functional given by

$$\sigma_g[\phi_0(\mathbf{r})] = \sigma_0(\bar{\phi}_0) - e^2 \int \mathcal{X}(\mathbf{r} - \mathbf{r}')\delta\phi_0(\mathbf{r}') \, d^2\mathbf{r}'. \tag{6.47}$$

It should be noted that $\chi(\mathbf{q})$ and hence $\mathcal{X}(\mathbf{r})$ are strongly dependent on the equilibrium charge density $\sigma_0(\bar{\phi}_0)$ on graphene that is achieved in the dual gating process. This density may be evaluated from [22]

$$\sigma_0(\bar{\phi}_0) = \frac{2}{\pi} \frac{e}{(\hbar v_{\mathrm{F}}\beta)^2} \left[\mathrm{dilog}\left(1 + e^{\beta(\varepsilon_{\mathrm{F}}+e\bar{\phi}_0)}\right) - \mathrm{dilog}\left(1 + e^{-\beta(\varepsilon_{\mathrm{F}}+e\bar{\phi}_0)}\right)\right], \qquad (6.48)$$

where $v_F$ is the Fermi speed in graphene ($v_F \approx c/300$, where $c$ is the speed of light in free space), $\varepsilon_{\mathrm{F}}$ is the Fermi energy of doped graphene, and $\mathrm{dilog}$ is the standard dilogarithm function.

As for the density of mobile ions, which is only nonzero in the region $I_3$ by Eq. (6.32), we also write it as the sum of an average part and a fluctuation part as

$$\rho_3^{(\mathrm{ion})}(\Phi_3(\mathbf{R})) = \bar{\rho}_3^{(\mathrm{ion})}(\bar{\Phi}_3(z)) + \delta\rho_3^{(\mathrm{ion})}(\delta\Phi_3(\mathbf{R})). \qquad (6.49)$$

If we further assume that $|\delta\Phi_3(\mathbf{R})| \ll |\bar{\Phi}_3(z) - \bar{\Phi}_3(\infty)|$ in the region $I_3$, where $\bar{\Phi}_3(\infty) = \Phi_3(\infty) \equiv \phi_{tg}$, then Eq. (6.49) gives to the first order in $\delta\Phi_3$

$$\rho_3^{(\mathrm{ion})}(\Phi_3(\mathbf{R})) = \;-\; 2Zec\,\sinh\{\beta Ze[\bar{\Phi}_3(z) - \bar{\Phi}_3(\infty) + \delta\Phi_j(\mathbf{R})]\} \qquad (6.50)$$

$$\approx \;-\; 2Zec\,\sinh\{\beta Ze[\bar{\Phi}_3(z) - \bar{\Phi}_3(\infty)]\} \qquad (6.51)$$

$$-\; 2\beta(Ze)^2 c\,\delta\Phi_3(\mathbf{R})\,\cosh\{\beta Ze[\bar{\Phi}_3(z) - \bar{\Phi}_3(\infty)]\}. \qquad (6.52)$$

Thus, the average and the fluctuation parts of $\rho_3^{(\mathrm{ion})}$ in the region $I_3$ are written as

$$\bar{\rho}_3^{(\mathrm{ion})}(\bar{\Phi}_3(z)) \;=\; -2Zec\,\sinh\{\beta Ze[\bar{\Phi}_3(z) - \bar{\Phi}_3(\infty)]\}, \qquad (6.53)$$

$$\delta\rho_3^{(\mathrm{ion})}(\delta\Phi_3(\mathbf{R})) \;=\; -2\beta(Ze)^2 c\,\delta\Phi_3(\mathbf{R})\,\cosh\{\beta Ze[\bar{\Phi}_3(z) - \bar{\Phi}_3(\infty)]\}. \qquad (6.54)$$

Finally, Eq. (6.31) now becomes in the three regions with $j = 1, 2, 3$

$$\nabla^2[\bar{\Phi}_1(z) + \delta\Phi_1(\mathbf{R})] = -\frac{4\pi}{\epsilon_1}[\bar{\rho}_{\mathrm{imp}}(z) + \delta\rho_{\mathrm{imp}}(\mathbf{R})], \qquad (6.55)$$

$$\nabla^2[\bar{\Phi}_2(z) + \delta\Phi_2(\mathbf{R})] = 0, \qquad (6.56)$$

$$\nabla^2[\bar{\Phi}_3(z) + \delta\Phi_3(\mathbf{R})] = -\frac{4\pi}{\epsilon_3}[\bar{\rho}_3^{(\mathrm{ion})}(\bar{\Phi}_3(z)) + \delta\rho_3^{(\mathrm{ion})}(\delta\Phi_j(\mathbf{R})) + \delta\rho_{\mathrm{bio}}(\mathbf{R})], \qquad (6.57)$$

where in the last equation we set $\bar{\rho}_{\mathrm{bio}}(z) = 0$, by assumption. In the following sections we shall solve separately the averaged and the fluctuating parts of each of these equations.

94

### 6.3.1 Averaged part of partially linearized Poisson-Boltzmann equation

For the averaged parts of Eqs. (6.55), (6.56) and (6.57) we obtain the following set of ODEs in regions $j = 1, 2, 3$,

$$\epsilon_1 \frac{d^2 \bar{\Phi}_1(z)}{dz^2} = -4\pi \bar{\rho}_{\text{imp}}(z), \tag{6.58}$$

$$\epsilon_2 \frac{d^2 \bar{\Phi}_2(z)}{dz^2} = 0, \tag{6.59}$$

$$\frac{d^2 \bar{\Phi}_3(z)}{dz^2} = 8\pi \frac{Zec}{\epsilon_3} \sinh\{\beta Ze[\bar{\Phi}_3(z) - \bar{\Phi}_3(\infty)]\}. \tag{6.60}$$

We assume that the averaged potential satisfies the same BCs,

$$\bar{\Phi}_1(-t) = \phi_{bg}, \tag{6.61}$$

$$\bar{\Phi}_3(\infty) = \phi_{tg} \tag{6.62}$$

and the same MCs,

$$\bar{\Phi}_1(0) = \bar{\Phi}_2(0) \equiv \bar{\phi}_0 \tag{6.63}$$

$$\bar{\Phi}_2(h) = \bar{\Phi}_3(h) \equiv \bar{\phi}_h \tag{6.64}$$

$$-\epsilon_2 \frac{d\bar{\Phi}_2(0)}{dz} + \epsilon_1 \frac{d\bar{\Phi}_1(0)}{dz} = 4\pi\sigma_0(\bar{\phi}_0) \tag{6.65}$$

$$\epsilon_2 \frac{d\bar{\Phi}_2(h)}{dz} = \epsilon_3 \frac{d\bar{\Phi}_3(h)}{dz}, \tag{6.66}$$

as the full potential in the previous subsection, but using the average charge density on graphene in Eq. (6.65). Note that in Eq. (6.64) we have defined the surface average of the potential $\bar{\phi}_h$ in the plane $z = h$, i.e., at the boundary between the Stern layer and electrolyte.

Solving Eq. (6.58) with the BC in Eq. (6.61) gives

$$\bar{\Phi}_1(z) = -\frac{4\pi}{\epsilon_1} \int_{-t}^{z} (z - z') \, \bar{\rho}_{\text{imp}}(z') \, dz' + A(z + t) + \phi_{bg}, \tag{6.67}$$

whereas the general solution of Eq. (6.59) in the Stern layer is simply

$$\bar{\Phi}_2(z) = B\,z + C. \tag{6.68}$$

95

Using the MCs in Eqs. (6.63), (6.64), (6.65) and (6.66) we can determine the coefficients $A$, $B$ and $C$, as well as the average potential $\bar{\phi}_h$.

In the region $I_3$, Eq. (6.60) can be reduced to the one-dimensional case given in Eq. (6.8) by introducing a non-dimensional average potential in the electrolyte by $\psi(z) = \beta Z e[\bar{\Phi}_3(z) - \bar{\Phi}_3(\infty)]$, and solving it subject to the BC in Eq. (6.62), which gives $\psi(\infty) = 0$. The result is given by [43]

$$\psi(z) = 4 \tanh^{-1}[e^{-\kappa(z+z_0)}] \, \text{sign}(\psi_h), \tag{6.69}$$

where $\psi_h \equiv \psi(h) = \beta Z e(\bar{\phi}_h - \phi_{tg})$ is a non-dimensional average of the potential drop across the EDL. In Eq. (6.69) we introduced an auxiliary parameter $z_0$ defined by

$$z_0 = -h - \frac{1}{\kappa} \ln \left| \tanh\left(\frac{\psi_h}{4}\right) \right|. \tag{6.70}$$

For the calculation of the fluctuation part in the next subsection, we also need an expression

$$\cosh[\psi(z)] = 1 + 2 \, \text{cosech}^2[\kappa(z + z_0)], \tag{6.71}$$

which is easily deduced from the solution in Eq. (6.69).

Finally, from the BCs in Eqs. (6.61) and (6.62) and from MCs in Eqs. (6.63), (6.64), (6.65) and (6.66) we obtain two transcendental equations, which determine the average potential on graphene $\bar{\phi}_0$ (and hence the average charge density on graphene $\sigma_0(\bar{\phi}_0)$), as well as the potential $\bar{\phi}_h$ (and hence the parameters $\psi_h$ and $z_0$ that determine the ionic charge accumulated in the EDL) in terms of the externally applied gate potentials $\phi_{bg} = \bar{\Phi}_1(-t)$ and $\phi_{tg} = \bar{\Phi}_3(\infty)$ as

$$C_{ox}(\bar{\phi}_0 - \phi_{bg}) + C_S(\bar{\phi}_0 - \bar{\phi}_h) = \sigma_0(\bar{\phi}_0) + \sigma_{\text{imp}} \tag{6.72}$$

$$C_{ox}(\bar{\phi}_0 - \phi_{bg}) + \frac{\epsilon_3 \kappa}{2\pi \beta Z e} \sinh\left(\frac{\psi_h}{2}\right) = \sigma_0(\bar{\phi}_0) + \sigma_{\text{imp}} \tag{6.73}$$

where $C_{ox} = \epsilon_1/(4\pi t)$ and $C_S = \epsilon_2/(4\pi h)$ are defined as the capacitances per unit area of the oxide layer and the Stern layer, respectively. In the above equations, $\sigma_{\text{imp}}$ is the effective surface density of charged impurities in the oxide defined by [8]

$$\sigma_{\text{imp}} = \int_{-t}^{0} \left(1 + \frac{z}{t}\right) \bar{\rho}_{\text{imp}}(z) \, dz. \tag{6.74}$$

## 6.3.2 Fluctuating part of partially linearized Poisson-Boltzmann equation

For the fluctuating parts of Eqs. (6.55), (6.56) and (6.57) we obtain in regions $j = 1, 2, 3$ the following set of linear second-order PDEs

$$\nabla^2 \delta\Phi_1(\mathbf{R}) = -\frac{4\pi}{\epsilon_1} \delta\rho_{\text{imp}}(\mathbf{R}), \tag{6.75}$$

$$\nabla^2 \delta\Phi_2(\mathbf{R}) = 0, \tag{6.76}$$

$$\nabla^2 \delta\Phi_3(\mathbf{R}) - \frac{8\pi\beta(Ze)^2 c}{\epsilon_3} \cosh\{\beta Ze[\bar{\Phi}_3(z) - \bar{\Phi}_3(\infty)]\} \delta\Phi_3(\mathbf{R}) = -\frac{4\pi}{\epsilon_3} \delta\rho_{\text{bio}}(\mathbf{R}), \tag{6.77}$$

which must satisfy the homogeneous BCs,

$$\delta\Phi_1(\mathbf{R})|_{z=-t} = 0, \tag{6.78}$$

$$\delta\Phi_3(\mathbf{R})|_{z\to\infty} = 0, \tag{6.79}$$

and the following MCs at $z = 0$ and $z = h$,

$$\delta\Phi_1(\mathbf{R})|_{z=0} = \delta\Phi_2(\mathbf{R})|_{z=0} \tag{6.80}$$

$$\delta\Phi_2(\mathbf{R})|_{z=h} = \delta\Phi_3(\mathbf{R})|_{z=h} \tag{6.81}$$

$$-\epsilon_2 \left.\frac{\partial\delta\Phi_2(\mathbf{R})}{\partial z}\right|_{z=0} + \epsilon_1 \left.\frac{\partial\delta\Phi_1(\mathbf{R})}{\partial z}\right|_{z=0} = 4\pi\,\delta\sigma_g[\delta\phi_0(\mathbf{r})] \tag{6.82}$$

$$\epsilon_2 \left.\frac{\partial\delta\Phi_2(\mathbf{R})}{\partial z}\right|_{z=h} = \epsilon_3 \left.\frac{\partial\delta\Phi_3(\mathbf{R})}{\partial z}\right|_{z=h}. \tag{6.83}$$

Note that $\delta\sigma_g(\mathbf{r})$ in Eq. (6.82) was defined in Eq. (6.46) as a linear functional of the fluctuating potential in the plane of graphene, $\delta\phi_0(\mathbf{r})$. However, following the procedure outlined in the section 2.7, we may safely omit graphene from the solution for the fluctuating part of the PB equation and include it in the GF by using the DS equation approach. Hence we set $\delta\sigma_g[\delta\phi_0(\mathbf{r})] = 0$ in Eq. (6.82) and proceed to find the GF for the structure in Fig. 6.1 without graphene.

It is noteworthy that we may replace $\cosh\{\beta Ze[\bar{\Phi}_3(z) - \bar{\Phi}_3(\infty)] = \cosh[\psi(z)]$ in the left-hand side of Eq. (6.77), and use the identity given in Eq. (6.71) to obtain a more compact form of the partially linearized PB equation in electrolyte,

$$\nabla^2 \delta\Phi_3(\mathbf{R}) - \kappa^2 \left\{1 + 2\operatorname{csch}^2[\kappa(z + z_0)]\right\} \delta\Phi_3(\mathbf{R}) = -\frac{4\pi}{\epsilon_3} \delta\rho_{\text{bio}}(\mathbf{R}), \tag{6.84}$$

where we have defined csch as a shorthand for the cosech function. Notice that, through the parameter $z_0$, this equation contains information about the average charge densities in the overall structure and the external gate potentials from Eqs. (6.72) and (6.73).

Owing to the 2D translational invariance of the structure, we may now apply the 2DFT to the fluctuating potentials $\delta\Phi_j(\mathbf{R}) \equiv \delta\Phi_j(\mathbf{r}, z)$ for all $j$, defined as

$$\tilde{\Phi}_j(\mathbf{q}, z) = \int e^{-i\mathbf{q}\cdot\mathbf{r}} \delta\Phi_j(\mathbf{r}, z)\, d^2\mathbf{r}, \tag{6.85}$$

with similar definitions for the fluctuating parts of the densities of charged impurities and bio-molecules, $\widetilde{\rho}_{\text{imp}}(\mathbf{q}, z)$ and $\widetilde{\rho}_{\text{bio}}(\mathbf{q}, z)$, respectively. As a result, we obtain from Eqs. (6.75), (6.77) and (6.77),

$$\frac{\partial\tilde{\Phi}_1(\mathbf{q}, z)}{\partial z^2} - q^2\tilde{\Phi}_1(\mathbf{q}, z) = -\frac{4\pi}{\epsilon_1}\widetilde{\rho}_{\text{imp}}(\mathbf{q}, z), \tag{6.86}$$

$$\frac{\partial\tilde{\Phi}_2(\mathbf{q}, z)}{\partial z^2} - q^2\tilde{\Phi}_2(\mathbf{q}, z) = 0, \tag{6.87}$$

$$\left\{ \frac{\partial^2}{\partial z^2} - q^2 - \kappa^2 - 2\kappa^2\text{csch}^2[\kappa(z + z_0)] \right\}\tilde{\Phi}_3(\mathbf{q}, z) = -\frac{4\pi}{\epsilon_3}\widetilde{\rho}_{\text{bio}}(\mathbf{q}, z). \tag{6.88}$$

It can be shown that there are two linearly independent eigenfunctions of the differential operator on the left-hand side in Eq. (6.88), which are defined for $z \geq h$ by

$$U_+(z) = e^{z\sqrt{q^2+\kappa^2}}\left\{ 1 - \frac{\coth[\kappa(z + z_0)]}{\sqrt{q^2 + \kappa^2}}\kappa \right\}, \tag{6.89}$$

$$U_-(z) = e^{-z\sqrt{q^2+\kappa^2}}\left\{ 1 + \frac{\coth[\kappa(z + z_0)]}{\sqrt{q^2 + \kappa^2}}\kappa \right\}, \tag{6.90}$$

with the corresponding derivatives being

$$U'_+(z) = \sqrt{q^2 + \kappa^2}\, U_+(z) + \frac{\kappa^2}{\sqrt{q^2 + \kappa^2}}e^{z\sqrt{q^2+\kappa^2}}\text{csch}^2[\kappa(z + z_0)], \tag{6.91}$$

$$U'_-(z) = -\sqrt{q^2 + \kappa^2}\, U_-(z) - \frac{\kappa^2}{\sqrt{q^2 + \kappa^2}}e^{-z\sqrt{q^2+\kappa^2}}\text{csch}^2[\kappa(z + z_0)]. \tag{6.92}$$

Hence the Wronskian of those functions is given by

$$W \equiv U_+(z)U'_-(z) - U_-(z)U'_+(z) = -\frac{2q^2}{\sqrt{q^2 + \kappa^2}}. \tag{6.93}$$

The above expressions for the eigenfunctions $U_+(z)$ and $U_-(z)$ of the partially linearized PB operator in Eq. (6.88) will be used to construct the components of the TFGF in the region occupied by electrolyte.

### 6.3.3 Results for Green's function for the fluctuating parts in 3 layers

By analogy with the procedure used in section 2.5, we can deduce now a set of second-order, linear ODEs with non-constant coefficients for the components $\widetilde{G}_{jk}(z, z')$ of the FTGF corresponding to the partially linearized PB equations (6.86), (6.87) and (6.88) as

$$\frac{\partial^2}{\partial z^2}\widetilde{G}_{jk}(\mathbf{q}; z, z') - Q_j^2(z)\widetilde{G}_{jk}(\mathbf{q}; z, z') = -\frac{4\pi}{\epsilon_j}\,\delta_{jk}\,\delta(z - z'), \text{ for } z \in I_j \text{ and } z' \in I_k, \quad (6.94)$$

where

$$Q_j^2(z) \;=\; \left\{ \begin{array}{ll} q^2 & \text{for } j = 1, 2 \\ q^2 + \kappa^2\left\{1 + 2\,\mathrm{csch}^2[\kappa\,(z + z_0)]\right\} & \text{for } j = 3. \end{array} \right. \quad (6.95)$$

We see in Eq. (6.94) that, in comparison with the set of ODEs for the PB equation in the DH approximation given in Eq. (6.13), the main difference is that now the parameter $Q_3(z)$ in the region $I_3$ depends on distance $z$ and includes, via the parameter $z_0$, all the information about the averaged features of the entire structure containing graphene in the regime of dual doping.

In the following, we shall find all the components of the FTGF in Eq. (6.94) by implementing FTs of the BCs in Eqs. (6.78) and (6.79) and the MCs in Eqs. (6.80), (6.81), (6.82), and (6.83), which give rise to the expressions already listed in the section 2.6. The only exception is that the BC at $z \to -\infty$ in Eq. (2.62) is now replaced by a homogeneous Dirichlet BC at the finite $z = -t$,

$$\widetilde{G}_{1k}(z, z')\Big|_{z=-t} = 0. \quad (6.96)$$

To be quite general, and for verification purposes, we assume that fluctuations of the external charge $\delta\rho_{\mathrm{ext}}(\mathbf{R})$ may occur in any of the three regions $I_k$ with $k = 1, 2, 3$, even though in application to electrochemistry of graphene the Stern layer in region $I_2$ generally does not contain charges.

**Source point in $I_1$ ($k = 1$)**

If the external charge is in region $I_1$, it corresponds to the case when $k = 1$. So now the system for the Poisson equation of the FTGF becomes:

$$\left( \tfrac{\partial^2}{\partial z^2} - q^2 \right) \widetilde{G}_{11}(\mathbf{q}, z, z') = -\tfrac{4\pi}{\epsilon_1} \delta(z - z') \tag{6.97}$$

$$\left( \tfrac{\partial^2}{\partial z^2} - q^2 \right) \widetilde{G}_{21}(\mathbf{q}, z, z') = 0 \tag{6.98}$$

$$\left\{ \tfrac{\partial^2}{\partial z^2} - q^2 - \kappa^2 - 2\kappa^2 \mathrm{csch}^2[\kappa \, (z + z_0)] \right\} \widetilde{G}_{31}(\mathbf{q}, z, z') = 0 \tag{6.99}$$

which have the general solutions with coefficients to be determined by BCs:

$$\widetilde{G}_{21}(z, z') = E\,e^{qz} + F\,e^{-qz} \tag{6.100}$$

$$\widetilde{G}_{31}(z, z') = G\,U_-(z) \tag{6.101}$$

where we have dropped a term with $U_+(z)$ in $\widetilde{G}_{31}(z, z')$ which becomes indefinitely large when $z \to \infty$ in order to satisfy the BC at infinity. Since now both $z$ and $z'$ are in the interval $I_1 = (-t, 0)$, we define two components of the corresponding diagonal element of the FTGF as:

$$\widetilde{G}_{11}^<(z, z') = A\,e^{qz} + B\,e^{-qz} \tag{6.102}$$

$$\widetilde{G}_{11}^>(z, z') = C\,e^{qz} + D\,e^{-qz} \tag{6.103}$$

Now, the seven constants $A$, $B$, $C$, $D$, $E$, $F$ and $G$ are determined by imposing the seven BCs, which comes from substituting Eqs. (6.102), (6.103), (6.100), (6.101) into the BC in Eq. (6.96) and the MCs listed in the section 2.6 (subsections 2.6.2-4) with $k = 1$ gives a non-homogeneous system of seven algebraic equations for $A$, $B$, $C$, $D$, $E$ $F$ and $G$,

$$A\,e^{qz'} + B\,e^{-qz'} = C\,e^{qz'} + D\,e^{-qz'}, \tag{6.104}$$

$$C + D = E + F, \tag{6.105}$$

$$E\,e^{qh} + F\,e^{-qh} = G\,U_-(h), \tag{6.106}$$

$$\epsilon_1(C - D) = \epsilon_2(E - F) \tag{6.107}$$

$$\epsilon_2 q \left( E\,e^{qh} - F\,e^{-qh} \right) = \epsilon_3\,G\,U_-'(h), \tag{6.108}$$

$$C\,e^{qz'} - D\,e^{-qz'} - A\,e^{qz'} + B\,e^{-qz'} = -\frac{4\pi}{q\epsilon_1}, \tag{6.109}$$

$$A\,e^{-qt} + B\,e^{-q(-t)} = 0. \tag{6.110}$$

100

The final expressions for $\widetilde{G}_{11}(z, z')$, $\widetilde{G}_{21}(z, z')$ and $\widetilde{G}_{31}(z, z')$ can be written in a compact form if we define parameters as

$$\Delta_t = e^{2qt}, \tag{6.111}$$

$$\Delta_h = e^{-2qh}, \tag{6.112}$$

$$\lambda_b = \frac{\epsilon_1 - \epsilon_2}{\epsilon_1 + \epsilon_2}, \tag{6.113}$$

$$\lambda_h = \frac{\epsilon_3 U'_-(h) + \epsilon_2 q U_-(h)}{\epsilon_3 U'_-(h) - \epsilon_2 q U_-(h)}, \tag{6.114}$$

$$\gamma = \frac{-\lambda_h \lambda_b \Delta_h + 1}{-\lambda_h \Delta_h + \lambda_b}, \tag{6.115}$$

$$\eta = \frac{\sinh(qt) - \frac{\epsilon_1}{\epsilon_2} \cosh(qt)}{\sinh(qt) + \frac{\epsilon_1}{\epsilon_2} \cosh(qt)}. \tag{6.116}$$

The final solution is:

$$\widetilde{G}_{11}(z, z') = \frac{4\pi}{q\epsilon_1} \sinh[q(z^< + t)] \frac{e^{qz^>} + \gamma e^{-qz^>}}{e^{qt}\gamma + e^{-qt}} \tag{6.117}$$

$$\widetilde{G}_{21}(z, z') = \frac{4\pi}{q\bar{\epsilon}_{12}} \frac{\sinh[q(z' + t)]}{-\lambda_h \Delta_h + \lambda_b} \frac{-e^{qz}\lambda_h \Delta_h + e^{-qz}}{e^{qt}\gamma + e^{-qt}} \tag{6.118}$$

$$\widetilde{G}_{31}(z, z') = \frac{4\pi}{q\bar{\epsilon}_{12}} \frac{\sinh[q(z' + t)]}{-\lambda_h \Delta_h + \lambda_b} \frac{e^{-qh}(1 - \lambda_h)}{e^{qt}\gamma + e^{-qt}} \frac{U_-(z)}{U_-(h)} \tag{6.119}$$

**Source point in $I_2$ ($k = 2$)**

By the same process as before, we acquire the PB equation for FTGF when external charge is placed at $I_2$ as:

$$\left(\frac{\partial^2}{\partial z^2} - q^2\right) \widetilde{G}_{12}(\mathbf{q}, z, z') = 0 \tag{6.120}$$

$$\left(\frac{\partial^2}{\partial z^2} - q^2\right) \widetilde{G}_{22}(\mathbf{q}, z, z') = -\frac{4\pi}{\epsilon_2}\delta(z - z') \tag{6.121}$$

$$\left\{\frac{\partial^2}{\partial z^2} - q^2 - \kappa^2 - 2\kappa^2\text{csch}^2[\kappa(z + z_0)]\right\} \widetilde{G}_{32}(\mathbf{q}, z, z') = 0 \tag{6.122}$$

which have the general solutions with coefficients to be determined by BCs:

$$\widetilde{G}_{12}(z, z') \;=\; A\,\mathrm{e}^{qz} + B\,\mathrm{e}^{-qz} \tag{6.123}$$

$$\widetilde{G}_{22}^{<}(z, z') \;=\; C\,\mathrm{e}^{qz} + D\,\mathrm{e}^{-qz} \tag{6.124}$$

$$\widetilde{G}_{22}^{>}(z, z') \;=\; E\,\mathrm{e}^{qz} + F\,\mathrm{e}^{-qz} \tag{6.125}$$

$$\widetilde{G}_{32}(z, z') \;=\; G\,U_{-}(z). \tag{6.126}$$

Again, the seven constants need to be determined by imposing the BC in Eq. (6.96) and the six MCs listed in the section 2.6 (subsections 2.6.2-4) as

$$A + B \;=\; C + D, \tag{6.127}$$

$$E\,\mathrm{e}^{qh} + F\,\mathrm{e}^{-qh} \;=\; G\,U_{-}(h), \tag{6.128}$$

$$\epsilon_1(A - B) \;=\; \epsilon_2(C - D) \tag{6.129}$$

$$\epsilon_2 q\left(E\,\mathrm{e}^{qh} - F\,\mathrm{e}^{-qh}\right) \;=\; \epsilon_3\,G\,U_{-}'(h), \tag{6.130}$$

$$C\,\mathrm{e}^{qz'} + D\,\mathrm{e}^{-qz'} \;=\; E\,\mathrm{e}^{qz'} + F\,\mathrm{e}^{-qz'}, \tag{6.131}$$

$$E\,\mathrm{e}^{qz'} - F\,\mathrm{e}^{-qz'} - C\,\mathrm{e}^{qz'} + D\,\mathrm{e}^{-qz'} \;=\; -\frac{4\pi}{q\epsilon_3}, \tag{6.132}$$

$$A\,\mathrm{e}^{-qt} + B\,\mathrm{e}^{-q(-t)} \;=\; 0. \tag{6.133}$$

So the final solution of those equations may be used to express the components $\widetilde{G}_{12}, \widetilde{G}_{22}, \widetilde{G}_{32}$ in a compact form as

$$\widetilde{G}_{12}(z, z') \;=\; \frac{2\pi}{q\epsilon_2}\,\frac{1 + \eta}{\sinh(qt)}\,\frac{\mathrm{e}^{-qz'} - \Delta_h \lambda_{\mathrm{h}} \mathrm{e}^{qz'}}{1 + \Delta_h \lambda_{\mathrm{h}} \eta}\,\sinh[q(z + t)] \tag{6.134}$$

$$\widetilde{G}_{22}(z, z') \;=\; \frac{2\pi}{q\epsilon_2}\left\{\frac{-2\Delta_h \lambda_{\mathrm{h}} \eta}{1 + \Delta_h \lambda_{\mathrm{h}} \eta}\,\cosh[q(z' - z)] + \frac{\eta\,\mathrm{e}^{-q(z'+z)} - \Delta_h \lambda_{\mathrm{h}} \mathrm{e}^{q(z'+z)}}{1 + \Delta_h \lambda_{\mathrm{h}} \eta}\right\}$$

$$+\; \frac{2\pi}{q\epsilon_2}\,\mathrm{e}^{-q|z - z'|} \tag{6.135}$$

$$\widetilde{G}_{32}(z, z') \;=\; \frac{2\pi}{q\epsilon_2}\,\mathrm{e}^{-qh}(-\lambda_{\mathrm{h}} + 1)\,\frac{\mathrm{e}^{qz'} + \eta\,\mathrm{e}^{-qz'}}{1 + \Delta_h \lambda_{\mathrm{h}} \eta}\,\frac{U_{-}(z)}{U_{-}(h)} \tag{6.136}$$

**Source point in $I_3$ ($k = 3$)**

As in the procedures for $k = 1$ and $k = 2$, the PB equations for the components of the FTGF with $k = 3$ have the form:

$$\left(\tfrac{\partial^2}{\partial z^2} - q^2\right) \widetilde{G}_{13}(\mathbf{q}, z, z') = 0 \tag{6.137}$$

$$\left(\tfrac{\partial^2}{\partial z^2} - q^2\right) \widetilde{G}_{23}(\mathbf{q}, z, z') = 0 \tag{6.138}$$

$$\left\{\tfrac{\partial^2}{\partial z^2} - q^2 - \kappa^2 - 2\kappa^2 \text{csch}^2[\kappa\,(z + z_0)]\right\} \widetilde{G}_{33}(\mathbf{q}, z, z') = -\tfrac{4\pi}{\epsilon_3}\delta(z - z') \tag{6.139}$$

which have the general solutions with coefficients to be determined from the BCs and MCs:

$$\widetilde{G}_{13}(z, z') = A\,e^{qz} + B\,e^{-qz} \tag{6.140}$$

$$\widetilde{G}_{23}(z, z') = C\,e^{qz} + D\,e^{-qz} \tag{6.141}$$

$$\widetilde{G}_{33}^{<}(z, z') = E\,U_-(z) + F\,U_+(z) \tag{6.142}$$

$$\widetilde{G}_{33}^{>}(z, z') = G\,U_-(z) \tag{6.143}$$

where we have dropped a term with $U_+(z)$ in $\widetilde{G}_{33}^{>}(z, z')$ which becomes indefinitely large when $z \to \infty$. Now by implementing the BC in Eq. (6.96) and the six MCs listed in the section 2.6 (subsections 2.6.2-4), we get the system of equations:

$$A + B = C + D, \tag{6.144}$$

$$\epsilon_1(A - B) = \epsilon_2(C - D) \tag{6.145}$$

$$C\,e^{qh} + D\,e^{-qh} = E\,U_-(h) + F\,U_+(h), \tag{6.146}$$

$$\epsilon_2 q\left(C\,e^{qh} - D\,e^{-qh}\right) = \epsilon_3\left[EU'_-(h) + F\,U'_+(h)\right], \tag{6.147}$$

$$E\,U_-(z') + F\,U_+(z') = G\,U_-(z'), \tag{6.148}$$

$$G\,U'_-(z') - E\,U'_-(z') - F\,U'_+(z') = -\frac{4\pi}{\epsilon_3}, \tag{6.149}$$

$$A\,e^{-qt} + B\,e^{-q(-t)} = 0. \tag{6.150}$$

In order to write the solutions for all the GF in a compact form, we introduce some notations as:

$$\Gamma_{1\pm} = \epsilon_2 q U_\pm(h) - \epsilon_3 U'_\pm(h) \tag{6.151}$$

$$\Gamma_{2\pm} = \epsilon_2 q U_\pm(h) + \epsilon_3 U'_\pm(h) \tag{6.152}$$

$$\Omega_\pm = \Gamma_{1\pm} - \Gamma_{2\pm}\Delta_h\eta. \tag{6.153}$$

By this way, we obtain the final solution of $\widetilde{G}_{13}, \widetilde{G}_{23}, \widetilde{G}_{33}$ corresponding to the BCs as:

$$\widetilde{G}_{13}(z, z') = 4\pi \frac{(1 + \eta)e^{-qh}}{\sinh(qt)\,\Omega_-} \sinh[q(t + z)]U_-(z') \tag{6.154}$$

$$\widetilde{G}_{23}(z, z') = \frac{4\pi e^{-qh}}{\Omega_-} \left(e^{qz} + \eta\, e^{-qz}\right) U_-(z') \tag{6.155}$$

$$\widetilde{G}_{33}(z, z') = \frac{4\pi}{\epsilon_3 W} \left[ \frac{\Omega_+}{\Omega_-} U_-(z)U_-(z') - U_+(z^<)U_-(z^>) \right], \tag{6.156}$$

where $z^< = \min(z, z')$ and $z^> = \max(z, z')$.

## 6.4  Conclusion

In this chapter we have considered a configuration of the FET based on a single graphene layer exposed to a thick layer of liquid electrolyte containing salt ions. This setting may be used for sensing of additional chemical or biological compounds in the electrolyte by either passing weak electrical current through graphene or measuring its electrical capacitance relative to two external gates. We assumed that graphene may be simultaneously gated by both a back gate separated from graphene by an oxide layer of finite thickness and a reference electrode immersed into the bulk regions of the electrolyte. It is important to note that both the electrical conductivity and the capacitance of graphene depend on two aspects of electrostatic interactions in such structure: a) equilibrium density of charge carrier on graphene, which is achieved through the process of duel gating, and b) fluctuations of the electric potential in the plane of graphene due to random distribution of charged impurities in the oxide layer [8, 22, 26].

Applying the gate potential through the ion solution gives rise to a spatial redistribution of the mobile ions through the electrolyte in the presence of a charged graphene surface, which may be modeled by the Boltzmann distribution. As a consequence, the resulting PB equation becomes non-linear and hence intractable by analytical methods in its full 3D form. In the case that variation of the electric potential across liquid electrolyte is small, this equation can be linearized, giving rise to the so-called DH approximation, which allows a very similar treatment to be applied to obtain the corresponding GF as in the case of a simple multilayered structure of dielectrics.

However, current experiments show that the electrolytically gated graphene transistors for biochemical sensing often operate with quite large charge carrier densities on graphene, which require application of large potential differences across the liquid electrolyte [9, 12]. We can then assume that the electrostatic potential and all the charge densities in the system are represented

by their average values taken over the large area of graphene, in which case the resulting 1D nonlinear differential equation for the potential can be solved analytically along the coordinate perpendicular to graphene. This solution can be next assumed to represent a ground state of the system, where the average charge densities of impurities, graphene and the salt ions in the diffuse layer of the electrolyte are fully determined by the prescribed values of the potential on both gates. If we further assume that the lateral fluctuations of the electrostatic potential in directions parallel to graphene are always much smaller than the local value of the average potential, then we can derive the so-called partially linearized PB equation, which may be solved analytically by applying a 2D FT parallel to graphene and solving the resulting linear, ODE with a non-constant coefficient as a function of the perpendicular coordinate in the electrolyte. Using the two linearly independent solutions of this equation allows as to construct a full GF, which can describe small fluctuations of the electrostatic potential across the surface of graphene, while keeping fully nonlinear dependence on its equilibrium charge density that is achieved in the process of dual gating in the presence of aqueous solution. Our GF can be used within the recently developed mathematical formulation of graphene conductance [8] in the presence of external charges in the electrolyte with an arbitrary distribution function describing, e.g., layers of DNA molecules, lipid membrane adjacent to graphene, etc.

# Chapter 7

# Concluding remarks and future work

We have outlined a formulation of the boundary-value problem for the Poisson equation for electrostatic potential in layered structures, paying special attention to boundary conditions. It was shown that either the Dirichlet or Neumann boundary conditions on a closed boundary yield a unique, stable solution to this equation. In this thesis we usually consider Dirichlet boundary conditions when the potential is prescribed on metallic electrodes, which serve as external gates for our structures. However, since the Poisson equation must be solved in a piece-wise manner in a layered structure, we have seen that the potential must also satisfy the electrostatic MCs of both the Dirichlet and Neumann type at the interfaces between adjacent regions having different dielectric properties. Moreover, we have shown that inclusion of a single sheet of graphene in the structure gives rise to the Robin type MC.

The main theme in this thesis is detailed evaluation of the GF for the Poisson equation in layered structures that may contain layers of finite or infinite thickness occupied with different materials, such as dielectric insulators, a metal slab, or liquid electrolyte. It was shown that treating the graphene layer as a zero-thickness sheet of charge that is proportional to the local value of the electrostatic potential allows a direct inclusion of graphene into the GF for any layered structure by means of the DS equation.

Taking advantage of translational invariance of layered structures, we have used a 2D spatial FT to reduce the PDE for the GF to a system of ODEs. The GF is written in the form of a tensor with components that satisfy different equations depending on the location of the source point and the solution point. We have found that, once the linearly independent solutions of the original Poisson equation are known, the easiest way to construct the GF components is by the method of undetermined coefficients, which are found from the boundary and matching conditions.

After outlining the main elements of the theory in chapters 1 and 2, we have studied several

specific configurations in some detail. In Chapter 3, we have reviewed a derivation of the GF for the system of two and three layers of simple dielectrics. In chapter 4, we have studied two semi-infinite regions with a randomly rough interface between them and derived an average GF to the second order in the surface roughness. In chapter 5, we have considered a single layer of metal containing EG sandwiched between two semi-infinite dielectrics. Three versions of the hydrodynamic model for the EG were studied in that chapter: a local model and two non-local models, labeled as the standard and the quantum hydrodynamic models. The latter two models give rise to wave equations for the electron gas density, which are of the second and fourth orders in the spatial variable, respectively. We have used the method of GFs for both the Poisson equation for the electrostatic potential and the wave equation for the electron gas density. It was shown that those two quantities are coupled via a physically motivated boundary condition of the Neumann type at the boundary of the metal layer in the case of standard model, whereas we had to search for an ABC for the case of the quantum model. Finally, in chapter 6 we have formulated a nonlinear PB equation for the electrostatic potential in a structure containing: a semi-infinite layer of aqueous electrolyte, a Stern layer with simple dielectric, a graphene sheet, and an oxide of finite thickness that separates metallic back gate from graphene. After reviewing the construction of GF for a fully linearized PB equation in the DH approximation, we have shown that it is possible to solve the nonlinear PB equation in a 1D limit for the surface average of all quantities and then linearize the equation about that solution. We have evaluated a GF for such partially linearized PB equation, describing small fluctuations of the electrostatic potential in graphene due to spatial heterogeneity of the nearby external charged species.

The main advantage of the GF method is that it can yield electrostatic potential in a structure by performing simple integration over the spatial distribution of external charges having arbitrary form. Hence, the results of this thesis can find a very broad range of applications, especially in the new areas of Physics that use layered nano-structures. So, GFs of the type described in chapter 3 were recently used to study the conductivity of graphene in a filed effect transistor with several dielectric layers and a nearby gate [7, 26]. Results for the GF similar to those described in chapter 4 were recently used to study plasmon excitation in a rough metal surface by external charges moving parallel to that surface [44]. Nonlocal effects in the interaction of a fast point charge moving though a metallic slab were studied in Ref. [42] by means of the QHD model discussed in chapter 5. While the plasmon dispersion relations were described in Ref.[41] based on the SHD model of chapter 5, a future publication will present the results for plasmon dispersion relations in a metal slab found in this thesis based on the QHD model. Finally, while the results for GF in the DH approximation for the Poisson equation were used to study ionic screening of charged impurities in electrolytically gated graphene [8], a future publication will explore the use of the GF for the partially linearized PB equation obtained in chapter 6 for graphene applications in bio-chemical sensing.

# References

[1] M. W. Shinwari, M. J. Deen, and D. Landheer, Microelectron. Reliab. **47**, 2025 (2007).

[2] M. I. Stockman, Phys. Today **64**, 39 (2011).

[3] L. Wei, S. Aldawsari, W.-K. Liu, and B. R. West, IEEE Photonics Journal, **6**, 4801010 (2014).

[4] P. Avouris and F. Xia, MRS Bulletin **37**, 1225 (2012).

[5] N. O. Weiss , H. Zhou , L. Liao , Y. Liu , S. Jiang , Y. Huang , and X. Duan, Adv. Mater. **24**, 5782 (2012).

[6] K. S. Novoselov, A. K. Geim, S. V. Morozov, D. Jiang, Y. Zhang, S. V. Dubonos, I. V. Grigorieva, and A. A. Firsov, Science **306**, 666 (2004).

[7] Z.-Y. Ong and M. V. Fischetti, Phys. Rev. B **86**, 121409(R) (2012).

[8] Z. L. Miskovic, P. Sharma and F. O. Goodman, Phys. Rev. B **86**, 115437 (2012).

[9] Y. Liu, X. Dong, and P. Chen, Chem. Soc. Rev. **41**, 2283 (2012).

[10] K. Balasubramanian and K. Kern, Adv. Mater. **26**, 1154 (2014).

[11] D. Jariwala, V. K. Sangwan, L. J. Lauhon, T. J. Marksab, and M. C. Hersam, Chem. Soc. Rev. **42**, 2824 (2013).

[12] L. H. Hess, M. Seifert, and J. A. Garrido, Proc. IEEE, **101**, 1780 (2013).

[13] Y. Yang, A. M. Asiri, Z. Tang, D. Du, and Y. Lin, Materials Today **16**, 365 (2013).

[14] F. Chen, Q. Qing, J. Xia, and N. Tao, Chem. Asian J. **5**, 2144 (2010).

[15] D. Chen, L. Tang and J. Li, Chem. Soc. Rev. **39**, 3157 (2010)

[16] T. Low and P. Avouris, ACS Nano, **8**, 1086 (2014).

[17] J. D. Jackson, *Classical Electrodynamics*, John Wiley and Sons, New York (1962).

[18] C. Ciracì, J. B. Pendry, and D. R. Smith, Chem. Phys. Chem. **14**, 1109 (2013).

[19] C. Ciracì, R. T. Hill, J. J. Mock, Y. Urzhumov, A. I. Fernández-Domínguez, S. A. Maier, J. B. Pendry, A. Chilkoti, and D. R. Smith, Sceince **337**, 1072 (2012).

[20] C. David and F. J. G. de Abajo, J. Phys. Chem. C **115**, 19470 (2011).

[21] A. Wiener, A. I. Fernández-Domínguez, A. P. Horsfield, J. B. Pendry, and S. A. Maier, Nano Lett. **12**, 3308 (2012).

[22] M. I. Katsnelson, Graphene: Carbon in Two Dimensions, Cambridge University Press (2012).

[23] R. C. McOwen, *Partial Differential Equations: Methods and Applications*, Second edition, Prentice-Hall (2003)

[24] D. Siegel, *Partial Differential Equations II*, Course Notes for AMATH 453, University of Waterloo (2013).

[25] R. Haberman, *Applied Partial Differential Equations with Fourier Series and Boundary Value Problems*, Fourth Edition, Pearson (2004).

[26] R. Anicic and Z.L. Miskovic, Phys. Rev. B **88**, 205412 (2013).

[27] M. L. Brongersma and P. G. Kik (editors), *Surface Plasmon Nanophotonics*, Springer, Berlin (2007).

[28] F. J. Garcia de Abajo, Rev. Mod. Phys. **82**, 209 (2010).

[29] T. S. Rahman and A. A. Maradudin, Phys. Rev. B **21**, 504 (1980).

[30] F. Haas, G. Manfredi and M. Feix, Phys. Rev. E **62**, 2763 (2000).

[31] G. Manfredi and F. Haas, Phys. Rev. B **64**, 075316 (2001).

[32] J. F. Dobson and H. M. Le, J. Mol. Struct.: THEOCHEM **501-502**, 327 (2000).

[33] R. H. Ritchie and A. L. Marusak, Surf. Sci. **4**, 234 (1966).

[34] F. J. García de Abajo and P. M. Echenique, Phys. Rev. B **45**, 8771 (1992).

[35] C. L. Gardner and C. Ringhofer, SIAM (Soc. Ind. Appl. Math.) J. Appl. Math. **58**, 780 (1998).

[36] C. Chainais-Hillairet, M. Gisclon, and A. Jüngel, Numer. Methods Part. Differ. Eqs. **27**, 1483 (2011).

[37] L. Chen and M. Dreher, in *Partial Differential Equations and Spectral Theory*, edited by M. Demuth, B.-W. Schulze, and I. Witt (Birkhäuser, Basel, 2011), Vol. 211, p. 1.

[38] O. K. Harsh, B. K. Agarwal, Phys. Rev. B **39**, 8150 (1989).

[39] K. Dharamvir, B. Singla, K. N. Pathak, V.V. Paranjape, Phys. Rev. B **48**, 12330 (1993).

[40] G. Barton, Rep. Prog. Phys. **42**, 65 (1979).

[41] N. Kang, Z. L. Miskovic, Y.-Y. Zhang, Y.-H. Song, and Y.-N. Wang, Nanoscale Systems: Mathematical Modeling, Theory and Applications **3**, 44 (2014).

[42] Y.-Y. Zhang, S.-B. An, Y.-H. Song, N. Kang, Z. L. Miskovic, and Y.-N. Wang, Phys. Plasmas. **21**, 102114 (2014).

[43] A. J. Bard and L. R. Faulkner, *Electrochemical Methods: Fundamentals and Applications*, 2nd ed., John Wiley and Sons, New York (2001).

[44] K. Lyon, Y.-Y. Zhang, Z. L. Miskovic, Y.-H. Song, and Y.-N. Wang, Surf. Sci., in press (2015).